



SAPIENZA
UNIVERSITÀ DI ROMA

PhD course in Biochemistry
XXXIV Cycle (Academic year 2018-2021)

Dysregulation of stress response in Down Syndrome

PhD Student

Sara Pagnotta

Tutor

Prof. Marzia Perluigi

PhD Coordinator

Prof. Stefano Gianni



Alla mia famiglia e ad Alessandro

1. INTRODUCTION.....	8
1.1 Down Syndrome	8
1.1.1 Down Syndrome and development of Alzheimer’s disease neuropathology ...	10
1.1.2 APP processing and neurofibrillary tangles in Down Syndrome	13
1.2 Oxidative damage in Down Syndrome.....	17
1.2.1 Gene dosage and oxidative stress: SOD-1, APP, CBR.....	20
1.3 BACH-1/Nrf-2 Signalling	24
1.3.1 Involvement of BACH-1 in AD and DS.....	28
1.4 Caffeic Acid Phenethyl Ester (CAPE) and VP961 and their therapeutical implications	34
2. AIMS OF THE WORK.....	37
3. MATERIALS AND METHODS	39
PROJECT 1.....	39
3.1 Materials (CAPE and VP961).....	39
3.2 Mouse colony	40
3.3 Cell Cultures.....	40
3.3.1 SHSY-5Y (experimental design).....	40
3.3.2 LCLs (experimental design)	42
3.3.3 Primary cell cultures.....	43
3.4 MTT Assay	46
3.5 Nuclear and cytosolic proteins extraction.....	47
3.6 Protein extraction and Western Blot.....	47
3.7 mRNA extraction	49
3.8 Reverse Transcription and Quantitative Real Time PCR.....	49
3.9 Immunofluorescence and confocal microscopy.....	51
3.10 Statistical analysis	52
PROJECT 2.....	52
3.11 Study population	52
3.12 Sample collection of Peripheral Bloo Mononuclear Cells from HD and DS Subjects.....	54
3.13 Protein Sample extraction	55

3.14	Protein Expression Analysis by nLC–HDMSE	55
3.15	Bioinformatics and network analysis	58
3.16	Western Blot	58
3.17	Slot Blot analysis and Protein Carbonylation	59
3.18	Statistical analysis	60
4.	<i>RESULTS</i>.....	61
	PROJECT 1.....	61
4.1	CHARACTERIZATION OF BACH-1/Nrf-2 pathway in DOWN SYNDROME MODELS.....	61
4.1.1	Characterization of BACH-1 /Nrf-2 pathway in primary cultures of neurons and astrocytes isolated from Ts2cje and Euploid mice.....	61
4.1.2	Characterization of BACH-1/Nrf-2 pathway in the hippocampus of Ts2cje and Euploid mice at 3 months of age	67
4.1.3	Characterization of BACH-1/Nrf-2 pathway in the LCLs from Down Syndrome and Healthy donors' children	69
4.2	CAPE and VP961	72
4.2.1	Effects of CAPE and VP961 on neuroblastoma cell viability	72
4.2.2	Protective effect of CAPE and VP961 pre-treatment against H2O2-induced toxicity on SHSY-5Y.....	74
4.2.3	The treatment with CAPE and VP961 is able to induce Nrf-2 nuclear translocation on SHSY-5Y under oxidative stress conditions	75
4.2.4	The effects of CAPE and VP961 on HO-1 and NQO1 gene and protein levels, as target of Nrf-2.....	77
4.3	CAPE and VP961 treatment on Down syndrome LCLs	80
4.3.1	VP961 induce Nrf-2 nuclear translocation in DS LCLs	81
	PROJECT 2.....	84
4.4	PBMC proteomes from DS and HD young patients were investigated using an in-depth Label-Free shotgun Proteomics Approach	84
4.4.1	Protein included in intracellular trafficking	94
4.4.2	Proteins involved in stress response	95
4.4.3	Cytoskeleton proteins	95
4.4.4	Protein involved in DNA structure	96
4.5	Validation of the results obtained by proteomic analysis.....	97
5.	<i>DISCUSSION</i>	99
5.1	Discussion Project 1	99

5.2 Discussion Project 2	104
6. <i>CONCLUSIONS</i>	111
7. <i>REFERENCES:</i>	112
8. <i>APPENDIX</i>	126
Appendix A	126
Appendix B	127
Appendix C	128
Appendix D	129

List of Abbreviations:

AD: Alzheimer disease

ADH: alcohol dehydrogenase

ALDH: aldehyde dehydrogenase

APP: amyloid precursor protein

ARE: antioxidant response element

A β : amyloid-beta peptide

BACH-1: BTB and CNC homology 1

BBB: blood-brain barrier

CAPE: Caffeic Acid Phenethyl Ester

CAT: catalase

CBR: carbonyl reductase

CNS: central nervous system

Cx: Cortex

DS: Down syndrome

DS-AD: DS-associated AD

DYRK1A: Dual specificity tyrosine-phosphorylation-regulated kinase 1A

ETS2: Protein C-ets-2

GPX: glutathione peroxidase

H₂O₂: hydrogen peroxide

Hip: hippocampus

HNE: 4-hydroxynonenal

HO•: hydroxyl radical

HO-1: heme oxygenase 1

HSA21: abnormal triplication of chromosome 21

Keap1: Kelch-like ECH-Associating protein 1

LCLs: Lymphoblastoid cell lines

MAPKs: mitogen-activated protein kinases

NFTs: neurofibrillary tangles

NQO1: NADPH quinone oxidoreductase 1

Nrf-2: nuclear factor erythroid 2-related factor 2

O₂••: superoxide anion

OS: oxidative stress

PBMCs: Peripheral blood mononuclear cells

RCAN1: regulator of calcineurin 1

RNS: reactive nitrogen species

ROS: reactive oxygen species

S100B: S100 calcium-binding protein B

SOD-1: superoxide dismutase

1. INTRODUCTION

1.1 Down Syndrome

Down syndrome (DS) is a genetic disorder affecting about 6 million people worldwide [1, 2]. Although the primary cause of this condition is the abnormal triplication of chromosome 21 (HSA21), DS may be considered as a multifactorial disease, where an abnormal expression of trisomic genes arises not only from genetic, but also environmental factors. Thus, trisomy leads to a deregulated scenario that also affects disomic genes and that ultimately results in largely different phenotypes. The increased dosage of the gene encoded on chromosome 21 (Fig.1) is known to affect diverse pathways, including those involved in brain development, metabolism, and neuronal networks [3, 4]. The genetic alterations indeed are responsible of the major clinical features of the disease such as craniofacial abnormalities, small brain size, accelerated aging, and cognitive defects. Individuals with DS are also more likely to develop certain health conditions, including hypothyroidism, autoimmune diseases, epilepsy, haematological disorders, and Alzheimer-like dementia [5]. Because of recent advance in health care and management of co-occurring illnesses, life expectancy of people with DS has largely improved [6, 7]. As a matter of fact, the average lifespan of DS individuals has approximately doubled over the past 30 years to 55-60 years of age [8, 9]. Consequently, up to 35 years old, mortality rate of adults with DS is comparable to that of adults affected by other intellectual disabilities. However, after age 35, mortality rates double every 6.4 years in DS as compared to every 9.6 years for people without DS [8]. Despite the consistent increase in life expectancy, one of the reasons that

strongly compromise adult DS subjects quality of life has to be found in the development of a form of dementia similar to Alzheimer's disease [10, 11].

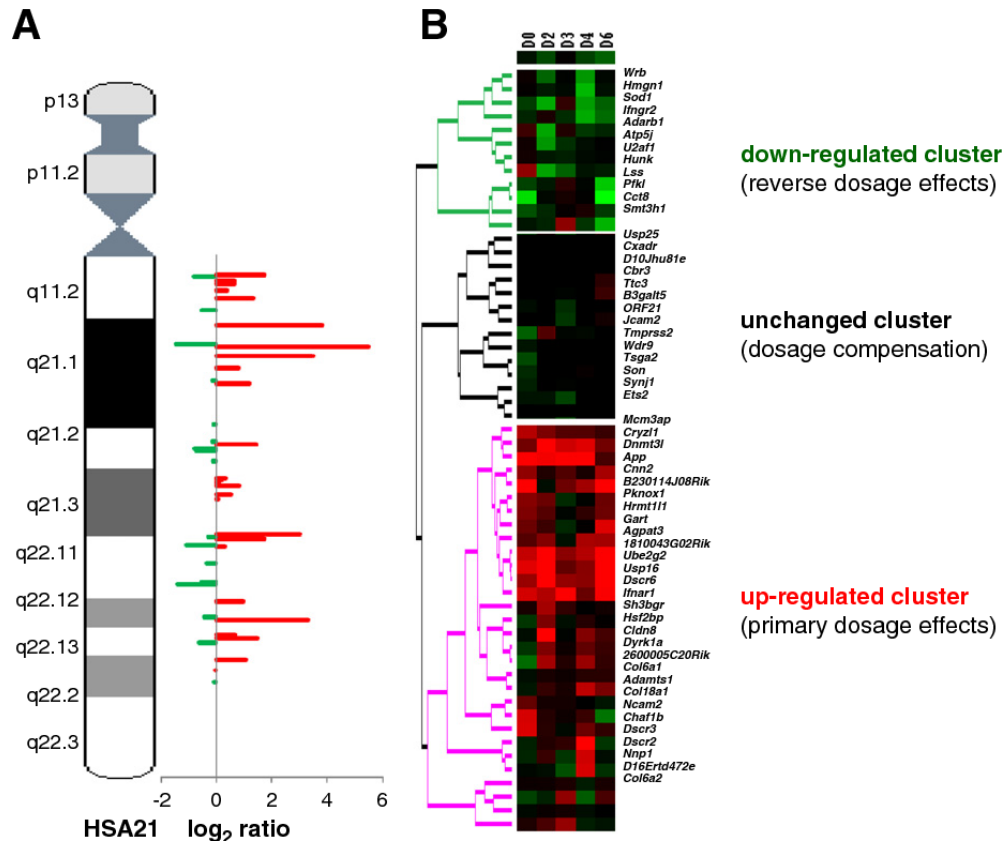


Figure 1. Gene dosage clusters of HSA21 orthologs. (A) The expression levels of the HSA21 genes and under-expressed genes along the chromosome HSA21. (B) K-mean hierarchical clustering green dendrogram indicates the down regulated trisomic genes and red dendrogram shows the up-regulated cluster genes [12].

1.1.1 Down Syndrome and development of Alzheimer's disease neuropathology

The aging process in DS population leads to increased risk of developing Alzheimer's disease (AD) since adult age. Recent findings suggest that 75% of adults with DS survive to 50 years old and 25% reach the age of 60 [13]. The portion of these surviving individuals that develop clinical signs of dementia can fluctuate considerably. In the range of age of 20-29, virtually no individual show symptoms of dementia [14, 15]. Between the ages of 30-39 years, reports of prevalence range between 0 to 33% of individuals being clinically demented. From 40-49 years of age, 5,7-55% may be demented and between 50-59 years prevalence ranges from 4-55%. In the end, the range of individuals affected by dementia over the age of 60 years is between 15-77% [9]. For DS people older than 40 years old, dementia follows a similar course to that seen in Alzheimer's disease [16, 17], with declines in recall and explicit memory [18] and in language function usually preceding dementia. However, early-onset dementia in younger DS individuals (aged 30-40 years) often manifests as changes in behaviour and personality [16, 17], with symptoms including apathy, increasing impulsivity and executive dysfunction. Understanding the factors that underlie the variation in symptom presentation and age of clinical onset of dementia in people with DS may provide insights into the pathophysiological mechanisms of both sporadic and DS-associated AD (DS-AD) [19, 20]. Thus, DS offers a unique model to investigate the early molecular changes that precede the appearance of the manifest clinical signs of AD-related dementia. Alzheimer's disease (AD) is a chronic neurodegenerative disease with well-defined pathophysiological mechanisms, mostly affecting medial temporal lobe and associative neocortical structures.

Neuritic plaques and neurofibrillary tangles represent the pathological hallmarks of AD and are respectively related to the accumulation of the amyloid-beta peptide ($A\beta$) in brain tissues, and to cytoskeletal changes that arise from the hyperphosphorylation of microtubule-associated Tau protein in neurons (Fig. 2, A and B).

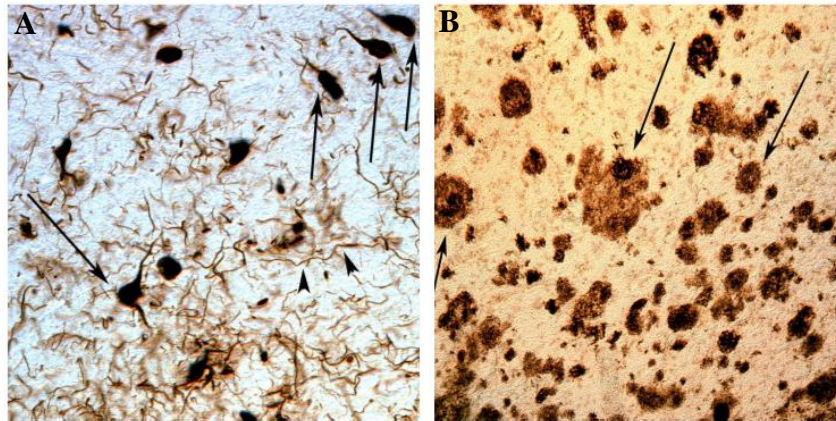


Figure 2. Neuropathological features of DS brain. (A) Neurofibrillary tangles labeled using PHF-1 antibody in the frontal cortex of a 46 years old male with DS and AD. (B) Significant cerebral amyloid angiopathy in a 46 years old male with DS and AD detected by immunostaining of the frontal cortex with $A\beta$ 1-40 antibody. Neurofibrillary tangles and amyloid plaques are both indicated in the figure by arrows. (Head E.).

According to the amyloid hypothesis of AD, the overproduction of $A\beta$ is a consequence of the disruption of homeostatic processes that regulates the proteolytic cleavage of the amyloid precursor protein (APP) [21]. Several studies on this topic revealed that from a molecular point of view, DS neuropathology and AD have many common features (Fig. 3), counting the deposition of senile plaques and neurofibrillary tangles, together with cellular dysfunction such as mitochondrial defects, increased oxidative stress, and

metabolic alterations [4, 11, 22, 23]. One of the main links between AD and DS is related to the triplication of the amyloid precursor protein gene (APP), which is encoded on chromosome 21. As a matter of fact, a small percentage of DS individuals having only a partial trisomy for APP gene do not have the same elevated risk to develop AD, even still more consistent than the rest of the population [24, 25]. Likewise, high expression of APP in fibroblasts of individuals with DS is necessary and enough to cause morphological and functional anomalies in early endosomes, which participate in neuron growth, homeostasis, and synaptic functions [26]. Taken together these findings support the conclusion that an extra dose of the APP gene is sufficient to cause AD in DS subjects. Moreover, trisomy of chromosome 21 results in increased gene dosage for all genes on this chromosome, including several genes in addition to APP that may also be involved in related mechanisms. Among triplicated genes, both dual specificity tyrosine phosphorylation regulated kinase 1A (DYRK1A) and the regulator of calcineurin 1 (RCAN1) have a well-established role in the aberrant phosphorylation of tau protein, which is one of the main mechanisms underlying the formation of toxic neurofibrillary tangles in AD [27-30]. Furthermore, trisomy 21 is characterized by mitochondrial dysfunction and enhanced production of reactive oxygen species (ROS) [27, 31] that may contribute to accelerated aging reported in DS people [32]. Indeed, oxidative damage is increased in prenatal DS brain compared to non-DS controls [33, 34] and is also higher in adult DS brain compared to age-matched controls [22, 35]. Interestingly, superoxide dismutase 1 (SOD-1), which has a pivotal role in ROS processing, is encoded on chromosome 21. Consistent with this, increased SOD-1 activity has been suggested to cause accelerated cell senescence by the abnormal accumulation of toxic hydrogen peroxide [36]. According these evidences, several genes can modulate the

course of AD neuropathology in DS population and further work is required to determinate their role and relative importance.

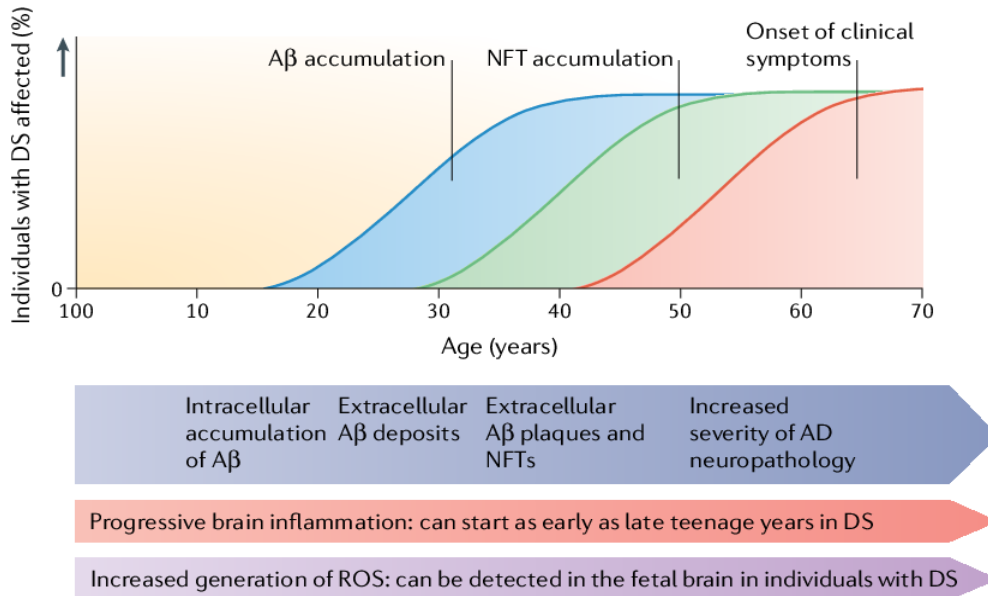


Figure 3. Hypothetical progression of Alzheimer-like neuropathology in Down syndrome. A proposed timeline from birth to over 60 years of age of Alzheimer's disease (AD) pathology in individuals with Down syndrome (DS).

1.1.2 APP processing and neurofibrillary tangles in Down Syndrome

Among the aberrantly over-expressed genes in DS individuals, the gene encoding the amyloid precursor protein (APP) is thought to have the key role in the pathology of AD. The additional copy of APP may drive the development of AD in DS population by increasing the levels of amyloid- β (A β), a cleavage product of APP that misfold and accumulates in the brain

forming toxic plaques. APP is a type I transmembrane protein essential for normal brain development and possibly also for adult brain plasticity [37]. This protein can undergo two major proteolytic pathways by different sets of enzymes: a canonical via (non-amyloidogenic) and an amyloidogenic one that leads to the formation of amyloid plaques. In the non-amyloidogenic pathway APP is initially cleaved by an α -secretase in the middle of the A β sequence, thus precluding the formation of A β (Fig. 4). This activity generates a soluble APP fragment (sAPP α) and a membrane-bound C-terminal fragment of APP (α -CTF). α -CTF can be further cleaved by γ -secretase generating the so-called p3 fragment and the amyloid intracellular domain (AICD). On the other hand, the potentially amyloidogenic pathway consists of a β -secretase-mediated cleavage of APP that results in the secretion of sAPP β , and a second membrane-bound C-terminal fragment of APP (β -CTF). Further cleavage of β -CTF by γ -secretase generates several aggregation-prone A β peptides that results in the progressive formation of senile plaques in the brain parenchyma [38]. The additional copy of APP in DS does not typically result in substantial A β accumulation until the second or third decade of life. This lack of early A β accumulation may be due to APP not becoming dosage sensitive until adulthood, as it's suggested by both animal and human studies [39-41]. Despite this, increased levels of soluble A β are found in one out of two DS foetal brain [42], suggesting that APP processing may not be sufficient to cause extensive A β accumulation in the developing brain but is still present even decades before the overt presence of clinical symptoms. In line with these findings, increased A β levels have been reported in human cell models like pluripotent stem cells derived from children and young adults affected by DS [26, 43, 44]. One of the possible explanations for the lack of early A β accumulation in DS is the initial efficiency of cellular clearance system. Indeed, the progressive

dysfunction of intracellular degradative systems that characterize DS neuropathology may contribute to the later accumulation of toxic aggregates [45, 46].

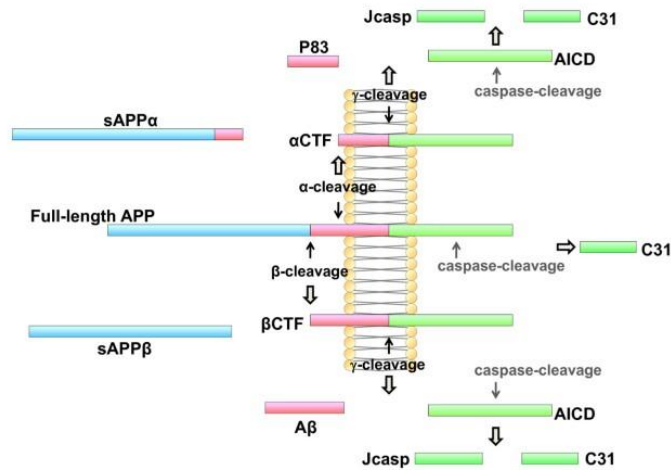


Figure 4. Schematic representation of amyloidogenic and non amyloidogenic APP processing. APP protein can be processed by two different pathways: the canonical via (non amyloidogenic) and the amyloidogenic one. In the non-amyloidogenic pathway APP is cleaved by an α -secretase precluding the formation of $A\beta$, this leads to the generation of a soluble fragment ($sAPP\alpha$) and a membrane-bound C-terminal fragment of APP (α -CTF). This last is subsequently cleaved by a γ -secretase generating the p3 fragment and the amyloid intracellular domain (AICD). In the amyloidogenic pathway APP is cleaved by β -secretase producing $sAPP\beta$ and a second membrane-bound C-terminal fragment of APP (β -CTF). The cleavage of β -CTF by γ -secretase generates several aggregation-prone $A\beta$ peptides that results in the progressive formation of senile plaques in the brain.

Other hallmark of AD is hyperphosphorylated state of tau, the major microtubule associated protein in neurons and interacts with tubulin to promote and stabilize its assembly into microtubules [47], allowing axonal transport of vesicles [48] (Fig. 5). In AD tau can no longer associate with microtubules,

leading to the formation of toxic neurofibrillary tangles (NFTs). Pathological brain changes of aged subjects affected by DS are nearly identical to those of patients with AD consisting of both amyloid plaques and NFTs. The potential factor that contributes to DS tau hyperphosphorylation may be the overexpression of the dual specificity tyrosine phosphorylation regulated kinase 1A (DYRK1A), a ubiquitously expressed protein kinases which is strongly expressed in heart and brain tissues [49, 50] and the overexpression of the regulator of calcineurin 1 (RCAN1). Both of them are encoded on chromosome 21. Furthermore, APP may also play a role in tau phosphorylation in DS brain since A β -42 peptide seems to upregulate both DYRK1A and RCAN1 [51]. Thus, the overexpression of chromosome 21-encoded genes appears to cooperate driving both precocious A β accumulation and aberrant tau

phosphorylation and consistently favouring the neurodegenerative process in DS.

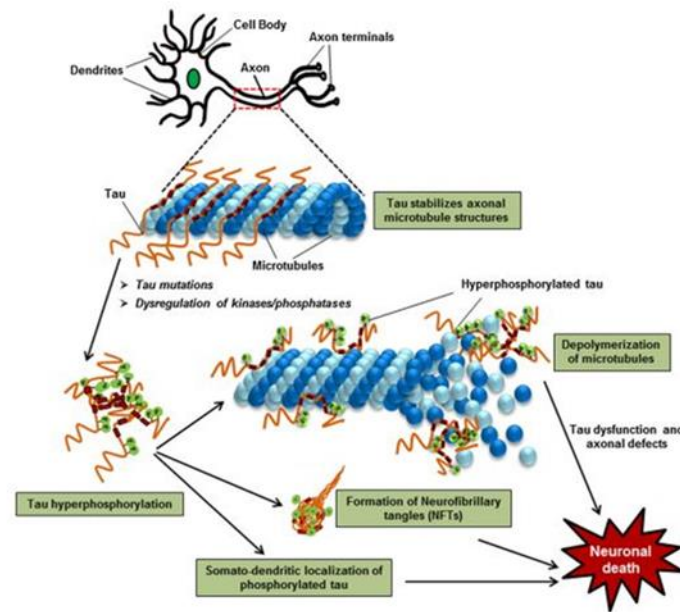


Figure 5. Schematic representation of some key events and role of tau hyperphosphorylation in formation of NFTs. Tau is a microtubule associated protein in neurons and physiological conditions it regulates microtubule stabilization. In AD, tau is not associated in microtubules leading a loss in microtubule affinity and the formation of toxic neurofibrillary tangles (NFTs) which consequently results in neurodegeneration and commencement of tauopathies.

1.2 Oxidative damage in Down Syndrome

DS is emerging as a disorder etiologically related to oxidative stress (OS) mainly due to triplication of Cu, Zn-superoxide dismutase (SOD-1),

encoded HSA21. However, recent reports showed that OS is driven not only from overexpression of some HSA21 genes, but also from a dysregulation of gene/protein expression associated with the trisomy [52]. OS results from either elevated production of reactive oxygen and nitrogen species (ROS/RNS) or by reduced antioxidant responses. The central nervous system (CNS) contains high levels of fatty acids that in the presence of high metabolic flux are a fertile ground for lipid peroxidation reactions responsible of generating increasing number of free radicals as well as highly reactive products, such as 4-hydroxynonenal (HNE) [22, 53-55]. In addition, superoxide anion ($O_2^{\bullet\bullet}$), hydrogen peroxide (H_2O_2), and hydroxyl radical (HO^{\bullet}), are continuously produced as by-products of aerobic respiration and various other catabolic/anabolic processes [56]. As a result, neuronal cells are highly susceptible to redox imbalance and to accumulate oxidative damage [57].

Accumulating studies implicate OS in DS pathological phenotypes [23, 58, 59], though the exact mechanisms through which oxidative damage translate into clinical features of DS need to be clarified. It is likely that OS is a chronic condition in DS brain, that initiates already during embryonic development and further accumulates with aging, representing a strong risk factor for subsequent neurodegeneration [60, 61]. In order to better understand and appreciate the causes of OS in DS brain, initial explanations can be obtained by mapping the HSA21 on which a number of genes (Table 1) such as SOD-1, amyloid precursor protein (APP), the transcription factor BTB and CNC homology 1 (BACH-1), the Protein C-ets-2 (ETS2), carbonyl reductase (CBR), S100 calcium-binding protein B (S100B), among others, are directly involved in the overproduction of ROS as found in DS individuals and in mouse models thereof [62].

Gene on Hsa21	Molecular Function	Biological Process	Relevance in Down Syndrome
SOD-1 , (<i>Cu,Zn-superoxide dismutase 1</i>)	Oxidoreductase	Antioxidant Response	Triplication of SOD-1 in DS brain results in an imbalance in the ratio of SOD-1 to CAT and GPX (two enzymes involved in its metabolism), thus leading to the accumulation of H ₂ O ₂ in the cells.
APP , (<i>amyloid precursor protein</i>)	Heparin-binding, Protease inhibitor	Apoptosis, Cell adhesion, Endocytosis, Notch signaling pathway and A β processing	Triplication of APP causes the over-production of A β (1-40/42) in DS brain. Deposition of senile plaques of A β is observed in post-mortem brain and plasma from DS compared with non-DS individuals.
BACH1 , (<i>BTB Domain and CNC Homolog 1</i>)	DNA-binding, Transcription regulation	Antioxidant Response	Triplication of BACH1, as a negative transcription regulator, in DS brain could block the induction of antioxidant genes, therefore promoting increased OS in the cell
CBR , (<i>Carbonyl reductase</i>)	Oxidoreductase	Oxidative stress Response	Triplication of CBR in DS play a role in exacerbating OS. Carbonyls are toxic metabolic intermediates that are mainly detoxified by aldehyde dehydrogenase or reduced by CBR and/or alcohol dehydrogenase to their corresponding alcohols. Increased levels of these enzymes were detected in the brain of DS patients, likely in response to elevated carbonyls production in DS

Table 1. List of genes located on Hsa21.

1.2.1 Gene dosage and oxidative stress: SOD-1, APP, CBR.

Among trisomic genes, SOD-1 is one of the first lines of antioxidant defence by catalyzing the conversion of $O_2 \bullet\bullet$ to molecular oxygen (O_2) and H_2O_2 , which can be neutralized by catalase (CAT) and by glutathione peroxidase (GPX) to water [63]. Moreover, the triplication of HSA21 is not accompanied by a parallel increase of CAT and GPX, resulting in imbalance in SOD-1/CAT levels and those of SOD-1/GPX, with an accumulation of H_2O_2 [11]. Interestingly, in all DS tissues an altered SOD-1/GPX activity ratio has been observed [22], that may partially explain higher levels of H_2O_2 and its by-products. In addition to CAT and GPX, a decreased expression of peroxiredoxin 2 also was detected in DS fetal brain, which further contribute to the increased susceptibility of DS neurons to undergo oxidative damage [10].

Intriguingly, aberrant expression of SOD-1 seems to be associated with mitochondrial impairment. Indeed, transgenic mice overexpressing wild-type human SOD-1 (Tg-SOD-1) show many mitochondrial defects such as increased mitochondrial swelling and vacuolization, that also are associated with learning and memory disturbance [54]. In addition, Tg-SOD-1 mice have altered levels of ATP synthase alpha/beta chain and elongation factor Tu, while no changes in the levels of antioxidant proteins were observed [54]. Taken together, these alterations correlate with synaptosomal damage and neuronal loss in the brain of Tg-SOD-1, ultimately leading to cognitive deficits in DS.

To the well-recognized role of SOD-1, increased OS could also be caused by the over-production of $A\beta$, due to triplication of APP. This hypothesis is confirmed by a number of reports demonstrating that both $A\beta$ (1-

40/42) are able to induce OS, as in the case of AD [55, 64]. Indeed, Butterfield and others [55, 58, 65, 66] proposed that A β (1-42), in the form of oligomers, is able to insert into the membranes initiating lipid peroxidation and downstream cascades [64]. Accordingly, the levels of both A β (1-42) and A β (1-40) in plasma are higher in DS compared with non-DS controls and deposition of senile plaques is observed in post-mortem brain from DS individuals [67, 68], very early in life. Further, A β has the ability to coordinate metal ions —Zn²⁺, Cu²⁺ and Fe²⁺—and the alteration of metal homeostasis is known to regulate both production and defence against ROS and is also involved in the regulation of neuronal activity in the synapses and other biological functions in the brain. It is interesting to underlie that, studies from Anandatheerthavarada et al. [69], for the first time provided evidence that full length APP itself is able to damage mitochondria. Consistent with their work, mice overexpressing wild type human APP show cognitive defects and neuronal pathology similar to what observed in AD models, though these mice do not show significant A β deposition in the hippocampus [70]. These findings support the notion that, in addition to effects from APP-generated A β oligomers on mitochondria, trisomy of APP itself may promote mitochondrial dysfunction in DS.

BACH-1, encoded on HSA21, is a key element in the regulation of the antioxidant response in DS [53]. BACH-1 is a transcription repressor that acts as a key regulator of the expression of genes involved in the cell stress response [71]. In DS, it is likely that upregulation of BACH-1 protein levels could block the induction of antioxidant genes, therefore promoting increased OS in the cell [53]. The molecular aspects of BACH-1 triplication will be discussed in the next section.

By mapping HSA21, another candidate gene that is related to OS is the enzyme carbonyl reductase (CBR). CBRs are NADPH-dependent cytosolic enzymes with broad substrate specificity for many endogenous and xenobiotic carbonyl compounds. They catalyse the reduction of endogenous prostaglandins, steroids, and other aliphatic aldehydes and ketones. Carbonyls are considered toxic metabolic intermediates, that can be detoxified both through oxidation by aldehyde dehydrogenase (ALDH) or by CBR-mediated reduction and/or alcohol dehydrogenase (ADH). Increased levels of both these enzymes were detected in the brain of both DS and AD patients, likely in response to elevated carbonyls production [72]. Published studies from our laboratories identified several oxidatively modified proteins in DS brain, prior and after development of AD [22, 45, 73]. Among several targets, oxidation of proteins could be particularly deleterious in aging and in age-related neurodegenerative diseases, due to a gradual loss of efficiency of clearance systems for their removal [72]. The role of OS in the development and progression of AD in the general population has been extensively discussed in several review papers [55, 74, 75]. Among the proteins identified by redox proteomics to be oxidatively modified, either by increased carbonylation or HNE modification, proteins involved in several intracellular processes such as (i) neuronal trafficking; (ii) the proteostasis network; (iii) energy metabolism; and (iv) mitochondrial function were found [53]. Reduced ATP levels, increased ROS, and altered mitochondrial permeability are characteristic mitochondrial defects of degenerating neurons not only in DS but also in many neurodegenerative disorders, including AD [55]. Overall, proteomics data demonstrate that oxidative damage is an early event in DS, and the dysfunction of protein clearance systems contributes to increased neuronal vulnerability to oxidative damage that accelerate neurodegenerative phenomena. As noted,

considering that several of the above-mentioned proteins have been already found to be oxidized in AD brain, our results strongly support the notion that aberrant protein oxidation in DS may contribute to age-dependent AD risk. This view is also confirmed by a longitudinal study analyzing some redox markers in plasma samples from DS subjects (1–57 years old) showing that changes in redox-related parameters are strongly age-dependent [59].

The picture that emerges from both brain and peripheral studies suggest that young DS individuals are characterized by an early pro-oxidant state [76] that results in a variety of pathological phenotypes. With age, adult DS persons accumulate oxidative damage associated with an increased risk to develop Alzheimer-like dementia [11, 62]. Understanding the complexity of factors regulating redox homeostasis may help to identify potential therapeutic treatments able to prevent the accumulation of oxidative damage. In this scenario, it is particularly interesting to discuss the role played by BACH-1/Nrf-2 axis in DS.

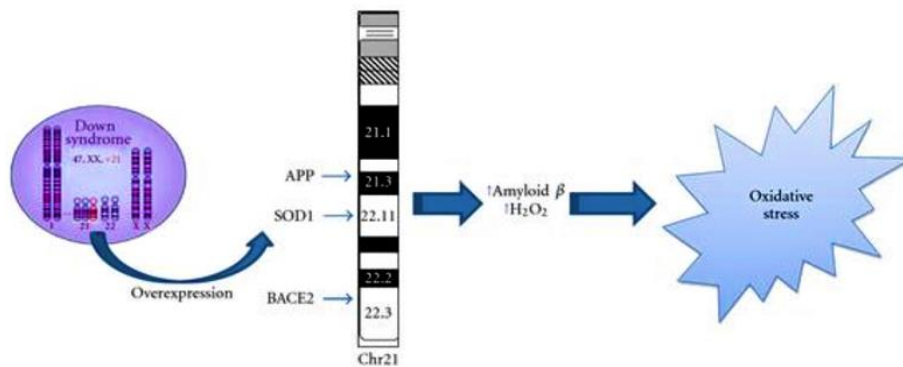


Figure 6. Oxidative stress and down syndrome. Increased conditions of oxidative stress are caused by the overexpression of some of the genes encoded by Chr21. Among these, amyloid precursor protein (APP), copper-zinc superoxide dismutase (SOD1), and beta secretase (BACE2) can directly or indirectly lead to OS.

1.3 BACH-1/Nrf-2 Signalling

Based on the considerations above, it is conceivable that OS occurs in DS pathogenesis and progression due to a dysregulation of gene/protein expression associated with the trisomy. As noted above, OS represents an imbalance between the production of ROS and the ability of a biological system to detoxify the reactive toxic intermediates—the antioxidant response—or to repair the resulting damage.

A prominent sensor involved in the antioxidant response is the Keap1-Nrf2-ARE (Kelch-like ECH-Associating protein 1- nuclear factor erythroid related factor 2-antioxidant response element) signalling complex. The transcription factor nuclear factor erythroid 2-related factor 2 (Nrf-2) mediates induction of multiple antioxidant enzymes through activation of ARE of DNA. Activation of Nrf-2 results in cellular protection by increasing the expression of antioxidant enzymes such as NADPH quinone oxidoreductase 1 (NQO1), heme oxygenase 1 (HO-1), and multiple components of the glutathione pathway. Promotion of this production of antioxidants is therefore a promising mechanism to protect against neurodegeneration. Under normal OS conditions, Keap1, a cysteine-rich protein that senses redox changes in the cell, binds to Nrf-2 leading to retention of Nrf-2 in the cytosol and causing its proteasomal degradation [77, 78]. Under OS, conformational changes in Keap1 lead to its dissociation from the Nrf-2/Keap1 complex and to the translocation of free Nrf-2 into the nucleus, where it binds to ARE regions in the genome, to activate the expression of stress response genes [79]. So far, there is no complete information on Nrf-2/Keap1 genes, protein levels or activities in DS. However, a recent study comparing gene expression profiles in DS and euploid astrocytes found that Nrf-2-associated oxidative stress response genes were differentially

regulated in DS [80]. In addition, a study from Swatton et al. in DS reported that mitogen-activated protein kinases (MAPKs) are highly phosphorylate in DS and AD brains [81], and this result can be linked to the mechanism whereby MAPKs phosphorylate Nrf-2 enabling its dissociation from the Nrf-2/Keap1 complex but preventing its translocation into the nucleus.

Compared to Nrf-2, ARE transcriptional repressors and their roles in DS, AD, and other neurodegenerative disorders have been minimally investigated.

Indeed, a novel hypothesis regards the implication of BACH-1 to compete with the Keap1-Nrf-2-ARE signalling complex. BACH-1 is a member of the Cap “n” Collar and basic region leucine zipper family (CNC-bZip) of transcription factors is encoded on HSA21 and functions primarily as a transcriptional repressor. Human BACH-1 is composed by 736 amino acids: (a) N-terminal region of BACH-1 contains a BTB/POZ domain, which functions as a protein interaction motif; (b) while the C-terminal bZip domain binds to DNA forming heterodimers with small Maf proteins (i.e., MafK, MafF, and MafG) [82]. Once into the nucleus, BACH-1-Maf heterodimers are able to inhibit the transcription of many oxidative stress-response genes. In addition, BACH-1 contains six cysteine-proline (CP) motifs, four of which are located in a heme-binding region near the C-terminus. Heme is able to inactivate BACH-1 by interacting with two of the CP motifs, leading to the exclusion of BACH-1 from the nucleus [83]. Under pro-oxidant condition, nuclear BACH-1 binds heme, changes its conformation, dissociates from ARE and allows transcription factors to bind and activate the expression of oxidative stress-responsive genes [84]. The export of BACH-1 from the nucleus is also the result of its tyrosine phosphorylation, activated by the antioxidant response, (BACH-1 tyrosine 486) [85] and by cadmium, which induces a cytoplasmic localization signal in the BACH-1 C-terminus [86]. After its release in the

cytoplasm, BACH-1 forms fiber-like structures on microtubules in the presence of intracellular hyaluronic acid-binding protein (IHABP), which regulates the subcellular localization of the former [86]. Many of the genes targeted by BACH-1 are in common with the genes regulated by Nrf2 and participate in redox regulation, including HO-1, that is crucial for cell survival upon detrimental oxidative stress conditions. HO-1 expression is negatively regulated by BACH-1 when heme levels are reduced, though higher heme levels are able to inhibit BACH-1-DNA interaction and also promote BACH-1 nuclear export and its subsequent degradation [87]. This event induces HO-1 expression, which in turn degrades heme while releasing antioxidant molecules such as carbon monoxide (CO), and biliverdin. Thus, the BACH-1/HO-1 pathway is considered to act as a feedback loop that regulates heme homeostasis during sustained oxidative stress. Taken together, BACH-1 is believed to displace Nrf-2 from AREs [84] and to act primarily as a transcriptional repressor for antioxidant genes, such as HO-1 [88] and NQO1 [89].

Specifically, BACH-1 competes with Nrf-2 for binding to the AREs in oxidative stress-response genes. In response to OS, Nrf-2 dissociates from Keap1, translocates into the nucleus, and binds to AREs as a heterodimer with Maf, thereby activating oxidative stress-response genes as previously described, while BACH-1 is displaced from AREs and exported out of the nucleus [84] (Fig. 7). A recent study suggests that both the nuclear import of Nrf-2 and the dissociation of BACH-1-ARE are promoted by sirtuin-6 (Sirt6) [90]. Research from Dhakshinamoorthy et al. demonstrated that positive and negative regulation of ARE-mediated gene expression depend on the critical balance between Nrf-2 and BACH-1 in the nucleus. This was clearly evident from the observation that BACH-1 repression of ARE-mediated gene

expression was relieved by co-expression of Nrf-2 with BACH-1, and BACH-1 failed to repress the ARE in cells overexpressing Nrf-2. However, BACH-1 repressed the ARE activation in cells expressing moderate levels of Nrf-2 [89]. Light on these findings, focusing on DS individuals, the triplication of genes (e.g., BACH-1) encoded on HSA21 is directly involved in the appearance of harmful conditions such as increased OS, which we hypothesize over time contributes to the early development of AD pathology in DS individuals. The presence of BACH-1 on HSA21 opens the possibility of seeking new therapies capable of controlling the possible imbalance between Nrf-2 and BACH-1 in the nucleus.

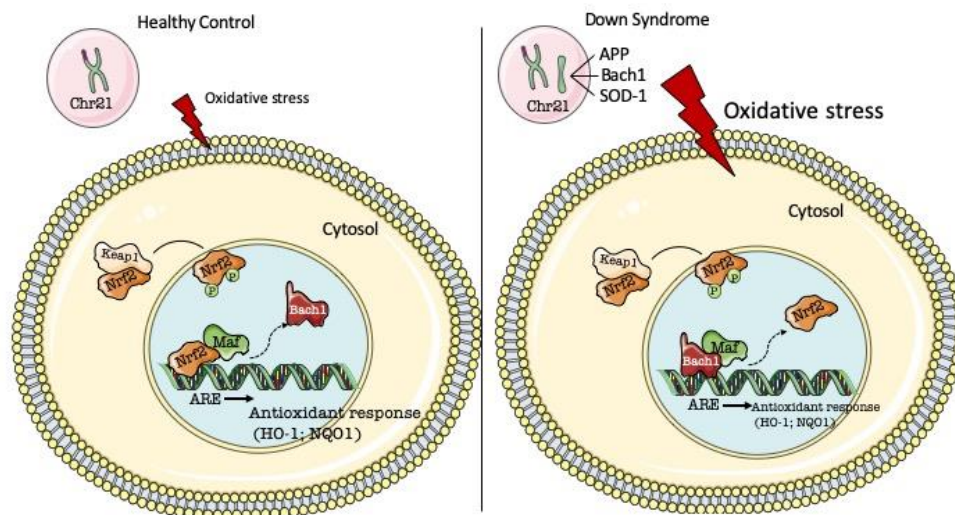


Figure 7. BACH-1/Nrf-2 signaling regulates antioxidant response. Under normal conditions (left), Keap1/Nrf-2 retains Nrf-2 in the cytoplasm. Exposure of cells to oxidative insult leads to the release of Nrf-2 from Keap1/Nrf-2. Nrf-2 then translocates into the nucleus and binds to AREs as a heterodimer with small Mafs, thereby activating oxidative stress-response genes (e.g., HO-1 and NQO1), while BACH-1 is displaced from AREs and exported out of the nucleus. In trisomic cells (DS) (right), triplication of BACH-1 competes with Nrf-2 thus resulting in reduced binding of Nrf-2 to AREs. This event may explain the increased oxidative stress levels

of DS individuals, that is likely the result of compromised induction of antioxidant response.

1.3.1 Involvement of BACH-1 in AD and DS

The evaluation of BACH-1 functions in the brain and particularly in neurodegenerative disorders characterized by a failure of antioxidant responses, represents a novel aspect of DS research. Indeed, only a limited number of studies addressed this topic to date. Studies performed in BACH-1 knock-out mice (BACH-1^{-/-}) showed significantly higher HO-1 mRNA expression levels with respect to control animals in all brain regions studied [91]. Moreover, higher induction of HO-1 was observed around damaged tissues in BACH-1^{-/-} mice [91]. Similar results were collected with regard to spinal cord where HO-1 protein levels were found significantly higher in BACH-1^{-/-} than WT mice either before or after injury [92]. Furthermore, neuronal loss and apoptotic cell death in the injured spinal cord was significantly reduced in BACH-1^{-/-} mice [92]. Thus, as described above, these results confirm that BACH-1 plays an important role in regulating HO-1 expression levels in the central nervous system. The first evidence about a possible involvement of BACH-1 in brain disorders came in 2003 when Shim et al. evaluated levels of BACH-1 protein levels in a small cohort of post-mortem frontal cortex samples collected from DS, AD, and related control individuals to test the hypothesis that DS-phenotype may be due to the overexpression of genes encoded on chromosome 21 [93]. Despite the prevalent hypothesis of a gene-dosage effect in DS, these authors found that BACH-1 protein levels were significantly reduced in DS samples, suggesting that DS features cannot be simply explained by the overexpression of

triplicated genes [93]. However, these findings were revised by the same group published in a subsequent study [94]. In the afore-mentioned work, fetal cortical specimens from DS fetuses and controls (females) from the 18–19th week of gestation were used to evaluate BACH-1 protein levels and levels of one of the targets of BACH-1 activity, i.e., HO-1, among the others [94]. BACH-1 was significantly overexpressed in fetal DS as compared to controls [94], while the levels of HO-1 were found comparable between the two groups [94]. In light of these results these researchers concluded that increased BACH-1 did not lead to decreased HO-1, which would have explained oxidative stress observed in fetal DS [94]. However, we suggest that the above conclusion could be criticized. Considering that HO-1 is inducible, with lower intracellular levels under physiological conditions, HO-1 levels are dynamically responsive to a variety of oxidative and inflammatory stimuli such as heme, A β , H₂O₂, heavy metals, UV light, hyperoxia, prostaglandins, nitric oxide (NO), peroxynitrite, lipopolysaccharide, oxidized lipid products and various growth factors [95-97]. Further, in the adult brain, HO-1 expression in basal conditions is restricted to sparse clusters of neurons and glia [95]. While in the unstressed rodent brain, low-level of HO-1 is observed in scattered neurons of the cerebral cortex, hippocampal dentate gyrus, thalamus, hypothalamus, and cerebellum [98-102]. Hence, reduced HO-1 levels in DS frontal cortex might not be expected. The reason could simply be that increased BACH-1 levels would prevent HO-1 overexpression, which remains at similar levels to those observed in the control group. If considered in this way, no changes observed for HO-1 levels would lead to increased oxidative stress levels in DS brain, since HO-1 is among the first proteins induced to elicit an antioxidant response under conditions of increased oxidative stress levels [103-105]. This hypothesis was further strengthened by proposing a role for BACH-

1 overexpression as one of the causes driving the development of neurodegeneration in DS [53]. Indeed, the expression levels and the ubiquitinylation of BACH-1 were evaluated in post-mortem frontal cortical samples isolated from postmortem DS persons before and after (DS-AD) the development of AD neuropathology, compared to age-matched controls [53]. Moreover, the incident effects of BACH-1 on HO-1 and on its physiological partner biliverdin reductase-A (BVR-A)—both involved in the production of the antioxidant molecule bilirubin [95, 96]—as well as the levels of NQO1, were determined. Results from this study highlighted that BACH-1 protein levels are significantly elevated in DS subjects, either before or after the development of AD [53]. Furthermore, the evaluation of BACH-1 post-translational modifications revealed that BACH-1 mono-ubiquitinylation levels were reduced only in DS, while increased levels of BACH-1 poly-ubiquitinylation were observed only in DS-AD subjects [53]. In parallel, it was observed that neither HO-1 or NQO1 protein levels (both regulated by BACH-1, [88, 89]) were different between DS and age-matched controls, while they were significantly increased in brains from the DS-AD group [53]. Observations collected from DS individuals agree with those previously reported by the group of Lubec and co-workers [94]. Moreover, further studies contributed to extending the knowledge about the regulation of BACH-1 in DS. Indeed, by taking into consideration that mono-ubiquitinylation is involved in modulating protein function, compartmentalization, and interactions, while polyubiquitinylation is a signal for protein degradation [106, 107], collectively, the results suggest that more than the expression levels, the regulation of BACH-1 activity/degradation plays a role in DS and contributes to the explanation of observed changes with regard to HO-1 [53]. Increased BACH-1 protein levels along with reduced BACH-1 mono-

ubiquitinylation would be responsible for the lack of HO-1 or NQO1 increase observed in DS, while increased BACH-1 poly-ubiquitinylation (degradation) would drive the observed increase of HO1 and NQO1 protein levels in DS-AD persons [53]. Increased BACH-1 poly-ubiquitinylation could result from increased oxidative stress levels in DS-AD individuals [53]. Similar analyses performed in a mouse model of DS, i.e., Ts65Dn mice, at different ages further suggest that BACH-1 overexpression results from the triplication of chromosome 21, although the mechanisms associated with BACH-1 regulation appear different between mice and humans [53]. Indeed, the overexpression of BACH-1 was not associated with differences in the ubiquitinylation profile between Ts65Dn and control mice [53].

Studies about the possible involvement of BACH-1 in AD neuropathology mostly rely with *in vitro* analyses. The only report aimed to evaluate levels of BACH-1 in AD brain shows no changes with respect to control subjects [93]. This gap in knowledge about functions of BACH-1 in AD needs to be fulfilled in future studies, particularly in light of the role for HO-1 and reduced antioxidant response in the onset and progression of AD pathology [95, 96, 108]. While HO-1 and NQO1 proteins levels are elevated in AD brain (reviewed in [96, 109]), reduced Nrf-2 activity was reported in a number of studies performed on human and animal samples. Indeed, reduced Nrf-2 nuclear expression in hippocampal samples from AD subjects were observed [110]. Similarly, a failure of Nrf-2-mediated processes in AD mouse models was reported [111-114]. Together, these observations spur the necessity for deeper investigations into a possible role for BACH-1 in AD. A previous study showed that BACH-1 also targets the gene for microtubule-associated protein tau (also known as MAPT)—known to drive AD progression [115]—by repressing its expression [116]. In this context,

Koglsberger et al. reported that BACH-1 expression contributes to molecular gender differences observed in tauopathies and AD and provides a new target for intervention strategies to modulate MAPT expression [117]. Since gender differences may influence the risk for brain disorders and the severity of their phenotypic manifestations, the role for BACH-1 appears of great interest. Indeed, there is evidence of a gender difference in the phenotypic expression of AD in DS. Female middle-aged DS individuals have an earlier onset and a more severe form of AD that correlates with higher neocortical neurofibrillary tangles (NFT) rather than senile plaques (SP) density. Among the in vitro studies that assessed a role for BACH-1 in neuronal injury, Piras et al. evaluated the effects of increased oxidative stress levels, mimicked by H₂O₂, in differentiated SH-SY5Y cells [118]. A striking finding of this work is represented by the fact that in differentiated cells BACH-1 is not displaced from the HO-1 promoter and Nrf-2 is not allowed to bind, while maintaining its ability to sense H₂O₂ moving into the nucleus [118]. In addition, BACH-1 and Nrf-2 mRNA levels were not modified by increased oxidative stress levels, further corroborating the hypothesis that the main regulation of both BACH-1 and Nrf-2 occurs at the post-transcriptional level [118]. These results agree with findings from our group with regard to DS (cited above) and reinforce the hypothesis that the sole evaluation of protein and/or transcripts levels are not sufficient to unravel the molecular mechanisms regulated by BACH-1 (Table 2).

<i>Pathology</i>	<i>BACH-1 changes</i>	<i>References</i>
Down Syndrome (DS)	↑ BACH-1 protein levels in fetal cortical specimens of human DS	<i>Ferrando-Miguel R. . J Neural Transm Suppl, 2003(67): p. 193-205</i> <i>Tili, E., et al., Ann Diagn Pathol, 2018. 34: p. 103-109.</i>
	↑ BACH-1 protein levels in human DS subjects, either before or after the development of AD	<i>Di Domenico, F., et al., J.Alzheimers Dis, 2015. 44(4): p. 1107-20.</i>
	Changes in post-traslational modifications of BACH-1: ↓ mono-ubiquitination of BACH-1 in young DS human brain ↑ poly-ubiquitinylation of BACH-1 only in DSAD subjects	<i>Di Domenico, F., et al., J.Alzheimers Dis, 2015. 44(4): p. 1107-20.</i>
	↑ BACH-1 protein levels in brain of Ts65Dn mice No changes were observed in BACH-1 ubiquitination in Ts65Dn mice compared to euploid mice.	<i>Di Domenico, F., et al., J.Alzheimers Dis, 2015. 44(4): p. 1107-20.</i>
Alzheimer Disease (AD)	NO changes were observed in BACH-1 protein levels in AD brain.	<i>Shim, K.S., R. Ferrando-Miguel, and G. Lubec, J</i>

		<i>Neural Transm Suppl, 2003(67): p. 39-49.</i>
	↑ BACH-1 protein levels in AD Brain using an immunohistochemistry approach	<i>Tili, E., et al., Ann Diagn Pathol, 2018. 34: p. 103-109.</i>

Table 2. Summary of BACH-1 changes in Down Syndrome and Alzheimer's pathology

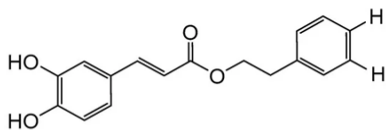
1.4 Caffeic Acid Phenethyl Ester (CAPE) and VP961 and their therapeutical implications

Caffeic Acid Phenethyl Ester (CAPE) is a natural compound obtained from propolis through extraction from honeybee hives. As confirmed by several studies in literature, CAPE has different biological activities: first it is an antioxidant compound, but it has also antimicrobial and anti-inflammatory activities [119]. CAPE is a hydrophobic polyphenolic compound, from the chemical point of view it is formed by three fragments: a catechol ring, responsible of its biological roles, linked to a phenethyl residue, through an α,β -unsaturated carboxyl chain (Fig. 8A) [120]. It is a Michael acceptor compound that reacts with the critical cysteine thiolate groups in Keap1 and subsequently breaks the complex Keap1/Nrf-2 and suppresses Nrf-2 ubiquitination. Thus, CAPE induces the nuclear Nrf-2 translocation and accordingly the expression of ARE mediated antioxidative and cytoprotective enzymes [121], including HO-1. Several studies have demonstrated its anti-inflammatory, antiviral, antioxidant and antitumor properties [122-124]. Its

beneficial effects against neurodegenerative diseases have also been suggested [125, 126]. CAPE is able to protect blood-brain barrier (BBB) in rodent model of traumatic brain injury [127], prevent neonatal hypoxic-ischemic brain injury [125] and attenuate dopaminergic neuronal loss in 6-OHDA Parkinson's model [128]. Scapagnini et al. reported that CAPE is a potent inducer of heme oxygenase-1 (HO-1) in astroglial cells and in neurons [129]. Moreover, its capacity to cross BBB was demonstrated by Silva et al., using parallel artificial membrane permeability assay (PAMPA) [129, 130]. Interestingly, Kumar et al. [131] demonstrated that CAPE administration ameliorated intracerebroventricular (i.c.v.) injection of streptozotocin -induced dementia through the attenuation of oxidative stress and inflammation. Morroni et al. investigate the neuroprotective effect of CAPE, through Nrf-2/HO-1 axis modulation, in a mouse model of AD in which an intraperitoneal administration of CAPE after i.c.v. A β O-injection counteracted oxidative stress induction [132].

To strengthen our research, we aim to investigate in our DS models not only the antioxidant effects of CAPE but we tested also its synthetic analogue. VP961 is a synthetic analogue of CAPE (Fig. 8B), synthesized by the Department of Drug Sciences of Catania University; Pittalà et al. tested VP961 focusing on the HO-1 induction. Their preliminary data demonstrated the antioxidant property of VP961 and its ability induce the HO-1 expression and activity, better than CAPE in Human Mesenchymal Stem Cells (hMSCs) [120].

A. CAPE



B. VP961

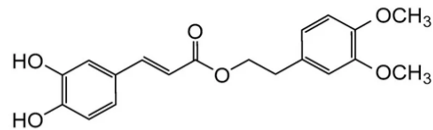


Figure 8. Chemical structures of CAPE (A) and VP961 (B).

Pittalà et al. [133], also investigated the potentially protective effects of CAPE and VP961 as heme oxygenase-1 (HO-1) inducers, in reducing pancreatic oxidative damage induced by excessive amount of glucose, in streptozotocin-induced type 1 diabetic rats. Their data demonstrated that CAPE and VP961 may be useful in diabetes and other stress-induced pathological conditions.

2. AIMS OF THE WORK

Several studies support the implication of oxidative stress (OS) in several phenotypical alterations of DS individuals; [23, 58, 59] however, the mechanisms through which OS damage leads to DS pathological phenotypes need to be clarified. The OS seems to be a chronic condition in DS brain and it can represent a strong risk factor for neurodegeneration [60, 61]. The mapping of HSA21 has been an aid to better understand the cause of OS in DS brain. This investigation showed several genes such as SOD-1, BACH-1, APP, CBR and S100B directly involved in the over-production of ROS in DS individuals and animal models [62].

The role of BACH-1 functions in the brain and its implication in the failure of anti-oxidant response - which can contribute to neurodegeneration- represents a novel aspect of DS research. Moreover, a number of studies demonstrated the importance of the balance between BACH-1 and Nrf-2 in the nucleus [89] to finely tune the anti-oxidant response.

In this scenario, we aimed to investigate BACH-1/Nrf-2 pathway and their related protein targets, including HO-1 and NQO1, to better understand if dysregulation of this axis plays a role in DS pathology. To achieve this goal, we have analyzed different DS models: (a) neurons and astrocytes isolated from cortex and hippocampus of Ts2cje mice, an animal model of DS; (b) hippocampus from Ts2cje mice at 3 months of age and (c) human DS lymphoblastoid cell lines (LCLs). On these selected models, we investigated if *bach-1* triplication would impair BACH-1/Nrf-2 axis and in turn downregulate the antioxidant responses.

In addition, we tested two compounds, CAPE and VP961, already proved to be anti-oxidant molecules that are able to act as inducers of Nrf-2 [120, 133]. The goal is to evaluate the ability of these two compounds to modulate BACH-1/Nrf-2 pathway, proposing them as a powerful strategy to restore OS conditions in DS.

In order to better understand the role of OS in DS pathology in the second project, we aimed to perform a comparative proteomic analysis on PBMCs from HD and DS young patients, to identify the pathway and the related proteins altered in DS PBMCs compared with HD. We focused our research to investigate the implications of these alterations on the increased OS in DS individuals that may confer them the characteristic features of the pathology. The aim of this second work is also to identify putative biomarkers for the early detection and exploration of the disease mechanisms.

3. MATERIALS AND METHODS

PROJECT 1

3.1 Materials (CAPE and VP961)

CAPE (Caffeic Acid Phenethyl Ester) and VP961 has been synthesized by the Department of Drug Sciences of Catania University [120]. In the table below all the chemical characteristics of the drugs has been reported (Table 3).

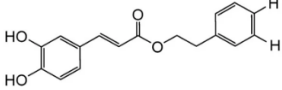
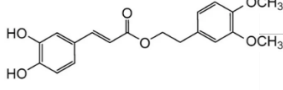
	CAPE	VP961
		
Molecular Formula	C ₁₇ H ₁₆ O ₄	C ₁₉ H ₂₀ O ₆
Molecular Composition	C=71,8%; H=5,7%; O=22,5%	C=66,27%; H=5,85%; O= 27,88%
Molecular Weight	284,30654	344,37
Exact Mass	284,10846	344
ALogP	3,5739	
Hydrogen Acceptor Count	4	
Hydrogen Donor Count	2	

Table 3. Chemical Characteristics of CAPE and VP961

3.2 Mouse colony

The mouse model used are Ts2Cje mice (Rb(12.Ts171665Dn)2Cje) and euploids animals (B6EiC3SnF1). Ts2Cje are a well-established murine model of DS characterized by a triple copy of a Robertsonian fusion chromosome carrying the distal end of Chr16 and Chr12. Parental generations were purchased from Jackson Laboratories (Bar Harbour, ME, USA). Mouse colony was raised by repeated crossbreed of Ts2Cje (Ts2) trisomic females with euploid (Eu) males. Since these breeding pairs produce litters containing both trisomic and euploid offspring, resultant progeny was genotyped to determine the presence of the trisomic segment using Quantitative-PCR, as previously described by Reinholdt et al. [134]. Mice were housed in clear Plexiglas cages (20 x 22 x 20 cm) under standard laboratory conditions with a temperature of $22 \pm 2^{\circ}\text{C}$ and 70% humidity, a 12-h light/dark cycle and free access to food and water. Ts2 and Eu mice were sacrificed by cervical dislocation at 3 months of age (n=5/groups) and the hippocampus was collected and frozen at -80°C . The samples were then used for Western Blot analysis and qRT-PCR.

3.3 Cell Cultures

3.3.1 SHSY-5Y (experimental design)

The human neuroblastoma cells SHSY-5Y were grown in Dulbecco's Modified Eagle Medium F-12, supplemented with Fetal Bovine Serum 10%, L-glutamine (200mM solution) 1% and a mixture of

penicillin-streptomycin solution 1% (200mM). First, the SHSY-5Y cells were plated in 96 well-culture dishes, at density of 30000 cells/well to perform a viability assay (MTT Assay) to select CAPE and VP961 concentrations able to protect the cells against oxidative stress induced by H₂O₂ and to use for the following experiments. The neuroblastoma cells were seeded at density of 100 x 10³ in 24 well-culture dishes for total proteins and mRNA extraction and at density of 300 x 10³ in 12 well-culture dishes for nuclear and cytosolic proteins extraction. These experiments were based on a pre-treatment with CAPE and VP961 (5uM) for 2h, thereafter, the medium was discarded and rechallenged with DMEM F-12 containing or not H₂O₂ 100uM for 4h (Fig. 9).

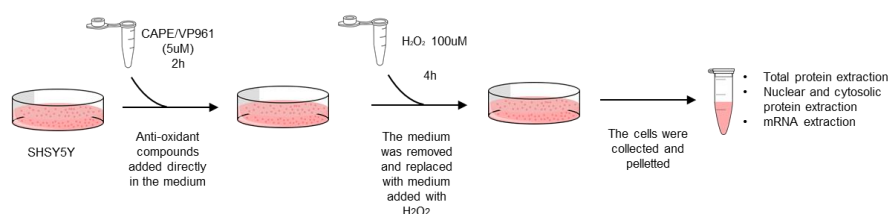


Figure 9. Schematic representation of SHSY-5Y treatment. Neuroblastoma cells were plated at an appropriate density in 24 or 12 well-culture dishes, after 24h SHSY-5Y were pre-treated with CAPE and VP961 (5uM) for 2h, then the medium was discarded and rechallenged with new DMEM-F12 containing or not H₂O₂ (100uM) for 4h. At the end of the treatment the cells were collected for subsequently use: totale protein, nuclear and cytosolic protein extraction and mRNA extraction.

3.3.2 LCLs (experimental design)

Lymphoblastoid cell lines (LCLs), immortalized using the Epstein-Barr virus [135], were obtained from a subset of PBMCs samples collected from Down syndrome (DS, n = 3) and Healthy Donors (HD, n = 3) (Table 4). For the DS LCLs the diagnosis of trisomy 21 was confirmed by karyotyping; individuals carrying a Robertsonian translocation or chromosome 21 mosaicism were excluded. The LCLs, non-adherent cells, were cultured in RPMI 1640 medium containing L-glutamine, 20% FBS, and 1% antibiotic. The study was approved by the Ethical Committee of Bambino Gesù Children Hospital in Rome, Italy (protocol # 1771_OPBG_2019). LCLs were seeded at density of 10×10^5 in 12 well-culture dishes for total proteins, nuclear and cytosolic proteins extraction and mRNA extraction. A viability assay (MTT) was used to detect the exact concentrations of CAPE and VP961 and time of treatment for the following experiment. HD and DS LCLs were treated with 10uM of CAPE and 5uM of VP961 for 6h.

Samples	n.	Gender (m/f)	Age (years) (avg \pm SD)
HD LCLs	3	2/1	9 \pm 3.0
DS LCLs	3	2/1	7 \pm 2.3

Table 4. Human Samples characteristics: number, gender and age are reported.

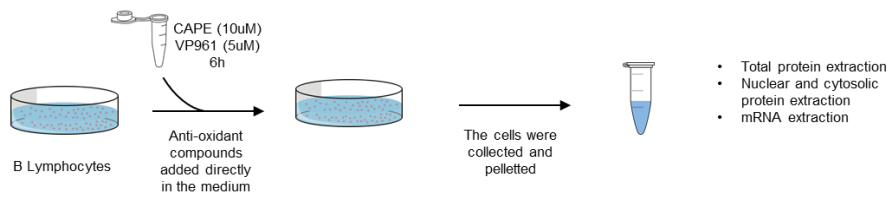


Figure 10. Schematic representation of LCLs treatment: the cells were seeded at an appropriate density in 12 well-culture dishes. After 24h were treated with 10uM of CAPE and 5uM of VP961 for 6h; there the LCLs were collected for subsequently use: total protein, nuclear and cytosolic extraction and mRNA extraction.

3.3.3 Primary cell cultures

For primary cell cultures, Ts2cje pups at 0-1 post-natal day (PND) has been used to isolate neurons and glial cells. Brain has been dissected and cortex (Cx) and hippocampus have been isolated to obtain neurons and astrocytes from Euploid and Ts2cje mice. Before brain dissection, all mice have been genotyped to process Euploid and Ts2cje separately.

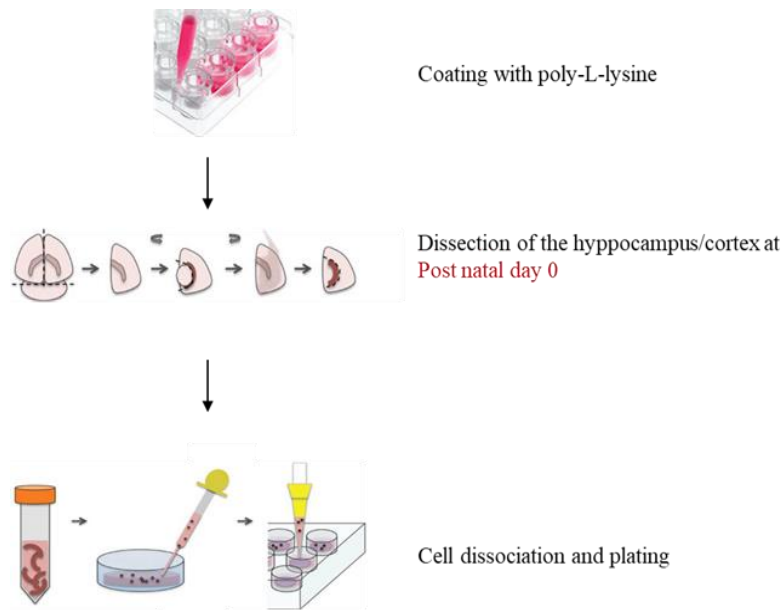


Figure 11. Schematic representation of primary cells isolation: brain from *Ts2cje* pups, after genotyping process to differentiate *Eu* and *Ts2cje* mice, has been dissected and cortex and hippocampus have been isolated. Using specific protocol and culture medium neurons and astrocytes were isolated.

Astrocytes: Cortex (cx) and hippocampus (hip) were mechanically dissociated in cold PBS (with Ca^{2+} and Mg^{2+}), followed by a chemical dissociation using Trypsin solution at 0.25% at 37°C for 20 minutes. The cells have been resuspended in of Dulbecco's Modified Eagle Medium High Glucose completed with FBS 10% and antibiotics. The cells were plated in 75-cm² flasks (1 brain/flask). The culture medium was changed within 24 h, and then twice a week until the astrocytes were grown to form a monolayer. At this time, the culture medium was replaced with PBS- without Ca^{2+} and Mg^{2+} and the flasks were vigorously shaken to remove non-adherent cells, oligodendrocytes and microglia. Subsequently, astrocytes were detached from the flask by a 5- min 0.05% trypsin–EDTA

treatment. Astrocytes obtained with this procedure were then sub-cultured twice, the first time in 75-cm² flasks and the second time directly in multi-well plates used for the experimental procedures, carried out in 1% FCS DMEM.

Neurons: cortex (cx) and hippocampus (hip) were mechanically dissociated in cold PBS (with Ca²⁺ and Mg²⁺) and centrifuged (3 minutes, 1100 rpm, 25°C). The supernatant was removed and a solution with PBS (w/o Ca²⁺ and Mg²⁺) with Trypsin 0,25% was added for 15 minutes for chemical dissociation and at the end the cells were centrifuged for 3 minutes at 1100 rpm at room temperature. The cells were, then, resuspended in MEM 1 medium* and centrifuged to 10 minutes, 1100rpm, 25°C. After centrifugation, the cells were resuspended in MEM2 medium**and plated in multi-well coated with poly-L-lysine. The cell medium has been replaced with Neurobasal medium 1*** after 24 hours to start the neurons differentiation, and then with Neurobasal medium 4**** after 4 days. The details of all medium used for neurons isolation have been listed below. After 8-10 days from the cell plating the neurons can be used for the experimental procedure.

LIST OF MEDIUM COMPOSITION FOR NEURONS DIFFERENTIATION:

***MEM1:** Minimum Essential Medium supplemented with FBS (1%), L-glutamine 200mM (1%), glucose 25mM (1%), Gentamycin 0,1mg/mL (1%);

****MEM2:** Minimum Essential Medium supplemented with FBS (5%), human serum (5%), L-glutamine 200mM (1%), glucose 25mM (1%), gentamycin 0,1mg/mL (1%);

*****NEUROBASAL 1:** Neurobasal Medium supplemented with B27 (2%), L-glutamine 200mM (1%), gentamycin 0,1g/mL (1%);

******NEUROBASAL 4:** Neurobasal Medium supplemented with B27 (2%), gentamycin 0,1mg/mL (1%).

3.4 MTT Assay

The viability of SHSY5Y and of LCLs from DS and HD was assessed using the MTT [-3(4,5-dimethylthiazol-2-yl)-2,5-diphenyltetrazolium bromide] reduction assay. SHSY5Y (30000 cells/well) and LCLs (50000 cells/well) were seeded in a 96-well plate in a final volume of 100 μ L/well. For SHSY5Y at the end of the treatment the medium was removed and the MTT solution (5mg/mL) was added to each well followed by 2h incubation at 37°C. Since LCLs are cells in suspension, at the end of the treatment MTT solution (5 mg/mL) was added directly to each well, followed by 4 h incubation at 37°C. The final concentration of MTT solution is 0,5mg/mL. Afterwards in order to dissolve the dark-coloured formazan crystals produced by reduction of the MTT tetrazolium salt, was added to each well a solution based on isopropanol supplemented with NP-40 0,1% and HCl 0,4M. The optical density of reduced MTT was measured at 570 nm with a reference wavelength at 690 nm using Appliskan Microplate Reader (Thermo Scientific, Waltham, MA, USA).

3.5 Nuclear and cytosolic proteins extraction

After the treatment the cells were washed in PBS, harvested and pelleted by centrifugation at 2700 rpm, 5 minutes at 4°C, the pellet obtained was washed with PBS. Subsequently the cells were resuspended in cell lysis buffer (HEPES 10mM pH 7,5, KCl 10mM, EDTA 0,1mM, DTT 1mM, NP-40 0,5%) with added protease and phosphatase inhibitors, and then allowed to swell on ice for 15-20 minutes with intermittent mixing. The samples were vortexed to disrupt the cell membranes and so centrifugated at 12000 rpm for 10 minutes at 4°C. The supernatant obtained contained the cytoplasmatic proteins and it was collected at -80°C. The pelleted nuclei were washed three times with the cell lysis buffer (centrifugation for each wash: 12000 rpm for 10 minutes at 4°C) and then resuspended in nuclear extraction buffer (HEPES 20mM pH 7,5, NaCl 400mM, EDTA 1mM, DTT 1mM) supplemented with protease and phosphatase inhibitors, and incubated on ice for 30 minutes. By centrifugation at 12000 rpm for 15 minutes at 4°C the nuclear extract is collected and then stored at -80°C. Both cytoplasmic and nuclear extracts were used to determine the total protein concentration by the BCA method (Pierce, Rockford, IL, USA).

3.6 Protein extraction and Western Blot

Cells and Tissues from Ts2cje and Euploid mice were homogenate in RIPA buffer (pH 7.4) containing 50mM Tris-HCl (pH 7.4), 150 mM NaCl, 1% NP-40, 0.25% sodium deoxycholate, 1 mM EDTA, 0,1% SDS, protease inhibitor cocktail, phosphatase inhibitor cocktail. All the experiments have

been conducted on a specific brain region, hippocampus. The samples were homogenized by 20 strokes of a Wheaton tissue homogenizer, sonicated, and centrifuged at 14 000 rpm for 40 minutes at 4°C to remove debris. Supernatant was collected and total protein concentration was determined by the BCA method according to manufacturer instructions. For western blot analysis, 15 μ g of proteins were separated via SDS-PAGE using Criterion™ TGX Stain-Free™ precast gel (Bio-Rad) and transferred to a nitrocellulose membrane by Trans-Blot Turbo Transfer System (Bio-Rad). The blot was imaged by ChemiDoc MP imaging system (Bio-Rad) using the Stain-Free Blot settings. Protein total load captured by Stain-Free technology was later used for total protein normalization. Following, nitrocellulose membrane was blocked using 3% BSA in 1X Tris Buffer Saline containing 0.01% Tween20 and incubated overnight at 4°C with the following primary antibodies: APP (1:5000; SAB5200113, Sigma-Aldrich); HO-1 (ADISPA 896F, Enzo; 1:1000), NQO1 (MA515926, Invitrogen; 1:1000), Nrf-2 (GTX 103322, GeneTex; 1:1000), pNrf-2 (Ser40) (ab76026, Abcam, 1:5000); BACH-1 (orb4401, biorbyt, 1:1000), b-actin (SC4778, Santa Cruz, 1:1000), lamin A/C (SC376248, Santa Cruz, 1:500), Polymerase II (SC47701, Santa Cruz, 1:1000), NeuN (14H6L24, Invitrogen, 1:500). Next day, all membranes were washed with 1X TBS containing 0.01% Tween20 and incubated at room temperature for 1-hour with respective horseradish peroxidase-conjugated secondary antibodies: anti-rabbit (1:10000; L005661, Bio-Rad Laboratories), anti-mouse (1:10000; L005662, Bio-Rad Laboratories). Blots were then imaged via the ChemiDoc MP imaging system using Chemiluminescence settings. Subsequent determination of relative abundance via total protein normalization was calculated using Image Lab 6.1 software (Bio-Rad Laboratories).

3.7 mRNA extraction

RNA was extracted from tissues and cells. In detail, RNA has been obtained: (a) from hippocampus of Ts2cje and Euploid mice at 3 months of age, (b) from neurons and astrocytes of Ts2cje and Euploid mice, (c) from LCLs and (d) from SHSY-5Y after treatment with CAPE and VP961.

Tissues and cells were lysed with an appropriate volume of Trizol Reagent and then incubated for 5 minutes at room temperature. Then, the chloroform was added for 3 minutes to the samples (V=20% of the Trizol Reagent volume) and all samples were centrifuge for 15 minutes (12000rpm, 4°C). To separate RNA, isopropanol was added to each sample and they were incubated at room temperature for 10 minutes. After isopropanol incubation, all samples were centrifugated for 15 minutes (12000rpm, 4°C). At the end of the centrifuge, the supernatant was discarded and the pellet has been washed with EtOH 75% (5 minutes, 7500rpm, 4°C). The samples has been resuspended in H₂O RNase free.

3.8 Reverse Transcription and Quantitative Real Time PCR

The RNA obtained was quantified using the Biospec Nano spectrophotometer (Shimadzu, Columbia, MD, USA), and RNA was reverse transcribed using the cDNA High Capacity kit (Applied Biosystems, Foster City, CA, USA), including reverse transcriptase, random primers and buffer according to manufacturer's instructions. The cDNA was produced through a series of heating and annealing cycles in the MultiGene OPTIMAX 96-well Thermocycler (LabNet International, Edison, NJ, USA).

Real time PCR (Q-PCR) was carried out using the following cycling conditions: 35 cycles of denaturation at 95°C for 20 s; annealing and extension at 60°C for 20 s, using the SensiFAST™ SYBR® No-ROX Kit (Bioline, London, UK). PCR reactions were carried out in a 20 µl reaction volume in a CFX Connect Real Time PCR machine (Bio-Rad Laboratories). Primers used for the RT-PCR are listed in Table 5 for mice samples and Table 6 for human sample.

Gene product	Forward primer (5'-3')	Reverse primer (5'-3')
APP	TGCTGAAGATGTGGGTTCTGA	GACAATCACGGTTGCTATGACAA
BACH-1	GAGTGAGTCACCTGACCGCC	TTGAGGCTGAGCAAGACGTT
NRF-2	CGCTGGAAAAGAAGTGGGC	GTGACAGGTCACAGCCTTCA
HMOX1	GGCTTAAGCTGGTGATGGC	TCTCTGCAGGGGCAGTATCT
NQO1	CCGATTCAGAGTGGCATCCT	GAGCAATTCCTTCTGCCCT
GAPDH	ACAGTCCATGCCATCACTGCC	GCCTGCTTACCACCTTCTTG

Table 5. Mouse primer used for qRT-PCR.

Gene Product	Forward primer (5'-3')	Reverse primer (5'-3')
APP	TGGCCAACATGATTAGTGAACC	AAGATGGCATGAGAGCATCGT
BACH-1	TGCAGCAGTTACTTCCAACAA	GTTTAGCAGTGTAGGCAAAC GAAT
NRF-2	ACACGGTCCACAGCTCATC	TGCCTCAAAGTATGTCAACTA
HMOX1	AGGGAATTCTTTGGCTGGC	GACAGCTGCCACATTAGGGT
NQO1	CGCAGACCTTGTGATATTCCAG	CGTTTCTCCATCCTTCCAGG
GAPDH	GACAGTCAGCCGCATCTTCT	TTAAAAGCAGCCCTGGTGAC

Table 6. Human primer used for qRT-PCR.

3.9 Immunofluorescence and confocal microscopy

The cells were plated on coverslips and, after the treatment, were fixed with 4% paraformaldehyde and washed three times with filtered PBS 1X. Then the coverslips were incubated for 30 minutes at room temperature with the permeabilization buffer (PBS 1X added with 0,2% Triton X-100). Afterwards 3 washes in PBS 1X the glasses were blocking for 1h at room temperature with the blocking buffer solution (PBS 1X added with Normal Goat Serum 5% and Triton X-100 0,3%). Cells were then incubated with Nrf-2 (GTX 103322, GeneTex; 1:200) primary antibody overnight at 4°C. The coverslips were then washed with PBS 1X three times and incubated with Alexa Fluor -488 nm secondary antibodies (1:1500; A11029, Invitrogen ThermoFisher Scientific) for 1-hour and a half at room temperature in the dark. Slides were then washed, incubated with DAPI (10 mg/mL) for 1 minute and washed again. At the end cover slip glasses were placed using a drop of Fluorimount aqueous mounting medium and glasses were kept at room temperature to dry. All coverslips were imaged using Zeiss AXio (Carl Zeiss, Oberkochen, Germany). All immunolabeling acquisition intensities, field sizes, and microscopy settings were kept consistent across all images. Images were analyzed using ImageJ.

To better define the Nrf-2 nuclear translocation all coverslips were imaged using the confocal microscopy. Confocal microscopy was performed on a Leica TCS-SP8X laser-scanning confocal microscope (Leica Microsystems, Mannheim, Germany) equipped with tunable white light laser (WLL) source, 405 nm diode laser, 3 Internal Spectral Detector Channels (PMT) and 2 Internal Spectral Detector Channels (HyD) GaAsP. Sequential confocal images were acquired using a HC PL APO CS2 40x

oil-immersion objective (1.30 numerical aperture, Leica Microsystems) with a 1024x1024 format, scan speed 400Hz, with an electronic zoom magnification up to 3x. Z-reconstructions were obtained from z-step size of 0.5 μm with an electronic zoom up to 4.4x. Maximum intensity projection (MIP) of z-series were obtained by LAS X (Leica Microsystems) software.

3.10 Statistical analysis

Statistical analyses were performed using Student t test for the evaluation of differences between 2 groups and a non-parametric 1-way ANOVA with *post-hoc* Bonferroni t-test for the evaluation of differences between more than two groups. Data are expressed as mean \pm SEM per group. All statistical analyses were performed using Graph Pad Prism 8.0 software (GraphPad, La Jolla, CA, USA).

PROJECT 2

3.11 Study population

For this study, we recruited individuals referring from the Down Syndrome and Pediatric outpatient Clinic of Bambino Gesù Children's Hospital in Rome. All the study participants underwent complete clinical workup including medical history collection, clinical examination, anthropometric measurements and laboratory test. In Table 7 are listed all the

clinical data of the subjects, Healthy Donors (HD) and Down Syndrome (DS), enrolled in the study including gender, age of participants, their body mass index calculated [BMI; weight (kg) \times squared height (m²)], and comorbidities; for children under the age of 2 years old we did not calculate the BMI but the ratio between weight/height and the relative's centile. The study was approved by the Ethical Committee of Bambino Gesù Children Hospital in Rome, Italy (protocol # 1771_OPBG_2019).

Subject	Diagnosis	Age	Sex	BMI	Centile	Comorbidities
HD 1	Healthy Donors	2	F	n/a	96	Asthma
HD 2	Healthy Donors	14	F	19.8	54	Rash
HD 3	Healthy Donors	9	F	17.6	68	Abdominal pain
HD 4	Healthy Donors	4	M	15.7	54	Kawasaki disease
HD 5	Healthy Donors	8	F	20	93	Headache
HD 6	Healthy Donors	3	M	16.2	49	Kawasaki disease
HD 7	Healthy Donors	12	M	19.6	54	Abdominal pain
HD 8	Healthy Donors	7	F	20	92	Headache
DS 1	Down Syndrome	6	M	14.9	9	Behavioral trouble
DS 2	Down Syndrome	4	M	20.6	40	CAV surgery, behavioral trouble
DS 3	Down Syndrome	5	M	17.5	64	sleep apnea
DS 4	Down Syndrome	17	F	24.5	35	leukopenia
DS 5	Down Syndrome	1	F	21.9	48	hypothyroidism
DS 6	Down Syndrome	1	F	n/a	0	prematurity
DS 7	Down Syndrome	1	F	n/a	31	FPIES
DS 8	Down Syndrome	3	F	16.1	35	FPIES

Table 7. Clinical characteristics of Down syndrome (DS) and healthy donors (HD) individuals

3.12 Sample collection of Peripheral Blood Mononuclear Cells from HD and DS Subjects

Peripheral blood mononuclear cells (PBMC) were isolated from DS and healthy donors (HD) blood samples. For the isolation of PBMC, ACD-A-anticoagulated blood was centrifuged at 800× g for 30 min and the top layer containing the plasma was removed. The remaining blood was diluted with an equal volume of phosphate-buffered saline, pH 7.4 (PBS), containing 0.05 M ethylenediaminetetraacetic acid (EDTA). Total of 12.5 mL of diluted blood was layered over 25 mL of the Ficoll-Paque PLUS (GE Healthcare, Chicago, IL, USA). Gradients were centrifuged at 400× g for 30 min at room temperature in a swinging-bucket rotor without applying brake. The PBMC interface was prudently removed by pipetting and washed with PBS-EDTA by centrifugation at 250× g for 10 min. PBMC pellets were suspended in ammonium-chloride-potassium (ACK) lysing buffer (Invitrogen Corporation, Carlsbad, CA, USA) and incubated for 10 min at room temperature with gentle mixing to lyse the contaminating red blood cells (RBC), then washed with PBS-EDTA. Cell number and viability were determined using a countess automated cell counter (Invitrogen Corporation, Carlsbad, CA, USA). Non-viable cells were identified by staining with trypan blue, and cell viability was calculated using the total cell count and the count of non-viable cells. PBMCs were cryopreserved in liquid nitrogen in fetal calf serum (FCS) containing 10% dimethyl sulfoxide (DMSO) and stored until required for downstream analyses.

3.13 Protein Sample extraction

The total protein extract from PBMCs was prepared in RIPA buffer (pH = 7.4) containing tris-HCl (50 mM pH = 7.4), NaCl (150 mM), 1% NP-40, 0.25% sodium deoxycholate, 1 mM EDTA, 0.1% SDS, supplemented with phosphatase and protease. Before clarification, the samples were sonicated on ice and then centrifuged at $16,000 \times$ rpm at 4 °C for 30 min to remove cellular debris. The supernatant was then used to determine the total protein concentration by the BCA method.

3.14 Protein Expression Analysis by nLC–HDMSE

Briefly, protein extracts derived from peripheral blood mononuclear cells (PBMCs) isolated from 6 DS subjects and 6 healthy donors (HD) blood samples were handled for enzymatic digestion according to the filter-aided sample preparation (FASP) protocol [136]. Briefly, as shown below the following steps were performed using filter tubes (Nanosep centrifugal device with Omega membrane-10 K MWCO): reduction (DTT 8 mM in urea buffer- 8 M urea, and 100 mM Tris), alkylation (IAA 50 mM in urea buffer 8 M urea, and 100 mM Tris), and trypsin digestion (final trypsin concentration of 0.01 $\mu\text{g}/\mu\text{L}$). Label-free proteomic analysis was performed, as previously described by Greco V et al. [137] with few modifications. First, 300 fmol/ μL of digested enolase from *Saccharomyces cerevisiae* (P00924) was added to each sample as an internal standard. Each digested sample (0.25 μg) was loaded onto a Symmetry C18 5 μm , 180 $\mu\text{m} \times$ 20 mm pre-column (Waters Corp., Milford, MA, USA), and was subsequently separated by a 120-min reversed-phase

gradient at 300 nL/min (linear gradient, 2–40% ACN over 90 min) using a HSS T3 C18 1.8 μm , 75 μm \times 150 mm nanoscale LC column maintained at 40 °C. Tryptic peptides were separated on an ACQUITY MClass System and then separated peptides were analyzed using a high-definition Synapt G2-Si mass spectrometer directly coupled to the chromatographic system. Differential protein expression was evaluated by a high-definition expression configuration mode (HDMSE), a data-independent acquisition (DIA) protocol where ion mobility separation (IMS) is integrated into LC-MSE workflow as described by Marini F. et al. [138]. The mass spectrometer parameters are set as: positive survey polarity of electrospray source (ES+), acquisition mode mass range 50–2000 m/z, capillary source voltage 3.2 kV, source T 80°C, cone voltage 40 eV, TOF resolution power 20,000, precursor ion charge state 0.2–4, trap collision energy 4eV, transfer collision energy 2eV precursor MS scan time 0.5 sec, and fragment MS/MS scan time 1.0 sec. All spectra have been acquired in ion mobility separation mode (IMS) cycles with wave height at 40 V, wave velocity of 650 m/s, transfer wave height 4 V, and transfer wave velocity of 175 m/s. Data were post-acquisition lock mass corrected using the doubly charged monoisotopic ion of [Glu1]-Fibrinopeptide B, sampled every 30 s. Each sample was run in four technical replicates. The analysis of differentially expressed proteins was performed according to Silva et al. [139] and Visser et al. [140]. Continuum LC-MS data from the four analytical replicates for each sample derived from both DS and HD PBMC were processed for qualitative and quantitative analysis using the ProteinLynx Global Server v3.0.3 software (PLGS). The qualitative identification of proteins was obtained using the embedded ion accounting algorithm of the software PLGS and by searching against Homo Sapiens database (UniProt KB/Swiss-Prot Protein Knowledgebase restricted to homo sapiens taxonomy) to which the sequence

from *Saccharomyces cerevisiae* Enolase (UniProtKB/Swiss-Prot AC: P00924) was appended. In order to obtain protein identifications, the PLGS software Search parameters include: automatic tolerance for precursor ions and for product ions, minimum 1 fragment ion matched per peptide, minimum 3 fragment ions matched per protein, minimum two peptide matched per protein, 2 missed cleavage, carbamydomethylation of cysteines and oxidation of methionine as fixed and variable modifications respectively. The identification of protein was based on the detection of more than two fragment ions per peptide, and more than two peptides measured per protein. False discovery rate (FDR) of the identification algorithm was set under 1%, based on a target decoy database. For quantitative expression analysis 300 fmol of Enolase has been set as calibration protein concentration. PLGS software uses the most reproducible proteotypic peptides for retention time and intensity of Enolase digestion (m/z 745.43, m/z 814.49, m/z 1288.70, m/z 1416.72, m/z 1578.80, and m/z 1840.89) to normalize the table of the exact mass on retention times (EMRTs). The expression analysis was performed considering two experimental groups, DS and HD, which include all the technical replicates derived from each sample (i.e., experimental condition, DS and HD: six biological samples \times four technical replicates) following the hypothesis that each group was an independent variable (DS and HD). The differentially expressed proteins dataset was screened and filtered according to the following MS established criteria by considering only those identifications from the alternate scanning LC-HDMSE data exhibiting a good replication rate (at least three out of four runs of the same sample) and with $p < 0.05$ for the relative protein fold change (two-tailed Student's t test). The significance of regulation level specified with a fold change of regulation higher than $\pm 30\%$, which is typically 2–3 times higher than the estimated error on the intensity

measurement, was used as a threshold to identify significant up- or down-regulation.

3.15 Bioinformatics and network analysis

To identify the biologically relevant molecular pathways, the proteomic datasets were analyzed using bioinformatic analysis tools based on QIAGEN'S Ingenuity Pathway Analysis (QIAGEN'S Ingenuity Pathway Analysis, Ingenuity Systems, <http://www.qiagen.com/ingenuity>) and STRING. Relevant functional associations have been explored. The analysis parameters were set as follows: direct and indirect relationships, endogenous chemical substances included all molecules, and/or relationships considered as the summary filter. The most significant categories associated with the loaded datasets were identified by calculating their significance (p-value, Fischer test). A p-value threshold was set at 0.05, which showed the probability of association between genes/proteins present in the datasets and each pathway (canonical pathway, and biological function).

3.16 Western Blot

All the western blot experiments were conducted as described in 'Material and Methods' of Project 1. The primary antibodies used in this project are: PRDX6 (A305-315A-M Bethyl, 1:1000), Gelsolin (sc-398244; Santa Cruz Biotechnology, Dallas, TX, USA; 1:500), and SOD-1 (sc-271014; Santa Cruz Biotechnology, Dallas, TX, USA; 1:500).

3.17 Slot Blot analysis and Protein Carbonylation

Protein carbonyls was used as a marker of protein oxidation and their levels were determined as described by Butterfield et al. [141]. Total of 5 μ L from PBMCs samples was derivatized at room temperature for 20 min in 10 mM DNPH and 5 μ L of 12% sodium dodecyl sulphate (SDS). Samples were than neutralized with 7.5 μ L of neutralization solution (2 M tris in 30% glycerol). The derived samples (250 ng) were then blotted onto a nitrocellulose membrane under vacuum pressure using a slot-blot apparatus (Bio-Rad, Hercules, CA, USA). Membranes were blocked for 1 h at room temperature with 3% of BSA in 1X tris buffer saline containing 0.01% Tween 20 and incubated for 2 hours at room temperature with a 1:1000 dilution of rabbit polyclonal anti-DNP primary antibody. Then, membranes were washed three times with 1X tris buffer saline solution containing 0.01% Tween 20 (T-TBS) and incubated for 1 h at room temperature with the respective alkaline phosphatase secondary antibodies from Sigma-Aldrich (1:10,000 dilution of anti-rabbit IgG alkaline phosphatase). The membranes were later washed three times in T-TBS and developed with a solution of nitro-tetrazolium blue chloride (0.2 mM) and 5-bromo-4-chloro-3-indolyl phosphate dipotassium (0.4 mM) in ALP buffer (0.1 M Tris, 0.1 M NaCl, 5 mM MgCl₂; pH 9.5). Blots were dried, acquired with Chemi-Doc MP imaging system Bio-Rad Laboratories, Hercules, CA, USA, # 17001402) and analyzed using Image Lab 6.0 software (Bio-Rad, Hercules, CA, USA).

3.18 Statistical analysis

For proteomics analysis six samples were employed for each group. As previously described [142], sample size was calculated using G-Power 3.1 software using the following parameters: Effect size = 2.5; Err- prob = 0.05; Power = 0.95; sample size of $n = 6$ for each group with an actual power of 0.97.

For Western blot analysis, we selected eight samples per group (G-power parameters are: Effect size = 2; Err- prob = 0.05; Power = 0.95; sample size of $n = 8$ for each group with an actual power of 0.96). The t-test was used to evaluate differences between HD and DS where p values equal * $p = 0.05$, ** $p = 0.01$. Data are expressed as mean \pm SEM per group. Values above or below two standard deviations of the mean were considered outliers and discarded from the data set. All statistical analyses were performed using Graph Pad Prism 8.0 software (GraphPad, La Jolla, CA, USA). As reported in the dedicated section, mass spectrometry raw data have been analyzed according to the well-established parameters for DIA-MSE acquisition [139, 140].

4. RESULTS

PROJECT 1

4.1 Characterization of BACH-1/Nrf-2 pathway in Down Syndrome models

4.1.1 Characterization of BACH-1/Nrf-2 pathway in primary cultures of neurons and astrocytes isolated from Ts2cje and Euploid mice

To test our hypothesis on the implication of BACH-1 to compete with the Keap1-Nrf-2-ARE signalling complex, several cellular models of DS has been studied in the following project.

Above all, once isolated neurons and astrocytes from Ts2cje and euploid mice to gain insight into the involvement of DS-related genes, we analyzed the gene expression of BACH-1 and APP, both genes encoded on HSA21. We detected a significant increase in gene expression and protein levels of APP (Fig. 12 C-D) and BACH-1 (Fig. 12 E-F) in Ts2cje-isolated neurons compared to euploid cells (*gene expression: APP 100%, $p=0,0011$; BACH-1 39%, $p=0,01$; protein levels: APP 80%, $p=0,0026$; BACH-1 54,7%, $p=0,03$). Further, the same data have been confirmed in astrocytes isolated from Ts2cje, where both APP (Fig. 13 C-D) and BACH-1 (Fig. 13 E-F) are significantly expressed compared to euploid cells (*gene expression: APP 32%, $p=0,046$; BACH-1 33%, $p=0,009$; protein levels: APP 43,5%, $p=0,02$; BACH-1 39,7%, $p=0,006$). Thus, these results obtained allowed us to confirm the presence of trisomy in our primary culture models and in particular, the over-**

expression of BACH-1 on neurons and astrocyte afforded to investigate deeply the BACH-1/Nrf-2 pathway.

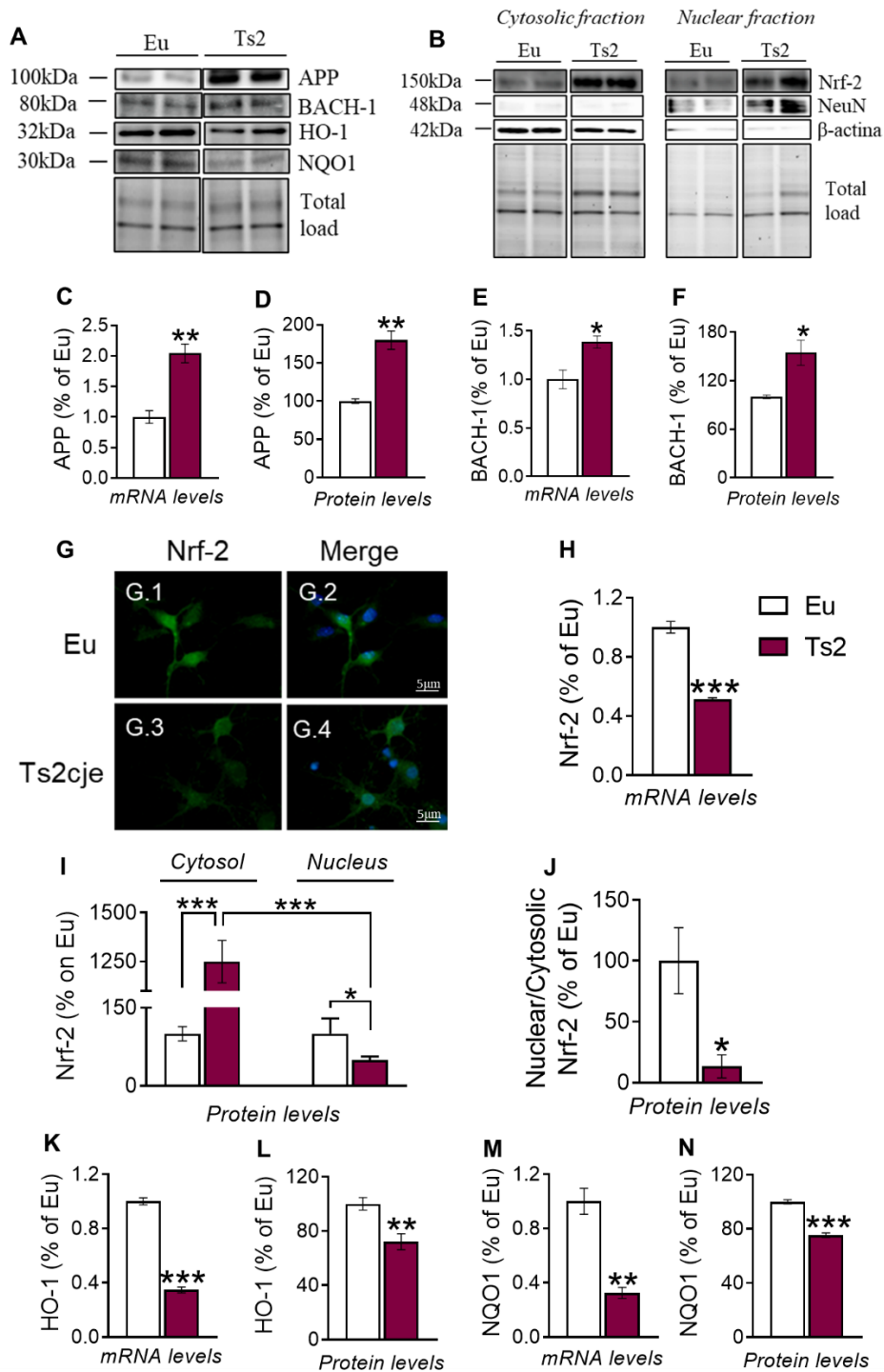


Figure 12. Comparative characterization of primary neurons from Eu and Ts2cje mice. A) Representative Western Blot showing total APP, BACH-1, HO-1 and NQO1 in Eu and Ts2cje primary neurons; B) Representative Western Blot showing Nrf-2, NeuN and β -actin levels in cytosolic and nuclear extract of Eu and Ts2cje primary neurons; C) and D) Gene expression changes of APP and quantification of panel A showing levels of total APP in Eu and Ts2cje primary neurons; E) and F) Gene expression changes of BACH-1 and quantification of panel A showing levels of total BACH-1 in Eu and Ts2cje primary neurons; G) Representative immunofluorescent images showing Nrf-2 signal (green) in Eu (G.1-G.2) and Ts2cje (G.3-G.4) primary neurons. DAPI (blue) was used to identify cell nuclei. Scale bar represent 5 μ m; H) Gene expression changes of Nrf-2 in Eu and Ts2cje primary neurons; I) Quantification of panel B showing levels of cytosolic and nuclear Nrf-2 in Eu and Ts2cje neurons; J) Bar graph represents nuclear and cytosolic Nrf-2 ratio; K) and L) Gene expression changes of HO-1 and quantification of panel A showing levels of total HO-1 in Eu and Ts2cje primary neurons; M) and N) Gene expression changes of NQO1 and quantification of panel A showing levels of total NQO1 in Eu and Ts2cje primary neurons. Densitometric values shown in the bar graph are the mean of 3 independent cultures/group normalized for total load, for NeuN and β -actin (as nuclear and cytosolic markers respectively) and are given as percentage of Eu, set as 100%. Data are presented as means \pm SEM. Statistical significance was determined using Student *t*-test analysis and 1-way ANOVA (**p* < .05, ***p* < .01 and ****p* < .001). The gene expression data were normalized to GAPDH expression. Fold change was determined using $2^{-\Delta\Delta Ct}$ method.

Several studies further suggested that BACH-1 and Nrf-2 compete with each other to regulate ARE-mediated gene expression in transfected cells [89]. In keeping with what observed, we evaluated changing in Nrf-2 gene expression, protein levels and its nuclear translocation. A significant reduction of Nrf-2 gene expression was observed in Ts2cje neurons (Fig. 12H 48,7%, *p*<0,0001) and astrocytes (Fig. 13H 24%, *p*=0,026) respectively compared with their euploid control. In addition, we observed a significant reduction of Nrf-2 protein levels into the nucleus of Ts2cje neurons compared with euploid cells (Fig. 12I 50,28%, *p*=0,0372). This reduction of Nrf-2 is maintained, also between cytosolic and nuclear portion of Ts2cje neurons (Fig. 12I 1200%, *p*<0,0001), probably due to the accumulation of Nrf-2 in the cytosolic fraction

of Ts2cje neurons (Fig. 12I 1150%, $p < 0,0001$). These results obtained are supported by measuring the Nrf-2 nuclear translocation, where the ability of Nrf-2 to translocate from the cytosol into the nucleus is significantly lower in Ts2cje neurons (Fig. 12J 86,73%, $p = 0,0234$).

All the results collected on neurons have been confirmed on Ts2cje astrocytes. We found a significant reduction of nuclear Nrf-2 (Fig. 13I 46,28%, $p = 0,0025$), also associated to a lower translocation into the nucleus (Fig. 13J 46,73%, $p = 0,0038$) in Ts2cje cells. The immunochemical data were further supported by confocal microscopy analysis of Nrf-2 nuclear buildup. The immunofluorescence staining demonstrates reduced overlapping of Nrf-2 signal with DAPI, supporting a lower translocation of Nrf-2 into the nucleus of Ts2Cje neurons (Fig. 12G) and astrocytes (Fig. 13G).

In order to verify the reduction Nrf-2 nuclear translocation related to the antioxidant response we analyzed HO-1 and NQO1 gene and protein expression in Ts2cje neurons and astrocytes. Our results showed a significant reduction of both HO-1 (Fig. 12K-L, *gene expression* 65%, $p < 0,0001$ and *protein levels* 28%, $p = 0,0086$) and NQO1 (Fig. 12M-N, *gene expression* 67%, $p = 0,0002$ and *protein levels* 26%, $p < 0,0001$) in Ts2cje neurons. The same results on HO-1 target have been collected in Ts2cje astrocytes (Fig. 13K-L, *gene expression* 56%, $p = 0,0002$ and *protein levels* 66,6%, $p < 0,0001$). Unlike what observed in neurons, no changes have been revealed on NQO1 gene and protein expression in Ts2cje astrocytes (Fig. 13M-N).

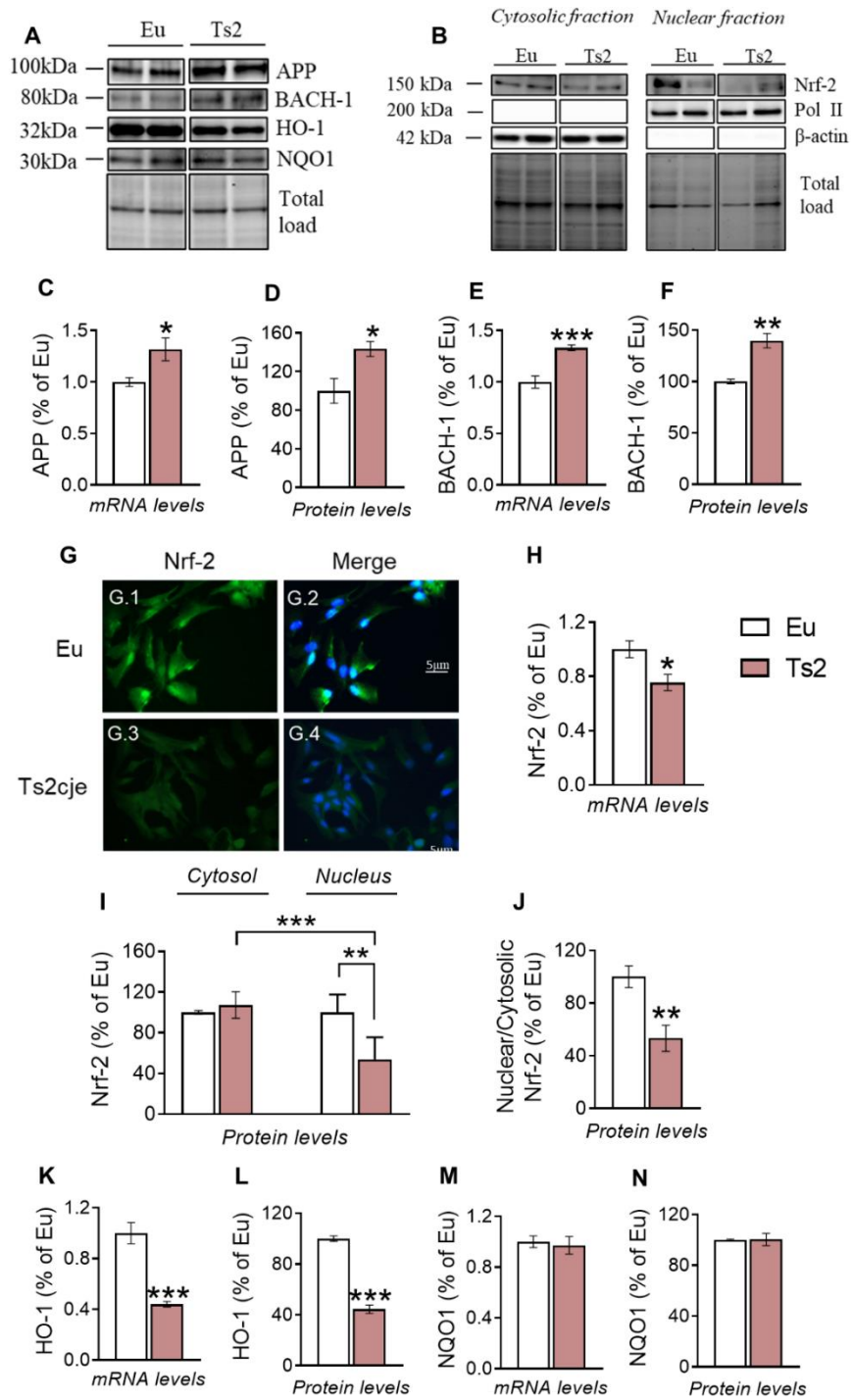


Figure 13. Comparative characterization of primary astrocytes from Eu and Ts2cje mice. A) Representative Western Blot showing total APP, BACH-1, HO-1 and NQO1 in Eu and Ts2cje primary astrocytes; B) Representative Western Blot showing Nrf-2, Pol II and β -actin levels in cytosolic and nuclear extract of Eu and Ts2cje primary astrocytes; C) and D) Gene expression changes of APP and quantification of panel A showing levels of total APP in Eu and Ts2cje primary astrocytes; E) and F) Gene expression changes of BACH-1 and quantification of panel A showing levels of total BACH-1 in Eu and Ts2cje primary astrocytes; G) Representative immunofluorescent images showing Nrf-2 signal (green) in Eu (G.1-G.2) and Ts2cje (G.3-G.4) primary astrocytes. DAPI (blue) was used to identify cell nuclei. Scale bar represent 5 μ m; H) Gene expression changes of Nrf-2 in Eu and Ts2cje primary astrocytes; I) Quantification of panel B showing levels of cytosolic and nuclear Nrf-2 in Eu and Ts2cje astrocytes; J) Bar graph represents nuclear and cytosolic Nrf-2 ratio; K) and L) Gene expression changes of HO-1 and quantification of panel A showing levels of total HO-1 in Eu and Ts2cje primary astrocytes; M) and N) Gene expression changes of NQO1 and quantification of panel A showing levels of total NQO1 in Eu and Ts2cje primary astrocytes. Densitometric values shown in the bar graph are the mean of 3 independent cultures/group normalized for total load, for Pol II and β -actin (as nuclear and cytosolic markers respectively) and are given as percentage of Eu, set as 100%. Data are presented as means \pm SEM. Statistical significance was determined using Student *t*-test analysis and 1-way ANOVA (**p* < .05, ***p* < .01 and ****p* < .001). The gene expression data were normalized to GAPDH expression. Fold change was determined using $2(-\Delta\Delta Ct)$ method.

4.1.2 Characterization of BACH-1/Nrf-2 pathway in the hippocampus of Ts2cje and Euploid mice at 3 months of age

To confirm the results collected from primary cell cultures on the BACH-1/Nrf-2 pathway, we investigated the BACH-1/Nrf-2 signaling in the hippocampus of Ts2cje and Euploid mice at 3 months of age. The results obtained revealed an increase of gene expression (Fig. 14B 63,6%, *p*=0,0016) and protein levels (Fig. 14C 14,5%, *p*=0,048) of BACH-1 in Ts2cje mice compared to the Euploid.

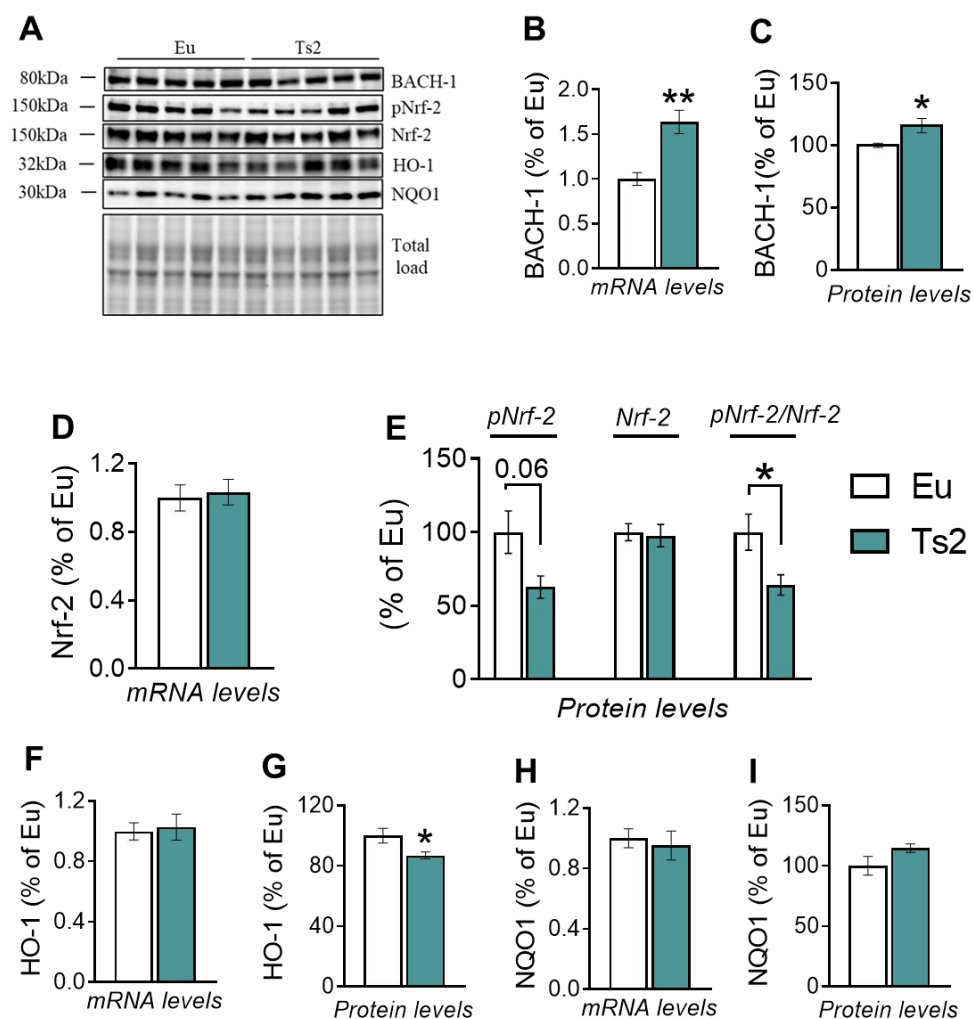


Figure 14. Comparative characterization of hippocampus of Ts2cje mice at 3 months of age. A) Representative Western Blot showing total BACH-1, p-Nrf2(Ser⁴⁰), Nrf-2, HO-1 and NQO1 in Eu and Ts2cje mice at 3 months of age; B) and C) Gene expression changes of BACH-1 and quantification of panel A showing levels of total BACH-1 in Eu and Ts2cje mice; D) Gene expression changes of Nrf-2 in Eu and Ts2cje mice; E) Quantification of panel A showing levels of total Nrf-2, p-Nrf2(Ser⁴⁰) and Nrf2(Ser⁴⁰)/total Nrf-2 ratio; F) and G) Gene expression changes of HO-1 and quantification of panel A showing levels of total HO-1 in Eu and Ts2cje mice; H) and I) Gene expression changes of NQO1 and quantification of panel A showing levels of total NQO1 in Eu and Ts2cje mice. Densitometric values shown in the bar graph are the mean of 5 samples for each group normalized for total load and are given as percentage of Eu, set as 100%. Data are presented as means \pm SEM. Statistical

significance was determined using Student *t*-test analysis (* $p < 0.05$, ** $p < 0.01$). The gene expression data were normalized to GAPDH expression. Fold change was determined using $2^{-\Delta\Delta Ct}$ method.

Subsequently, we evaluated the Nrf-2 phosphorylation on Ser⁴⁰ as an index of its nuclear import and a significant decrease of p-Nrf-2(Ser⁴⁰)/Nrf-2 was found in the hippocampus of Ts2cje mice (Fig. 14E 35,8%, $p=0,04$) compared to euploid mice. In light of this data, we analyzed the activity of Nrf-2 in promoting the transcription of its target genes: HO-1 and NQO1 and no significant changes have been detected in gene and protein levels in Ts2cje mice (Fig. 14F-I).

4.1.3 Characterization of BACH-1/Nrf-2 pathway in the LCLs from Down Syndrome and Healthy donors' children

Thanks to a collaboration with 'Bambino Gesù Hospital of Rome' we used LCLs from DS and healthy donors' (HD) children as a control, to investigate the BACH-1/Nrf-2 in DS peripheral cells, which may serve as a further model to study genetic disorders and mechanistic insights driving neurodegeneration in living subjects.

Initially, we analyzed the gene and protein levels of APP and BACH-1 and our data showed a significant increase of gene and protein levels of APP and BACH-1 (Fig. 15C-F, respectively, *gene expression* 113% $p=0,047$; 64%, $p=0,03$; and *protein levels* 276%, $p=0,0017$; 38,6%, $p=0,0155$) in DS LCLs compared to HD cells.

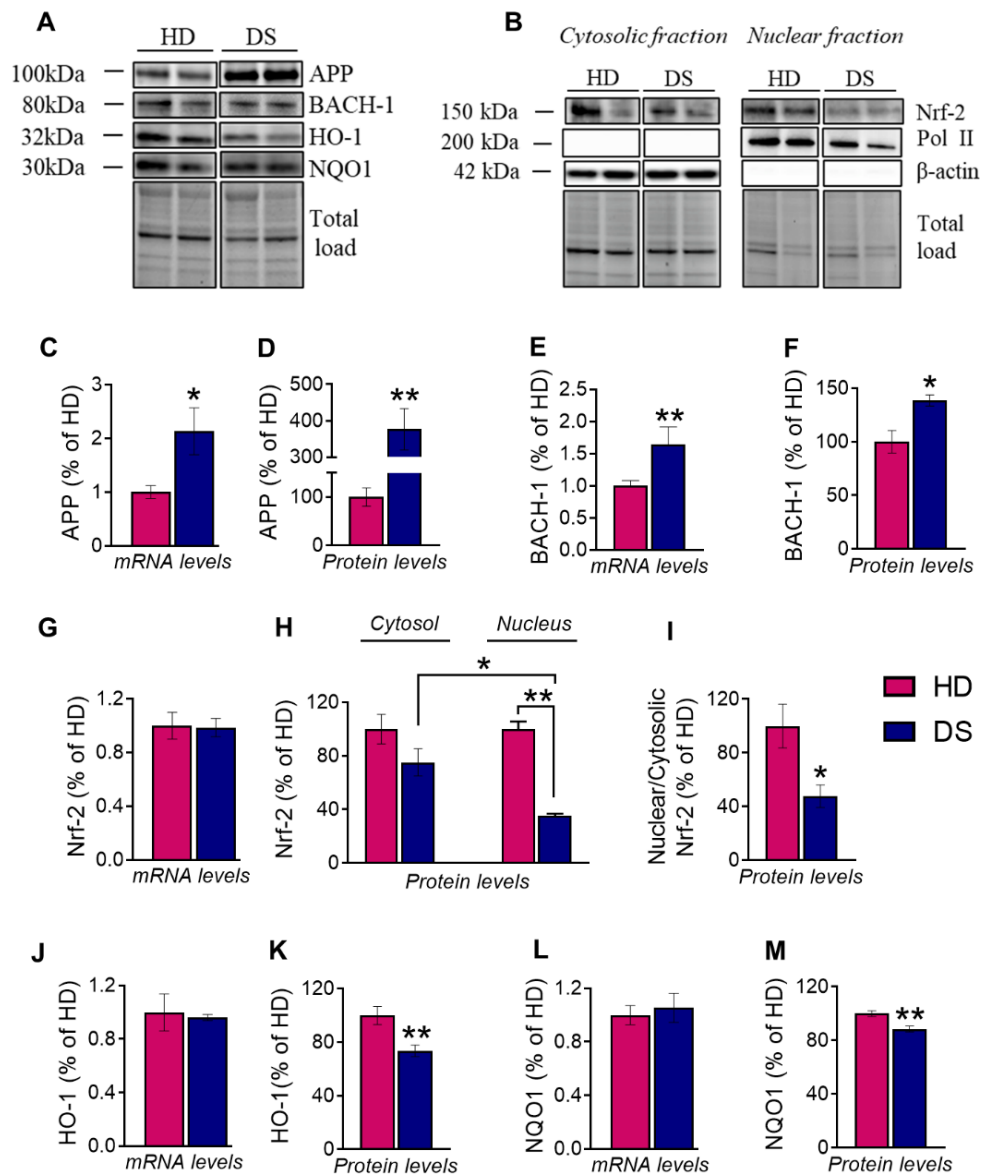


Figure 15. Comparative characterization of LCLs from HD and DS young patients. A) Representative Western Blot showing total APP, BACH-1, HO-1 and NQO1 in DS and HD LCLs; B) Representative Western Blot showing Nrf-2, Pol II and β -actin levels in cytosolic and nuclear extract of HD and DS LCLs; C) and D) Gene expression changes of APP and quantification of panel A showing levels of total APP in HD and DS LCLs; E) and F) Gene expression changes of BACH-1 and

quantification of panel A showing levels of total BACH-1 in HD and DS LCLs; G) Gene expression changes of Nrf-2 in HD and DS LCLs; H) Quantification of panel B showing levels of cytosolic and nuclear Nrf-2 in HD and DS LCLs; I) Bar graph represents nuclear and cytosolic Nrf-2 ratio; J) and K) Gene expression changes of HO-1 and quantification of panel A showing levels of total HO-1 in HD and DS LCLs; L) and M) Gene expression changes of NQO1 and quantification of panel A showing levels of total NQO1 in HD and DS LCLs. Densitometric values shown in the bar graph are the mean of 3 samples for each group normalized for total load, Pol II (as nuclear marker) and β -actin (as cytosolic marker) and are given as percentage of HD, set as 100%. Data are presented as means \pm SEM. Statistical significance was determined using Student *t*-test analysis (* $p < 0.05$, ** $p < 0.01$) and 1-way ANOVA. The gene expression data were normalized to GAPDH expression. Fold change was determined using $2(-\Delta\Delta Ct)$ method.

As demonstrated above on primary cell cultures, Nrf-2 induction is impaired in DS cells likely due to the triplication of BACH-1, thus favoring oxidative stress conditions. Indeed, we found significant changes in the translocation of Nrf-2 into the nucleus in DS cells (Fig. 15I 52%, $p=0,046$) and this data can be related to a lower amount of Nrf-2 in the nucleus of DS LCLs compared to the HD cells (Fig. 15H 64,7%, $p=0,002$). In addition, a significant decrease of Nrf-2 protein levels has been detected comparing nuclear and cytosolic fraction of DS protein amount (Fig. 15H 39,9%, $p=0,0326$). To confirm that the alteration of Nrf-2 translocation can prevent the transcription of its target genes, we evaluated HO-1 and NQO1: no significant differences were revealed by measuring their gene expression (Fig. 15J and L), while we observed a decrease of HO-1 (Fig. 15H 26,4%, $p=0,006$) and NQO1 (Fig. 15M 11,5%, $p=0,0075$) protein levels in DS compared to HD cells.

4.2 CAPE and VP961

4.2.1 Effects of CAPE and VP961 on neuroblastoma cell viability

Given the results collected in DS models, where we demonstrated that the decrease in Nrf-2 translocation into the nucleus is due to the gene imbalance of BACH-1, we decided to treat our cells with compounds (CAPE and VP961) that are able to induce Nrf-2 expression. To select the appropriate dose of CAPE and VP961 to treat neuroblastoma cell lines (SHSY-5Y), we tested each compound at different concentrations and we evaluated the cell viability using MTT assay. The following doses has been tested: 100nM, 250nM, 500nM, 1uM, 5uM, 10uM, 50uM for 24h. The dose-response curve showed that higher concentrations of VP961 and CAPE can reduce cell viability (Fig. 16A and B) after 24 h.

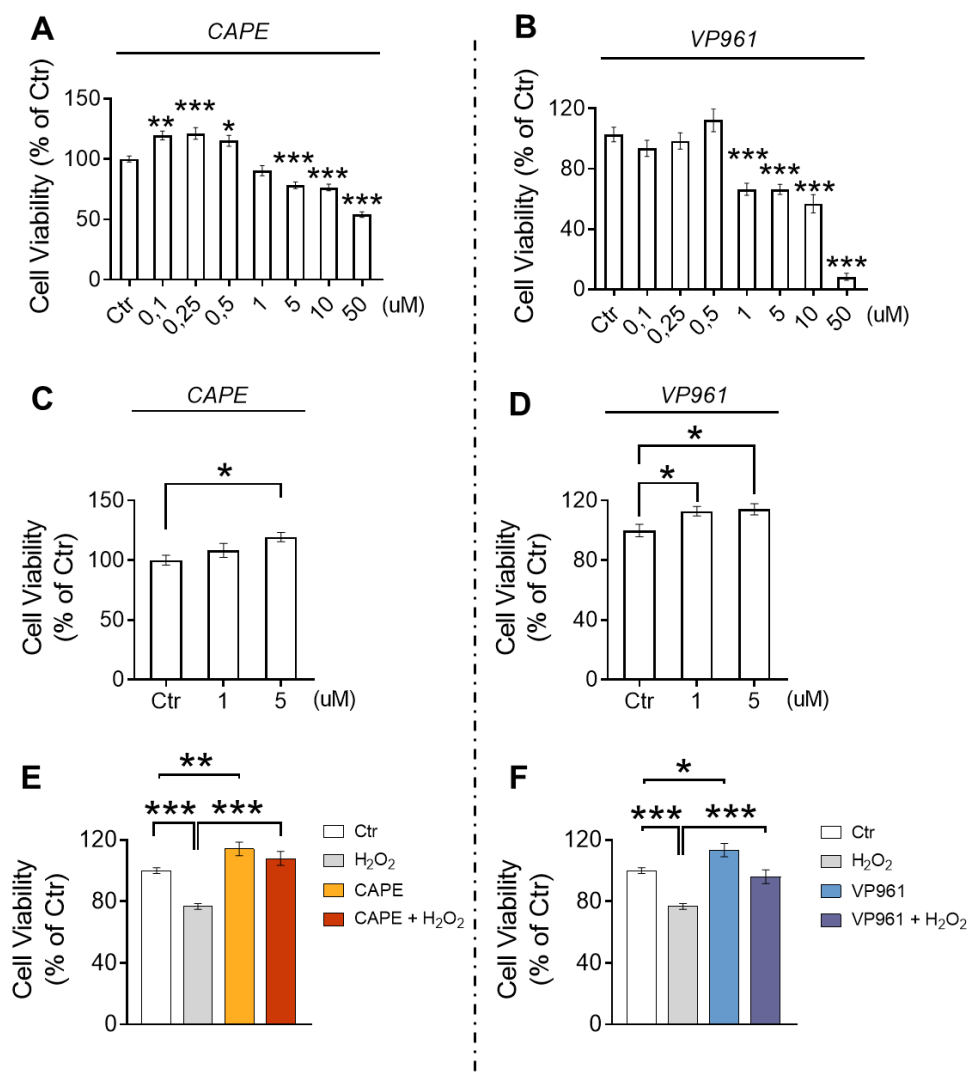


Figure 16. SHSY-5Y: CAPE and VP961 pre-treatment has a protective effect against oxidative stress stimulus. A) and B) Cell viability graphs of SHSY-5Y treated with different concentrations of CAPE and VP961 for 24h. C) and D) Cell viability graphs of SHSY-5Y treated with CAPE and VP961 for 2h and further 24h with only fresh medium; E) Cell viability graph of SHSY-5Y treated with CAPE, H₂O₂ or their combination; F) Cell viability graph of SHSY-5Y treated with VP961, H₂O₂ or their combination. Viability percentage is the mean of 8 different well for each experimental condition. The control cells are set as 100%. Data are presented as means \pm SEM. Statistical significance was determined using 1-way ANOVA (* $p < .05$, ** $p < .01$ and *** $p < .001$).

In light of the results, we selected two concentrations 1 and 5uM and we decided to pre-treat the cells for 2 hours and then remove the drug for the next 24 h, to avoid the toxic effects of the drugs. Indeed, pre-treatment with 1 and 5uM of CAPE and VP961 did not affect cell viability (Fig. 16C and D). Thus, these experimental conditions have been maintained for the following experiments to investigate the anti-oxidant and protective effects of CAPE and VP961.

4.2.2 Protective effect of CAPE and VP961 pre-treatment against H₂O₂-induced toxicity on SHSY-5Y

To evaluate the protective effect of CAPE and VP961, we treated SHSY-5Y cells acutely with H₂O₂ (100uM for 4h); the selected dosage of H₂O₂ was able to induce cell mortality around 20-30% on SHSY-5Y cell line. Thus, pre-treatment with CAPE and VP961 at 5uM for 2h replaced the cell viability under conditions of H₂O₂-induced toxicity (Fig. 16E and F).

All together these results have allowed us to set up a scheme for the next experiments, in order to characterize the antioxidant properties of CAPE and VP961 in modulating Nrf-2 activity.

4.2.3 The treatment with CAPE and VP961 is able to induce Nrf-2 nuclear translocation on SHSY-5Y under oxidative stress conditions

To achieve the goal of our project, we evaluated the ability of CAPE and VP961 to modulate Nrf-2 gene expression, protein level and its nuclear translocation under oxidative stress conditions. By performing RT-PCR, we observed that both compounds were not able to modify the gene expression of Nrf-2 (Fig. 17B and G). On the other hand, pre-treatment with CAPE and VP961 under oxidative stress conditions were able to modulate the nuclear protein levels of Nrf-2 and to induce its nuclear translocation (Fig. 17C-D and H-I). In details, analyzing the nuclear protein fractions, pre-treatment with CAPE and VP961 (2h) increased the protein levels of Nrf-2 in SHSY-5Y stimulated with H₂O₂ (Fig. 17C and H CAPE: 211,7%, $p < 0,0001$ – VP961: 93,7%, $p = 0,04$) compared with the cells treated acutely with H₂O₂. In addition, we can observe also that CAPE and VP961 can increase the nuclear Nrf-2 levels compared with the control cells (Fig. 17C and H CAPE: 155,4%, $p = 0,0002\%$ - VP961: 70,3%, $p = 0,07$). Moreover, we demonstrated that both these anti-oxidant molecules can induce the translocation of Nrf-2 into the nucleus under acutely oxidative stress conditions compared with the cells only treated with H₂O₂ (Fig. 17D and I; CAPE: 113%, $p = 0,0452$ – VP961: 79,3%, $p = 0,0387$).

The immunochemical data are further supported by confocal microscopy analysis of Nrf-2 nuclear buildup. The images demonstrate increased overlapping of Nrf-2 signal with DAPI supporting a higher translocation of Nrf-2 into the nucleus in SHSY-5Y treated with CAPE (Fig. 17E) and VP961 (Fig. 17J) in oxidative stress condition.

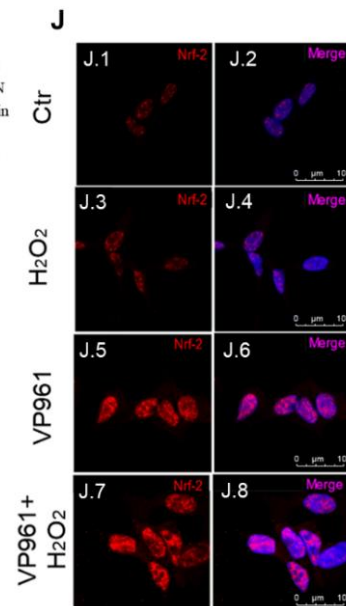
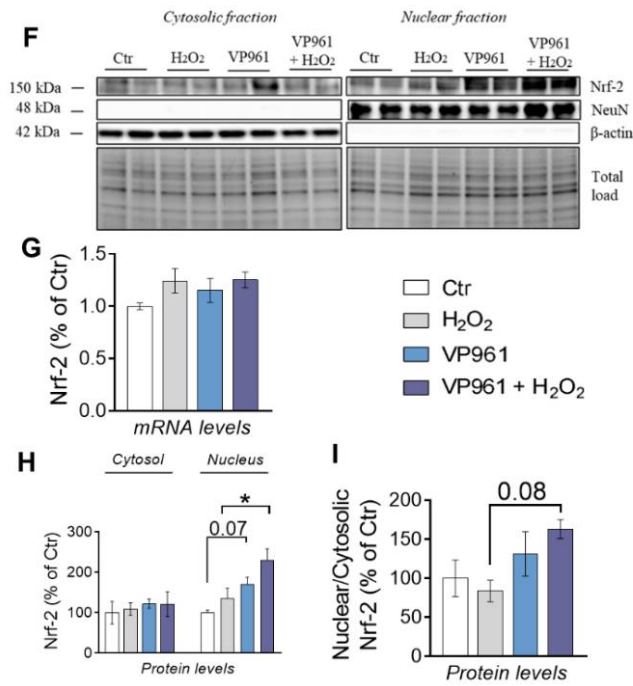
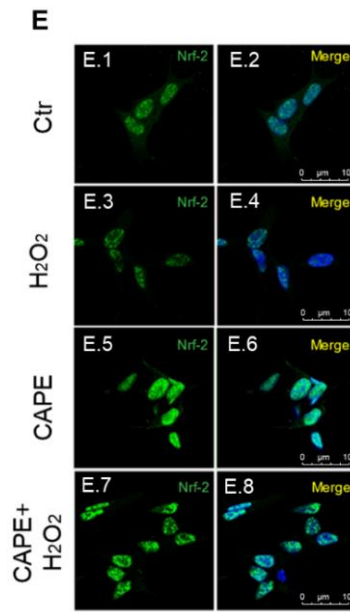
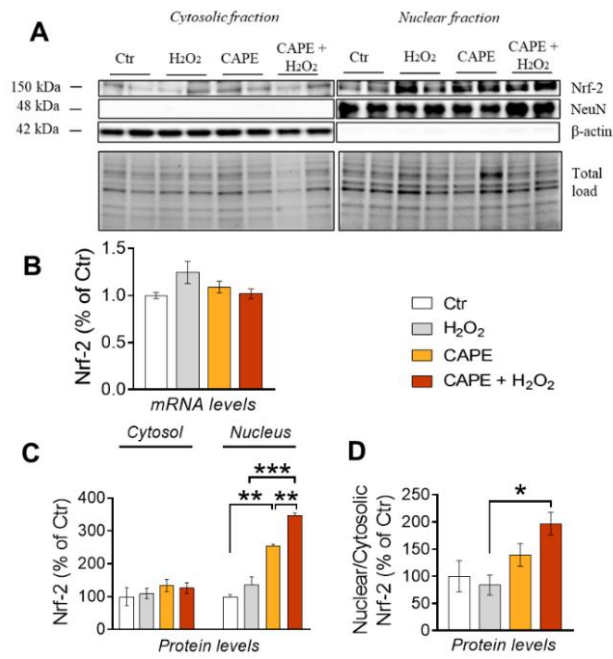


Figure 17. CAPE and VP961 pre-treatment promote increased Nrf-2 nuclear translocation and gene expressions and total levels of its targets in oxidative stress condition in SHSY-5Y. A) Representative Western Blot showing Nrf-2, NeuN and β -actin levels in cytosolic and nuclear extract of SHSY-5Y cells treated with CAPE; B) Gene expression changes of Nrf-2 in SHSY-5Y cells treated with CAPE; C) Quantification of panel A showing levels of cytosolic and nuclear Nrf-2 in SHSY-5Y cells treated with CAPE; D) Bar graph represents nuclear and cytosolic Nrf-2 ratio; E) Representative immunofluorescent images showing Nrf-2 signal (green) in SHSY-5Y treated with CAPE in oxidative stress condition (E.1-E.8). DAPI (blue) was used to identify cell nuclei. Scale bar represent 10 μ m. F) Representative Western Blot showing Nrf-2, NeuN and β -actin levels in cytosolic and nuclear extract of SHSY-5Y cells treated with VP961; G) Gene expression changes of Nrf-2 in SHSY-5Y cells treated with VP961; H) Quantification of panel G showing levels of cytosolic and nuclear Nrf-2 in SHSY-5Y cells treated with VP961; I) Bar graph represents nuclear and cytosolic Nrf-2 ratio; J) Representative immunofluorescent images showing Nrf-2 signal (red) in SHSY-5Y treated with VP961 in oxidative stress condition (J.1-J.8). DAPI (blue) was used to identify cell nuclei. Scale bar represent 10 μ m. Densitometric values shown in the bar graph are the mean of 3 independent cultures/group normalized for total load, NeuN (as nuclear marker) and β -actin (as cytosolic marker) and are given as percentage of control, set as 100%. Data are presented as means \pm SEM. Statistical significance was determined using 1-way ANOVA (* $p < .05$, ** $p < .01$ and *** $p < .001$).

4.2.4 The effects of CAPE and VP961 on HO-1 and NQO1 gene and protein levels, as target of Nrf-2

To confirm that both drugs were able to induce Nrf-2 activation, we evaluated their ability to modulate gene and protein levels of two main targets of Nrf-2, as HO-1 and NQO1. In details, we observed a significant increase of HO-1 gene expression (Fig. 18B and G, CAPE: 97%, $p=0,0027$ and VP961: 70%, $p=0,04$) and protein levels (Fig. 18C and H, CAPE: 397%, $p<0,0001$ and VP961: 69,42, $p= 0,0015$) in SHSY-5Y cells pre-treated with the compounds under oxidative stress compared to H₂O₂ conditions. Intriguingly, CAPE alone is able to increase HO-1 protein levels relative to control (Fig. 18C, 125%,

$p=0,02$), this data underlines the anti-oxidant properties of CAPE in our cell model.

Of what concern the other target of Nrf-2, pre-treatment with CAPE and VP961 under H_2O_2 stimulation increased NQO1 gene expression only related to drug-control (Fig. 18D and I, CAPE: 64%, $p=0,005$ and VP961: 20%, $p=0,07$). In addition, no changes were observed in NQO1 protein levels in cells pre-treated with drugs (Fig. 18E and J).

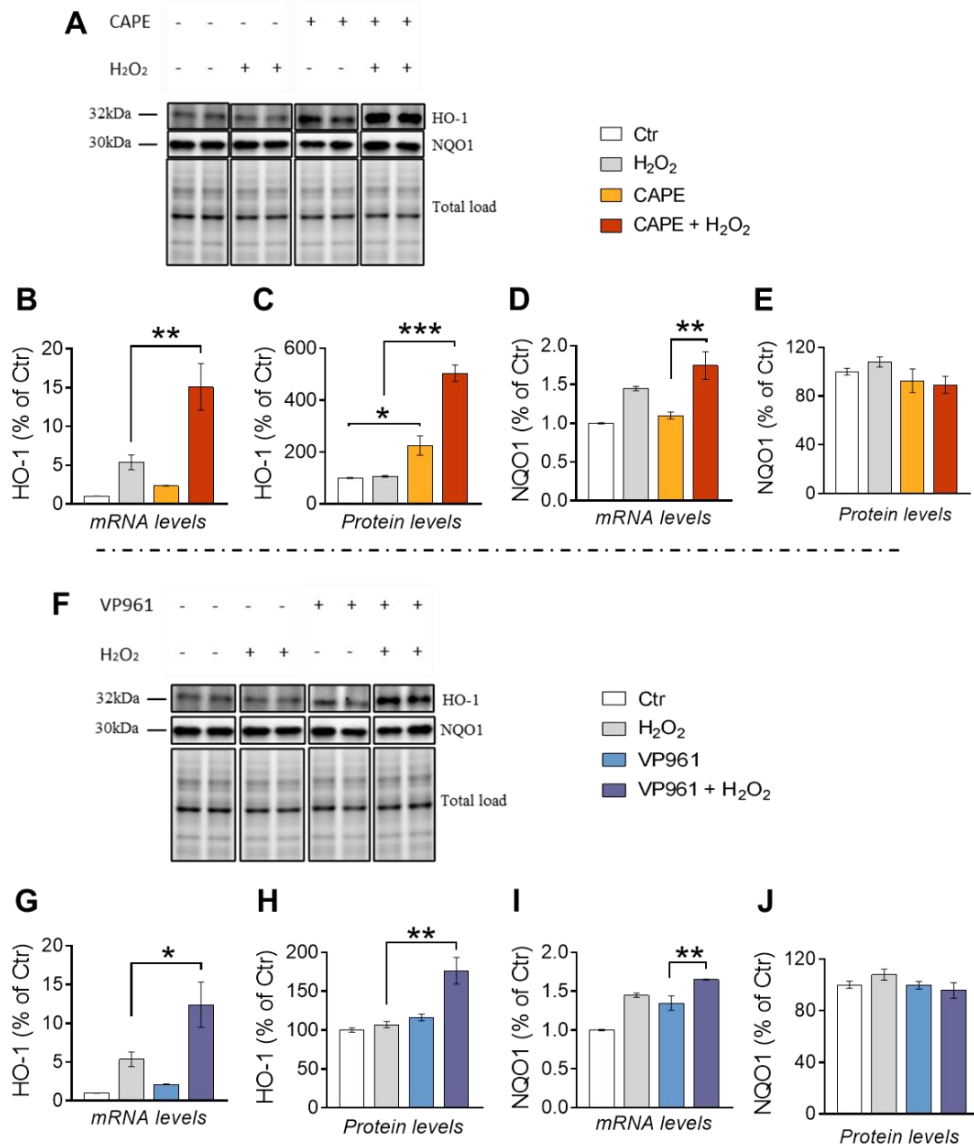


Figure 18. CAPE and VP961 pre-treatment induce HO-1 gene expression and protein levels in oxidative stress condition. A) Representative Western Blot showing total HO-1 and NQO1 in SHSY-5Y cells treated with CAPE; B) and C) Gene expression changes of HO-1 and quantification of panel A showing levels of total HO-1 in SHSY-5Y treated with CAPE; D) and E) Gene expression changes of NQO1 and quantification of panel A showing levels of total NQO1 in SHSY-5Y treated with CAPE; F) Representative Western Blot showing total HO-1 and NQO1 in SHSY-5Y cells treated with VP961; G) and H) Gene expression changes of HO-1 and

quantification of panel F showing levels of total HO-1 in SHSY-5Y treated with VP961; I) and J) Gene expression changes of NQO1 and quantification of panel F showing levels of total NQO1 in SHSY-5Y treated with VP961. Densitometric values shown in the bar graph are the mean of 3 independent cultures/group normalized for total load, and are given as percentage of control, set as 100 %. Data are presented as means \pm SEM. Statistical significance was determined using 1-way ANOVA ($p < .05$, ** $p < .01$ and *** $p < .001$).*

Our results suggested that CAPE and VP961 in oxidative stress condition can increase the gene and protein levels of HO-1 in a similar manner. The drugs are able, also to promote the gene expression of NQO1 but are not able to modulate protein levels, probably due to time setting of experimental conditions.

4.3 CAPE and VP961 treatment on Down Syndrome LCLs

Once we tested the beneficial effects of CAPE and VP961 under oxidative stress conditions on Nrf-2 pathway in SHSY-5Y, we conducted a new set of experiments on our DS cell model. Thus, to achieve our goal to demonstrate a role of BACH-1 in Nrf-2 regulation, we decided to test CAPE and VP961, since their ability to modulate Nrf-2 activity on DS LCLs. As previously described, DS LCLs showed an impairment of BACH-1/Nrf-2 pathway that allowed us to test CAPE and VP961 in DS in peripheral cells, which may serve as a further model to study genetic disorders and mechanistic insights driving neurodegeneration in living subjects.

4.3.1 VP961 induce Nrf-2 nuclear translocation in DS LCLs

From the results obtained on LCLs characterization, in which DS and HD cells differed in Nrf-2, HO-1 and NQO1 in terms of protein levels, we decided to test if CAPE and VP961 were able to modulate the Nrf-2 nuclear protein levels, its translocation in the nucleus and its targets proteins, as HO-1 and NQO1, as demonstrated in SHSY-5Y. Thus, we treated the DS LCLs with 10uM of CAPE and 5uM of VP961 for 6h, as determined by a dose-response curve where cell viability has been measured after treatment (Fig. 19A and B). We observed that both CAPE and VP961 treatment increased the nuclear Nrf-2 levels compared to DS control (Fig. 19D; CAPE: 196,7%, $p=0,05$ - VP961: 585,2%, $p=0,0019$). Interestingly, VP961 was more effective than CAPE to induce Nrf-2 protein levels into the nucleus (Fig. 19D; 388,5%, $p=0,0015$). Thus, only VP961 was able to improve the Nrf-2 nuclear translocation (Fig. 19E; 244,7%, $p=0,0005$) as reported by the ratio between nuclear and cytosolic Nrf-2.

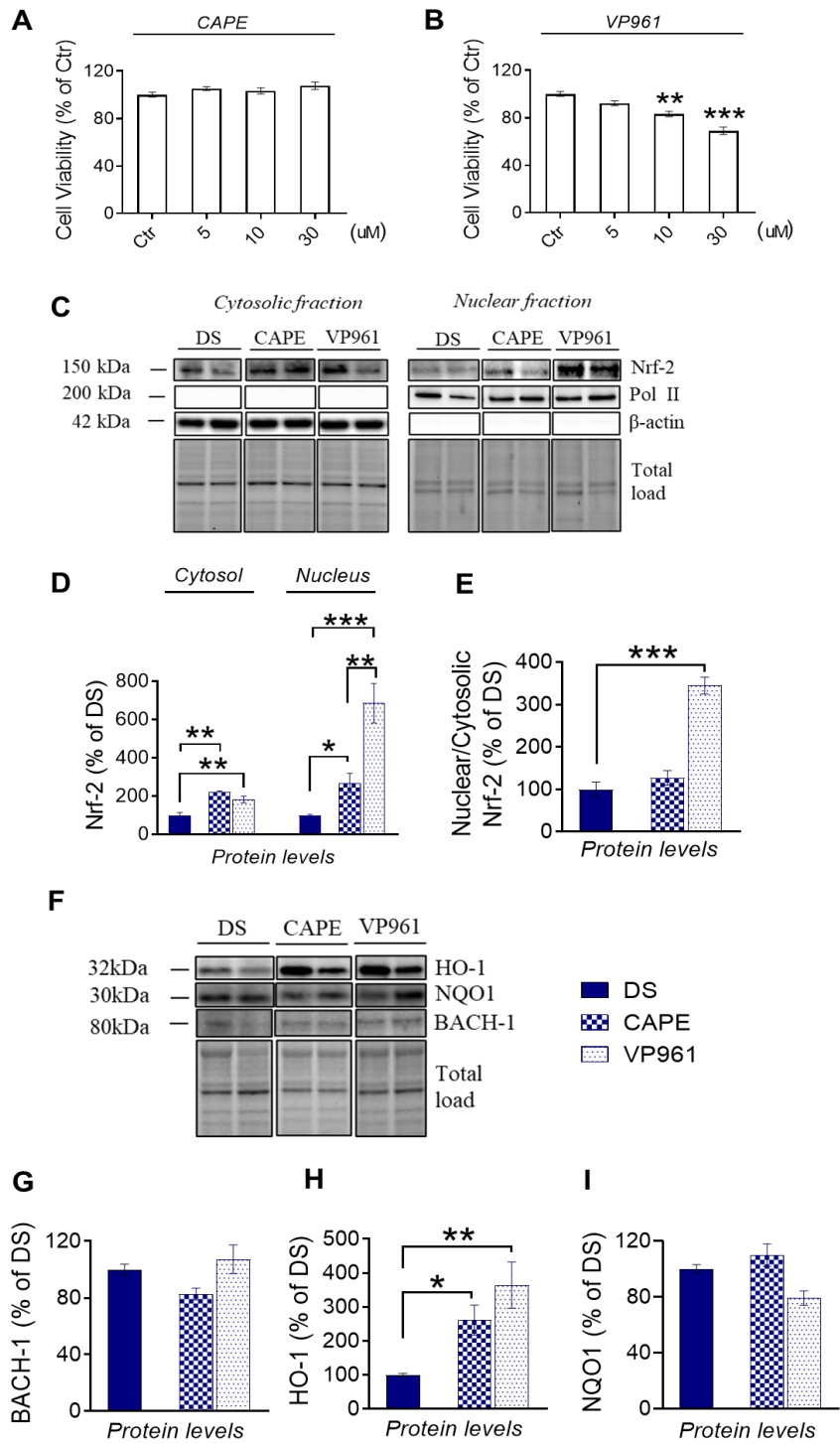


Figure 19. VP961 induce Nrf-2 nuclear translocation in DS LCLs. A) and B) Cell viability graphs of DS LCLs treated with different concentrations of CAPE and VP961 for 6h; C) Representative Western Blot showing Nrf-2, Pol II and β -actin levels in cytosolic and nuclear extract of DS LCLs treated cells; D) Quantification of panel C showing levels of cytosolic and nuclear Nrf-2 DS LCLs treated cells; E) Bar graph represents nuclear and cytosolic Nrf-2 ratio; F) Representative Western Blot showing total HO-1, NQO1 and BACH-1 in DS LCLs treated cells; G) Quantification of panel F showing levels of total BACH-1; H) Quantification of panel F showing levels of total HO-1; I) Quantification of panel F showing levels of total NQO1. Densitometric values shown in the bar graph are the mean of 3 samples for each group normalized for total load, Pol II (as nuclear marker) and β -actin (as cytosolic marker) and are given as percentage of DS, set as 100%. Data are presented as means \pm SEM. Statistical significance was determined using 1-way ANOVA (* $p < .05$, ** $p < .01$ and *** $p < .001$).

Regarding the two targets of Nrf-2, we found that both compounds increased the protein levels of HO-1 in a significant manner compared to control, but VP961 (Fig. 19H; 263,9%, $p=0,0015$) was able to induce Nrf-2 target more than CAPE (Fig. 19H; 161,3%, $p=0,0277$). Since our previous results obtained on DS LCLs characterization showed a significant increase of BACH-1 gene and protein levels, we tested if CAPE and VP961 were able to modulate not only Nrf-2 but also BACH-1. We observed that no changes of BACH-1 were produced by the treatment with CAPE and VP961 (Fig. 19G), suggesting that the two drugs can modulate Nrf-2 not involving BACH-1 alteration in DS LCLs model. Their beneficial effects on DS cells regards the modulation of Nrf-2 activity and in particular, VP961 had a stronger effect on Nrf-2 translocation into the nucleus than CAPE in DS LCLs.

PROJECT 2

4.4 PBMC proteomes from DS and HD young patients were investigated using an in-depth Label-Free shotgun Proteomics Approach

A comparative characterization of PBMC proteomes from 6 DS and 6 HD cases was performed to investigate putative changes in protein expression that could allow to gain insight into the molecular mechanisms of DS pathology. The differential protein expression analysis was carried out by a HD-MS^E isotope label-free profiling. Quality control measures were performed on the analytical replicates to ensure the reproducibility of the mass measurement and chromatographic retention time of each peptide. We acknowledge a limitation for sample size in the present study, however data obtained were consistent with previous analysis and have been partially confirmed by specific immunochemical analysis. As thoroughly described above, applying the statistical parameters on the identified proteins (such as fold change of regulation higher than $\pm 30\%$), 178 proteins have been shown as statistically differentially expressed across both conditions. Data obtained from this analysis and then bioinformatics-based speculations show that all the proteins, differently expressed in the experimental groups, clustered in a well-defined number of functions including stress response, trafficking, metabolism, DNA structure, cytoskeleton network and signalling, as represented in figures 20 and 21, and as listed in tables 8, 9 and 10.

(1) Group	(2) Protein Description	(3) Uni Prot Accession number	(4) Highly expressed	(5) DS/HD ratio
METABOLISM				
Unique HD	L-lactate dehydrogenase A, B, C	P00338; P07195; P07864		
	Malate dehydrogenase_ cytoplasmic	P40925	HD	
	Malate dehydrogenase_ mitochondrial	P40926	HD	
	ATP synthase subunit alpha_ mitochondrial	P25705	HD	
	Transaldolase	P37837	HD	
	Transketolase	P29401	HD	
	Triosephosphate isomerase	P60174	HD	
	Antizyme inhibitor 1	O14977	HD	
	Mitochondrial ornithine transporter 2	Q9BXI2	HD	
Over- expressed in HD	N/A	N/A	N/A	N/A
Unique DS	N/A	N/A	N/A	N/A
Over- expressed in DS	Glyceraldehyde-3-phosphate dehydrogenase	P04406		5,2
	Fructose-bisphosphate aldolase A, C	P04075; P09972		3,17
	Phosphoglycerate kinase 1, 2	P00558; P07205		1,86
TRAFFIKING				
Unique HD	Rab1 (A, B, C)	P62820; Q9H0U4; Q92928	HD	
	Rab3 (A, B, C, D)	P20336; P20337; Q96E17; O95716	HD	
	Rab4 (A, B)	P20338; P61018	HD	
	Rab6 (A, B)	P20340; Q9NRW1	HD	
	Rab8 (A, B)	P61006; Q92930	HD	
	Rab10	P61026	HD	
	Rab12	Q61Q22	HD	
	Rab13	P51153	HD	
	Rab14	P61106	HD	
	Rab15	P59190	HD	
	Rab30	Q15771	HD	
	Rab33 (B)	Q9H082	HD	
	Rab35	Q15286	HD	
	Rab37	Q96AX2	HD	
	Rab39 (A, B)	Q14964; Q96DA2	HD	
	Rab43	Q86YS6	HD	
	Peripherin	P41219	HD	
	Chloride intracellular channel protein 1	O00299	HD	
	AarF domain-containing protein kinase 1	Q86TW2	HD	
	Over- expressed in HD	Rho GDP-dissociation inhibitor 1	P52565	
	Protein bicaudal D homolog 1	Q96G01		0,15
	Membrane magnesium transporter	Q8N4V1		0,3
Unique DS	N/A	N/A	N/A	

Over-expressed in DS	N/A	N/A	N/A
DNA STRUCTURE			
Unique HD	Heterogeneous nuclear ribonucleoprotein A1	P09651	HD
	Heterogeneous nuclear ribonucleoprotein A1-like 2	Q32P51	HD
	Heterogeneous nuclear ribonucleoprotein C-like 1, 2, 3, 4	O6081; B2RXH8; B7ZW38; P0DMR1	HD
	Heterogeneous nuclear ribonucleoproteins C1/C2	P07910	HD
	TATA box-binding protein-associated factor RNA polymerase I subunit B	Q53T94	HD
Over-expressed in HD	Putative male-specific lethal-3 protein-like 2	P0C860	0,56
Unique DS	Histone H1.1,2, 3,4,5	Q02539; P16403; P16402; P10412; P16401	DS
	Histone H2B type 1-B, C, D, H, K, L, M, N, O	P33778; P62807; P58876; Q93079; O60814; Q99880; Q99879; Q99877; P23527	DS
	Histone H2B type 2- E, F	Q16778; Q5QNW6	DS
	Histone H2B type 3	Q8N257	DS
	Histone H3.1,2,3	Q16695; Q71DI3; P84243	DS
Over-expressed in DS	Shieldin complex subunit 3	Q6ZNX1	1,78
	Ribonuclease H2 subunit C	Q8TDP1	2,4
	Histone H4	P62805	2,51
STRESS RESPONSE			
Unique HD	Poliubiquitin B, C	P0CG47; P0CG48	HD
	Heat shock 70 kDa protein 1A, 1B	P0DMV8; P0DMV9	HD
	Heat shock 70 kDa protein 1, 2	P34931; P54652	HD
	Heat shock protein HSP 90-alpha, beta	P07900; P08238	HD
	Ubiquitin-40S ribosomal protein S27a	P62979	HD
	Calreticulin	P27797	HD
	Parkinson disease protein 7	Q99497	HD
Over-expressed in HD	Glutaredoxin-like protein C5orf63	A6NC05	HD
	T-complex protein 1 subunit beta	P78371	0,3
	Protein S100-A8, A9	P05109; P06702	0,26
Unique DS	Peptidyl-prolyl cis-trans isomerase A	P62937	0,4
	Nitric oxide synthase-interacting protein	Q9Y314	DS
	Glutathione S-transferase	P09211	DS
	Cyclic AMP-dependent transcription factor ATF-6 alpha and beta	P18850; Q99941	2,2

	DNA damage-inducible transcript 3 protein (CHOP)	P35638	3,4
	Endoplasmic reticulum chaperone BiP (GRP78)	P11021	2,07
Over-expressed in DS	ERO1-like protein alpha	Q96HE7	3,04
	Protein disulfide-isomerase (PDI)	P07237	8,7
	Peroxiredoxin-1, 2, 4, 6	Q06830; P32119; Q13162; P30041	2,88;3,7; 4,2; 4,8
	Endoplasmin	P14625	2,4
	Superoxide dismutase [Cu-Zn]	P00441	6,7
	Extracellular superoxide dismutase [Cu-Zn]	P08294	5,4
	CYTOSKELETON NETWORK		
	Gelsolin	P06396	HD
	Annexin A6	P08133	HD
Unique HD	Calmodulin-1, 2, 3	P0DP23; P0DP24; P0DP25	HD
	Protocadherin gamma	Q9Y5G3	HD
	Neurofilament medium polypeptide	P07197	HD
	Plastin-2	P13796	HD
	Adenylyl cyclase-associated protein 1	Q01518	HD
Over-expressed in HD	POTE ankyrin domain family member F	A5A3E0	- 0,6
	Radixin	P35241; P15311	0,7
	Na(+)/H(+) exchange regulatory cofactor NHE-RF2	Q15599	0,13
	Vimentin	P08670	- 0,8
Unique DS	Actin-related protein 2/3 complex subunit 1, 4, 5	O15143; P59998; O15511	DS
	Cofilin-1, 2	P23528; Q9Y281	1,67; 1,57
Over-expressed in DS	Tropomyosin alpha-1,3, 4 chain	P09493; P06753; P67936,	2,21; 2,18; 2,46
	Tropomyosin beta chain	P07951	2,46
	TUBA4B Putative tubulin-like protein alpha-4B Iso 1	Q9H853	2,43
	TUBA8 Tubulin alpha-8 chain Iso 2	Q9NY65	5,13
	TUBB1 Tubulin beta-1 chain Iso 1	Q9H4B7	4,28
	TUBB2B Tubulin beta-2B chain Iso 1	Q9BVA1	3,8
	Myosin-9	P35579	7,29
	Ezrin	P15311	2,8
	Profilin-1	P07737	7,4
	SIGNALLING		
Unique HD	Guanine nucleotide-binding protein G(i) subunit alpha-2	P04899	HD
Over-expressed in HD	Pleckstrin	P08567	0,53
	Platelet factor 4	P02776; P10720	0,24
	Platelet glycoprotein Ib alpha chain	P07359	0,22
	Platelet glycoprotein 4	P16671	0,26
	Embryonal Fyn-associated substrate	O43281	0,32

	SH3 domain-binding glutamic acid-rich-like protein	Q9H299	0,2
	Gap junction beta-4 protein	Q9NTQ9	0,4
	Casein kinase II subunit alpha	P19784	0,37
Unique DS	SHC SH2 domain-binding protein 1	Q8NEM2	DS
	Protein kinase C gamma	P05129	DS
Overexpressed in DS	GPR107	Q5VW38	8,4
OTHER FUNCTIONS			
	WD repeat-containing protein 1, 54	O75083; Q9H977	HD
	Cystatin-B	P04080	HD
Unique HD	Putative elongation factor 1-alpha-like 3	Q5VTE0	HD
	Coagulation factor XIII A chain	P00488	HD
	Coronin-1A	P31146	HD
	Hemoglobin subunit alpha, zeta	P69905; P02008	0,64; 0,45
	Protein tweety homolog 2	Q9BSA4	0,4
	Elongation factor 1-alpha 1	P68104; Q5VTE0; Q05639	0,09
Over-expressed in HD	Eukaryotic initiation factor 4A-II	Q14240	0,2
	Lysozyme C	P61626	0,39
	Shugoshin 2	Q562F6	0,46
	Fermitin family homolog 3	Q86UX7; Q13905; Q9UBZ9	0,34; 0,46;0,6
	39S ribosomal protein L45_ mitochondrial	Q9BRJ2	0,14
Unique DS	N/A	N/A	N/A
Overexpressed in DS	N-alpha-acetyltransferase	Q6N069	2,21

Table 8. Differentially expressed proteins in DS and HD groups identified using HD-MS^E label-free Mass spectrometry analysis clustered in the related molecular networks. (1): experimental group in which proteins are mainly expressed; (2): protein name; (3). accession number according to UniProtKB/Swiss-Prot Protein Knowledgebase; (4): protein found highly represented (defined as unique) in DS or HD PBMCs protein extracts; (5): ratio of expression between DS and HS according to quantitative expression analysis by PLGS 3.03.

<i>Reactome Pathways in HD</i>			
<i>Pathway</i>	<i>Description</i>	<i>Count in gene set</i>	<i>False discovery rate</i>
<u>HSA-8873719</u>	RAB geranylgeranylation	23 of 63	3.35E-31
<u>HSA-9007101</u>	Rab regulation of trafficking	16 of 118	2.57E-15
<u>HSA-8876198</u>	RAB GEFs exchange GTP for GDP on RABs	14 of 86	2.18E-14
<u>HSA-5653656</u>	Vesicle-mediated transport	26 of 64	6.66E-14
<u>HSA-199991</u>	Membrane Trafficking	23 of 612	1.27E-11

Table 9. Highlights of the 5 most significant reactome pathways involving proteins overexpressed in the HD group.

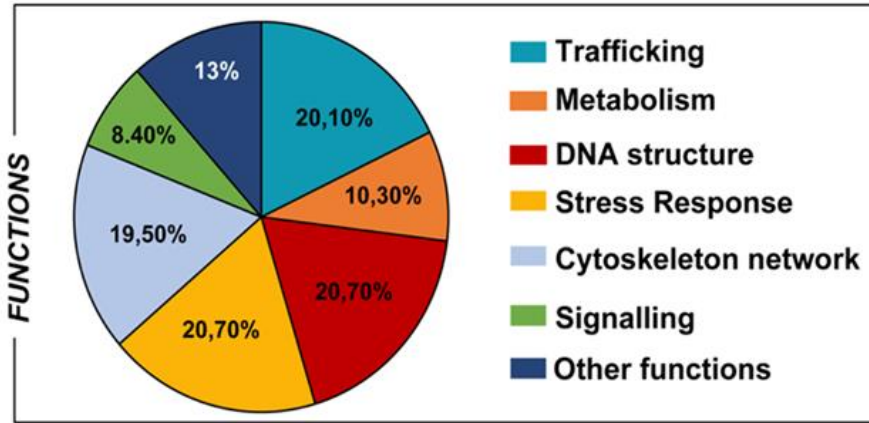
<i>Reactome Pathways in DS</i>			
<i>Pathway</i>	<i>Description</i>	<i>Count in gene set</i>	<i>False discovery rate</i>
<u>HSA-2262752</u>	Cellular responses to stress	27 of 384	1.17e-27
<u>HSA-2559586</u>	Cellular responses to external stimuli	27 of 459	5.50e-26
<u>HSA-2559586</u>	DNA Damage Stress Induced Senescence	15 of 61	3.98e-22
<u>HSA-2559583</u>	Cellular Senescence	15 of 161	1.70e-16
<u>HSA-195258</u>	RHO GTPase effectors	17 of 273	3.41 e-16

Table 10. Highlights of the 5 most significant reactome pathways involving proteins overexpressed in the DS group.

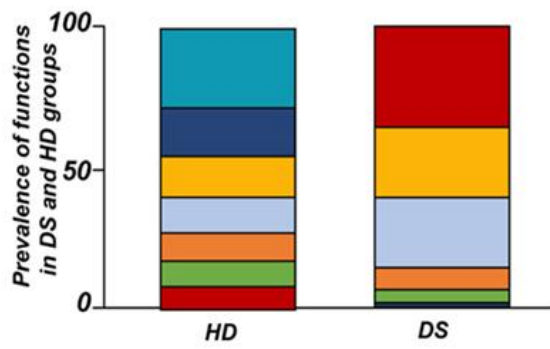
According to the analytical features of the mass spectrometer used and to the results from quantitative expression analysis, the identified proteins were then clustered as follows: proteins with a different expression comparing both DS and HD conditions (over-expressed or down-expressed, with fold change > 30%), and highly-expressed proteins, so-called “unique” proteins, whose compared expression ratio is more than 10 times higher so that they can be

considered present in only one specific group. Thus, we identified four groups of comparison: UNIQUE HD that include proteins over expressed in HD with a fold >10; overexpressed in HD (>HD) that include protein with a fold of increase >1.3 but <10; UNIQUE DS that include proteins over expressed in DS with a fold >10; overexpressed in DS (>DS) that include protein with a fold of increase >1.3 but <10. Intriguingly, the HD groups include proteins belonging to all 6 functional groups but demonstrate a high prevalence of trafficking proteins (28%) as also evident in Figure 20 and Table 8. We report also a 15% of stress response proteins, a 13% of cytoskeletal proteins, a 10% of metabolic proteins, a 9% of proteins related to signaling network and an 8% of DNA structure proteins. In addition, the 17% of proteins with increased expression in HD groups do not fall in any of the functional networks taken in considerations. The DS groups display an altered expression for proteins mainly involved in DNA structure (36%) and stress response (25%) as evident in figures 21 and 22B, while other functional groups that presents overexpressed protein in DS are: cytoskeleton network for the 25%, metabolic pathways for the 8%, cell signaling for the 5% and a broad array of function for the remaining 2% (Fig. 22B).

A



B



C

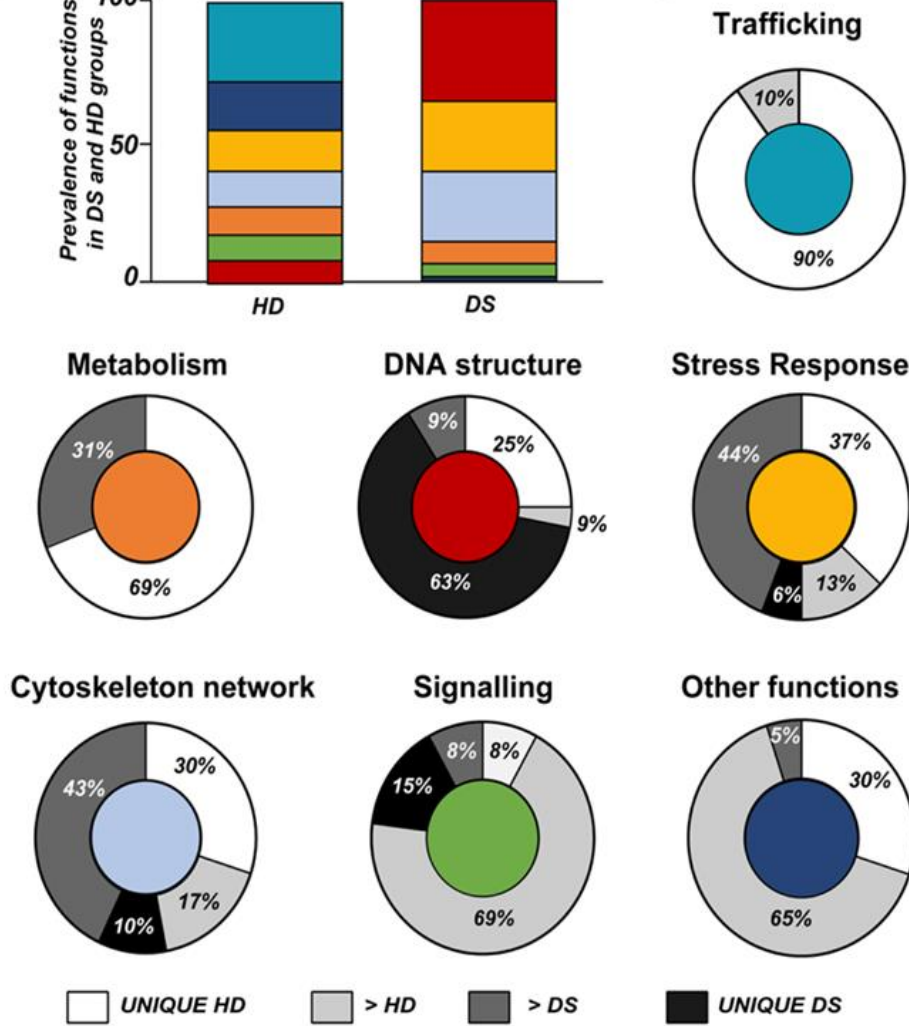


Figure 22. A) Pie chart representing all the proteins grouped according to their function. B) Representative graph showing the prevalence distribution of the listed functions in the HD and DS groups, respectively. C) Pie chart representing all the functions reported in the work and the related alterations among the groups of analysis (UNIQUE HD, UNIQUE DS, >HD and >DS).

Subsequently, by analyzing for each identified functional set, the percentage and the identity of the proteins belonging to UNIQUE HD, >HD, UNIQUE DS and >DS groups, we sought to delineate the pathways that are mainly affected during DS pathology, their role in disease progression and their potential value as biomarkers.

4.4.1 Protein included in intracellular trafficking

The 100% of all the proteins included in intracellular trafficking group are over increased in HD groups with the 90% and 10% belonging to UNIQUE HD and to >HD respectively (Fig. 20 and 22C); in details as listed in table 8 we identified 25 proteins belonging to the Rab family, a member of the Ras superfamily of small G proteins. In the cell metabolism group, UNIQUE HD proteins account for the 69%, while the 31% belong to >DS (Figure 22C). Pathway analysis revealed that these proteins are related to energy metabolism, glucose metabolism, ornithin metabolic pathway and urea cycle. In details, the protein linked to energy metabolism are: cytoplasmatic and mitochondrial malate dehydrogenase, lactate dehydrogenase, ATP synthase subunit alpha mitochondrial, Glyceraldehyde-3-phosphate dehydrogenase, Fructose-bisphosphate aldolase A/C, Phosphoglycerate kinase 1,2, transaldolase, transketolase. Protein linked to the ornithin metabolic pathway and urea cycle are the Antizyme inhibitor 1 and the mitochondrial ornithine transporter 2.

4.4.2 Proteins involved in stress response

Analyzing the stress response proteins network, it is evident that the 37% of the proteins are UNIQUE HD, the 13% are >HD, the 6% belong to UNIQUE in DS and the 44% are overexpressed in DS (Fig. 21 and 22C). Some notable proteins include those involved in the response to ER stress, protein folding in the ER (ERO1 and PDI), ER-nucleus signaling pathway (ATF6, ATF6-alpha, B and CHOP) and in cellular chaperoning, such as GRP78 (Table 8). Focusing on ER stress, endoplasmic reticulum chaperone that functions in the processing and transport of secreted proteins, and functions in endoplasmic reticulum associated degradation (ERAD). Intriguingly, all the over mentioned proteins, associated with ER stress, were found to be over-expressed in DS compared to HD, thus confirming the involvement of increased UPR in the pathophysiology of Down Syndrome. Furthermore, other relevant over-expressed proteins in DS involved in stress response with antioxidant properties are SOD-1, Peroxiredoxin 1,2,4,6 and glutathione S-transferase.

4.4.3 Cytoskeleton proteins

Regarding the cytoskeleton network statistical analysis reveals that these proteins fall into the HD groups for the 47% (specifically, 30% UNIQUE in HD and 17% >HD) and into the DS group for the 53% (specifically, 10% are UNIQUE DS, and 43% are overexpressed in DS). The UNIQUE HD group include the following proteins: Gelsolin, Annexin A6, Calmodulin-1, 2, 3, WD repeat-containing protein 1, 54, Vimentin, Protocadherin gamma, Plastin-2, Adenylyl cyclase-associated protein 1 and Fermitin family homolog 3. The

only protein unique in DS cases is Actin-related protein 2/3 complex subunit, while the proteins over-expressed in DS are: Cofilin-1, 2, Tropomyosin alpha and beta chain, Tubulin alpha and beta with different isoforms, Myosin-9, Ezrin and Profilin-1.

4.4.4 Protein involved in DNA structure

An altered expression of the proteins involved in the DNA structure strongly affects the DS groups, indeed, only the 28% of protein belong to the HD groups including the heterogeneous nuclear ribonucleoprotein A1 and heterogeneous nuclear ribonucleoprotein C1/C2, while the 72% of the identified protein are part of both the UNIQUE DS and >DS groups.

In details, 5 types of histone proteins, H1, H2A, H2B, H3 and H4, have been identified as increased in DS (Fig. 21). The proteins involved in signaling network group represents a small amount of the total identified proteins (8%) and comprises: Pleckstrin OS, Platelet glycoprotein 4, Platelet glycoprotein Ib alpha chain, SHC SH2 domain-binding protein 1, Protein kinase C gamma and GPR107. The distribution of these proteins between the groups of comparisons revealed that the 77% belong to the HD groups (specifically, 8% UNIQUE HD and 69% >HD) and the 27% to DS groups (respectively, 15% to UNIQUE DS and 8% to the >DS).

At final we identified 20 proteins (13% of the total), which do not fall in any of the above-mentioned networks and may hold various biological functions, have been identified in HD groups (95%).

4.5 Validation of the results obtained by proteomic analysis

To validate the results obtained with Label-Free Proteomic Analysis and to underline the notion that oxidative stress plays an important role in DS pathogenesis and progression we analyzed, by slot blot, protein carbonylation as a surrogate index for total protein oxidation and, by western blot, the proteins involved in OS response.

We found a significant increase of protein carbonylation in DS PBMCs compared to HD. As can be seen from Fig.23B, the global protein carbonylation load was higher in DS group respect to HD group (+42%, $p=0.02$). The elevation of protein carbonylation parallel with the increase of SOD-1, triplicated in DS, whose overexpression is observed both by mass spectrometry-based proteomics and WB (+115.4%; $p<0.001$) (Fig.23F). As a further validation of the MS data, the over expression of PRDX-6 in DS was also confirmed by WB analysis (+18%; $p=0.03$) and support the induction of antioxidant responses to counteract OS in DS PBMCs (Fig.23E).

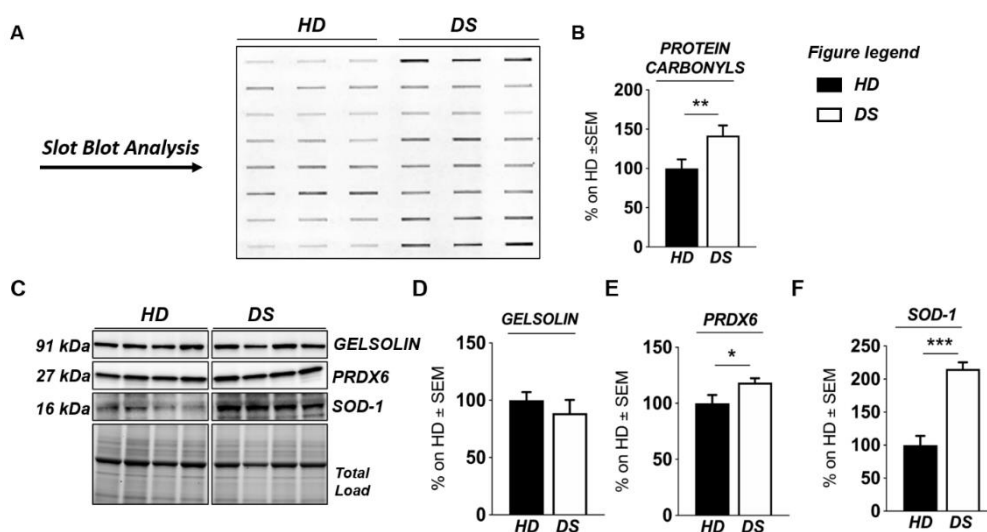


Figure 23. Human PBMCs from DS individuals show the induction of antioxidant responses to counteract OS. Slot blot analysis of total protein carbonylation. Panel A (left hand side): Slot blot of representative samples from healthy donors (HD) and down syndrome (DS) groups. A triplicate of 6 samples per group is showed. Panel B (right hand side): Densitometric analysis of total protein carbonylation in healthy donors (HD) and down syndrome (DS) groups. C) Representative Western Blot showing SOD-1, PRDX6 and GELSOLIN in PBMCs from DS and HD. D) Quantification of panel C showing levels of total GELSOLIN; E) Quantification of panel C showing levels of PRDX6 E) Quantification of panel C showing levels of total GELSOLIN; F) Quantification of panel C showing levels of SOD1. Densitometric values shown in the bar graph are the mean of 6 samples for each group normalized for total load and are given as percentage of HD, set as 100%. Statistical significance was determined using Student t-test analysis (* $p < 0.05$, ** $p < 0.01$).

5. DISCUSSION

5.1 Discussion Project 1

Down Syndrome is a genetic disorder etiologically related to oxidative stress (OS) due to the triplication of some genes encoding on HSA21. However, recent studies showed that OS is related not only to the over-expression of gene located on HSA21 but also to the dysregulation of gene/protein expression outside the HSA21 [52].

Several studies support the idea that OS is strongly related to phenotypical characteristics of DS pathology [23, 58, 59], despite the mechanisms through which OS damage leads to the diversity of pathological features of DS need to be clarified. Published studies from our group supported the idea that OS is a chronic condition in DS brain, that initiates already during embryonic development representing, with the aging process, a strong risk factor for neurodegeneration [60, 61]. It's well accepted that the aging process in DS population leads to increased risk of developing Alzheimer's disease (AD) by the age of 50ys. The mapping of HSA21 made an important contribution to better understand the causes of OS in DS brain; this investigation reveal a number of genes, such as SOD-1, APP, BACH-1, ETS2, CBR, S100B, involved in the over-production of ROS, as demonstrated in DS individuals and in mouse models of the disease [62].

Among triplicated genes, we focused our attention on *BACH-1*. BACH-1 is a transcription repressor that acts as a key regulator of the expression of genes involved in the cell stress response [71]; thus, since it is encoded on HSA21, BACH-1 is strongly related to the anti-oxidant response in DS [53]. As transcription repressor, BACH-1 competes with Nrf-2 for binding to the

AREs in oxidative stress-response genes. Once in the nucleus, BACH-1 is able to inhibit the transcription of oxidative stress response-genes such as HO-1 and NQO1. Moreover, it was demonstrated that positive and negative regulation of ARE-mediated gene expression depend on the critical balance between Nrf-2 and BACH-1 in the nucleus [89].

These evidences prompted us to investigate the role of BACH-1/Nrf-2 pathway in DS mouse model, the Ts2cje. We first set up a specific protocol to obtain primary cells, neurons and astrocytes, from cortex and hippocampus of Ts2cje pups. We characterized these primary cells as a model to study the molecular features of DS neuropathology. The results obtained from the cells characterization confirmed the over-expression of BACH-1 in Ts2cje cells compared to the euploid cells. Moreover, the Nrf-2 gene expression resulted to be decrease in Ts2cje neurons and astrocytes, along with reduced Nrf-2 protein levels and its consequent decreased translocation in the nucleus. These data suggested an impairment of Nrf-2/BACH-1 axis, due probably to the over-expression of BACH-1. To confirm the impairment of Nrf-2/BACH-1 axis in DS, we evaluated gene and protein expression of their related targets, HO-1 and NQO1, to better understand the involvement of this axis in DS neuropathology. Indeed, the transcription factor Nrf-2 is a key player in the antioxidant defense, as it can induce the transcription of antioxidant and cytoprotective genes. Once translocated into the nucleus, Nrf-2 is able to induce transcriptional activation of antioxidant response element that involves HO-1 and NQO1, among others [143]. Thus, the decreased translocation into the nucleus of Nrf-2, in Ts2cje primary cultures, results in a reduction of gene and protein levels of HO-1 and NQO1, as an index of an impaired anti-oxidant response. Intriguingly, such effect in DS samples is detected at an early time point most likely as the result of the triplication of BACH-1, which competes

with Nrf-2 for ARE sequences [71]. Accordingly, as shown in this study and in our previous work, BACH-1 demonstrates increased expression of the transcript and of the total protein, thus resulting in the lack of HO-1 and NQO1 induction [53]. In addition, our data have been supported by several studies showing the involvement of BACH-1 in HO-1 regulation [91, 92]. Indeed, Sakoda et al. performed studies on BACH-1 knock-out mice (BACH-1^{-/-}) and they showed significantly higher HO-1 gene expression levels with respect to control animals in all brain regions studied [91]. This regulation of HO-1 by BACH-1 was confirmed also by our analysis performed on Ts2cje primary cells that revealed a reduction of HO-1 gene and protein levels compared to the euploid cells, according with the demonstrated impairment of Nrf-2.

To further characterize our DS cell models, we also evaluated the gene and protein levels of APP, another relevant gene coding on HSA21, and we demonstrated its expected increase in the DS.

In addition, to endorse our results obtained in primary cell cultures, we evaluated the gene and protein expressions of BACH-1, also in the hippocampus isolated from Ts2cje mice at 3 months of age. Interestingly, our data obtained in the Ts2cje mice confirmed both an over-expression of BACH-1 and a decrease in Nrf-2 activity, as indexed by its phosphorylation on Ser residue (Ser40). The decreased Nrf-2 phosphorylation on Ser40 is associated to a reduction of the HO-1 protein levels. All together, our results proved a reduction of Nrf-2 activity, likely associated to BACH-1 over-expression in both primary cultures and Tg mice.

To strengthen our understanding of BACH-1/Nrf-2 dysregulation in DS, we characterized LCLs obtained from DS and HD donor, which may serve as a further model to study the genetic of this disorder and provide mechanistic insights on age-associated degeneration in DS.

The DS LCLs showed the same scenario observed in Ts2cje cell models. The results showed an increase of BACH-1 and APP gene and protein levels in DS LCLs compared to the HD control. On the other hand, in LCLs model we observed an impairment of Nrf-2 and its target only on the protein expression. Collected data suggest that in human LCLs cells the trisomy of HSA21 affects BACH-1 and Nrf-2 pathway, as we demonstrated in Ts2cje neuronal cells, and in particular the Nrf-2 impairment could be associated also to a dysregulation of the proteostasis network [144, 145]. In contrast, a study from Zamponi et al. demonstrated that the increased induction of Nrf-2 in human and mouse DS fibroblasts increased along with OS [146]. The observed discrepancy of results between these studies could be ascribed to the variance of gene dosage occurring in DS [147, 148]. The results of the current study suggested that DS brain and blood- derived cells are characterized by the chronic induction of OS, including the Nrf-2/BACH-1 pathway that is a master regulator of the anti-oxidant response. Moreover, the evaluation of BACH-1 functions in the brain, and particularly in neurodegenerative disorders, represents a novel molecular aspect of DS research. Considering that only a limited number of studies addressed this topic to date, our study provides novel evidence on the mechanisms enrolled in DS that lead to compromised antioxidant response, suggesting the gene-dosage hypothesis of BACH-1 as a key player in the dysregulation of Nrf-2 signalling and its downstream modulation of stress response machinery.

Further, we also proposed the efficacy of antioxidant compounds to restore the BACH-1/Nrf-2 axis and their potential application to modulate oxidative stress-phenotype in DS.

Several studies suggest the use of anti-oxidant molecules as an intervention to attenuates OS in DS individuals. Parisotto et al. demonstrated

that the anti-oxidant supplementation in the diet of DS children and teenagers for 6 months can restore the levels of OS biomarkers, that were found over-expressed before the treatment in DS individuals compared with control [149]. Moreover, Valenti D et al, demonstrated the ability of two anti-oxidant polyphenols, resveratrol and epigallocatechin-3-gallate, to reverse the severe impairment of mitochondrial bioenergetics and biogenesis in Ts65Dn-derived hippocampal progenitor cells rescuing the *in vitro* impaired neurogenesis [150]. According with these evidences, we selected two anti-oxidant polyphenols on our human model of DS LCLs: CAPE and VP961. The first compound is a natural polyphenol with demonstrated several biological activities [119] and beneficial effects against neurodegenerative diseases [125, 126], although CAPE has never been proposed as a possible anti-oxidant intervention in DS. While VP961 is a synthetic compound with demonstrated ability to induce HO-1 [120]. Above all, we performed a treatment on neuroblastoma cell line (SHSY-5Y) both to set the experimental condition and to test the anti-oxidant effects of our drugs. Our results confirmed the ability of the two antioxidant compounds to induce Nrf-2 nuclear translocation and to improve the HO-1 gene and protein levels under OS conditions in the same manner.

Interestingly, the DS LCLs were found to be sensitive to the treatment with CAPE and VP961. Indeed, the Nrf-2 nuclear protein amount and its nuclear translocation resulted restored in DS treated cells both with CAPE and VP961. Surprisingly, the synthetic compound, VP961, was more effective than natural one, CAPE, to induce Nrf-2 translocation into the nucleus and also, to increase protein levels of HO-1 in DS LCLs compared to untreated DS. We suggest that treatment with VP961 could be beneficial, compared to CAPE, in modulating Nrf-2/HO-1 pathway in this model.

Based on these collected data, we suggest that further studies on CAPE and VP961 mechanisms need to be performed to confirm their translational application for attenuating DS pathological phenotypes.

5.2 Discussion Project 2

In the present study, a comparative proteomic investigation was performed to identify the putative protein biomarkers of DS that could allow to get a deeper comprehension of the complex mechanisms responsible for DS pathological phenotypes. Gene dosage is believed to play a significant role in determining the wide variability of DS phenotypes [148, 151-153]. While gene dosage may contribute to the phenotype associated with DS, an exact mechanism and specific gene network underlying DS abnormalities are yet to be elucidated [154, 155]. Differentially expressed proteins were identified and a comprehensive study on the proteins associated with DS imbalance was carried out in PBMCs isolated from young DS individuals compared with healthy age-matched donors. PBMCs, by reflecting at systemic level cellular alterations driven by trisomic condition, represent a valuable model to elucidate the molecular mechanisms of DS pathology, including those that characterize neurodegeneration [145, 156]. Collected results agree with published studies from our group and others showing the early alterations of specific cellular pathways in DS individuals that are considered to contribute to the accelerated-aging phenotype, ultimately resulting in the early onset of Alzheimer dementia in DS [19, 26, 45, 62, 157-162].

We suggest that a well-defined number of pathways, including intracellular trafficking, stress responses, cytoskeleton network, and energy

metabolism are significantly disrupted in PBMCs from young DS individuals, reflecting alterations already observed in other tissues [45, 157, 163]. The presence of Rab GTPases, increasingly expressed in HD cases only, demonstrate a massive dysfunction of the intracellular membrane trafficking in DS. Alterations of Rab GTPases, or of the membrane compartments that they regulate, are associated with virtually all cellular activities in health and disease. They mediate fundamental processes of vesicle sorting and transport between target membranes [164, 165]. Consequently, Rab GTPases are commonly used as markers and identifiers of various organelles and vesicles in the endocytic and secretory systems. Of particular interest in the present study is Rab-3A, whose downregulation was already reported in human frontal cortex from DS individuals [166].

In this scenario, our data suggest that the reduction of Rab3A could be an early event in DS that occurs at different body compartments thus representing a shared mechanism of cell alteration. Furthermore, in the present study we found both Rab10 and Rab2 as UNIQUE proteins in HD cases. Rab1 and Rab2 regulate the transport of vesicles between ER and Golgi [167]. Amber R. English et al. have also identified Rab10 as an ER-specific Rab GTPase that regulates ER structure and dynamics [168]. Another major finding of this study was that the protein levels of Rab GDP-dissociation inhibitor 2 (GDI-2) were significantly decreased in DS, as observed in a fetal Down syndrome brain by R. Weitzdoerfer et al. [169]. Rab GDP-dissociation inhibitor 2 (GDI-2) is a regulatory protein involved in membrane release of Rabs [170] that holds an essential role in vesicle formation, vesicle docking, and membrane fusion [171]. The depletion of the GDI gene in yeast led to various transport defects in the cell, demonstrating the high importance of GDIs function [172]. Furthermore D'Adamo et al. showed that GDI has an

important role in neuronal function and a mutation in the gene encoding GDI-1 is responsible for X-linked mental retardation [172]. Taken together these results suggest that decreased levels of GDI-2, together with the alteration of Rab proteins, found in PBMCs from DS patients may represent one of the multiple factors leading to impaired vesicles transport observed in DS [173].

Membrane trafficking is essential for protein synthesis, processing, sorting, and turnover in the ER and Golgi apparatus. The ER is a multifunctional organelle that coordinates protein folding, lipid biosynthesis, and calcium storage and release [174]. The alteration of ER trafficking is associated with the perturbations of ER homeostasis that lead to ER stress and to the activation of specific stress responses involved in protein folding and/or degradation. These response mechanisms include the induction of the unfolded protein response (UPR) and of re-folding proteins such as PDIs. Our proteomics analysis demonstrates the differential expression, in PBMCs from DS children, of proteins belonging to ER stress responses with a role in protein folding and unfolded protein binding. We found the altered expression of GRP78, ATF6, and CHOP components of the UPR, and of ERO1 and PDIA1.

Interestingly, our current data confirm that ER stress and UPR are primary events in DS and might have a prominent role in pathological processes [156]. Such hypothesis is further corroborated by different authors that observed dysfunctional UPR and ISR (integrated stress response) in DS human and mice, supporting a role for trisomy-related aberrant UPR/ISR induction in the disruption of the proteostasis network [145, 175]. Over the above-cited proteins involved in the UPR and folding related to the ER, the selective recognition of oxidized/misfolded proteins by molecular chaperones (HSPs) is the first step toward their elimination. Heat shock protein 70 (HSP70) and heat shock protein 90 (HSP90) are chaperones that interact with

the outer mitochondrial membrane, stabilizing the unfolded state of the nascent proteins and thereby preventing their aggregation. We showed that HSP70 and HSP90 were significantly downregulated in DS suggesting a prevention in the formation of the appropriate interactions with the proteins target resulting in protein misfolding and a consequent exacerbation of oxidative stress. The increase of oxidative stress is demonstrated to occur in our sample and is known to be involved in DS phenotype as an effect of the increased production of pro-oxidant species due to the triplication of SOD-1 gene, among other. However, an involvement of differentially induced antioxidant responses has been also documented. We previously observed in DS blood-derived and brain samples the depletion of Nrf2-related antioxidant response, as an effect of BACH-1 triplication, and its uncoupling with UPR defining a further degree of connection between proteostasis and OS [156]. Here we show that the increased expression levels of peroxiredoxins subtypes (Prx-proteins) in DS PBMCs suggest the activation of the Prx system due to unbalanced redox homeostasis [176]. Overall, the increased expression of Prx subtypes was already observed in brain patients with AD and DS [177].

Histones proteins represent a common target of ROS and RNS irreversible damage, that is able to alter their folding, expression, and stability, as well as, to induce their aberrant post-translational modification [178] thus severely impacting the global structure of chromatin, gene expression, genome stability, and replication. The alteration of proteins involved in DNA structure found by proteomic data concern mainly the DS group. We identified the altered expression of all the five types of histone proteins: H2A, H2B, H3, H4, and H1; and, except for H4, they all were identified as multiple isoforms. The increase in histone transcript levels that normally occurs during aging suggest a protection of the cells from premature aging, while the reduced histone

expression in the short-lived mutants is a cause of their shortened lifespan. In agreement, Feser et al. demonstrated that the increase in the gene expression of all four core histones extended the median lifespan of *asf1* mutants by 65% [179]. Within this context, our data suggest that the increased histones expression might represent a response to counteract the accelerated aging observed in DS.

Proteomics data also highlight the alteration of a central cellular function, the energy production. Collected results suggest that young DS individuals show an altered metabolic profile as indicated by a reduced expression of mitochondrial enzymes and of enzymes belonging to the pentose phosphate pathway (PPP), while in the presence of increased expression of glycolytic enzymes, including aldolase, GAPDH, and PGK1,2. Glycolysis is a fundamental feature of all cells and is therefore involved in a range of cellular responses that have been associated with both neurodevelopmental and neurodegenerative disorders. This includes effects on the immune system, cytoskeletal abnormalities, synaptic plasticity, and neurogenesis. We suggest that upregulation of glycolysis may be a compensatory mechanism in response to impaired mitochondrial function. neurodegenerative disorders. This includes effects on the immune system, cytoskeletal abnormalities, synaptic plasticity, and neurogenesis. We suggest that upregulation of glycolysis may be a compensatory mechanism in response to impaired mitochondrial function. Abnormalities in glucose metabolism and the link to metabolic syndrome in DS patients have been recently proposed [163] with evidences deriving from metabolome profile of plasma from DS [180, 181], genes associated with glycolysis and signs of abnormal glucose metabolism evidenced in DS individuals and mouse models thereof [163]. Taken together, this signature suggests that a condition of hypometabolism occurs in DS individuals, likely

because of the lowered glucose uptake, an early occurrence of insulin resistance associated with reduced mitochondrial activity [160]. Interestingly, our group, highlighted for the first time that markers of brain insulin resistance are evident in DS brain even before the development of AD pathology [160], suggesting that these alterations might support the mechanisms associated with intellectual disability, as well as the early onset of AD in people with DS [19].

Increasing evidences indicates that cytoskeletal abnormalities are observed already in prenatal life and may be largely responsible for the cortical dysgenesis in DS [159]. Among cytoskeleton components, we found that actin-related protein 2/3 complexes, tropomyosin, tubulin, cofilin, and myosin are overexpressed in DS vs. healthy controls. The microtubule cytoskeleton network is made up of tubulin subunits and actin filaments and serves multiple roles in neurons [182]. It provides a structural framework for axons and dendrites, representing a major determinant of neuronal size and morphology. It also serves as a track for transport and plays essential roles in growth and development. In contrast to microtubules that function individually, actin filaments work in networks or bundles that function to control cell shape, distribution of membrane proteins, and cell–cell interactions. Interestingly, in DS, cytoskeleton integrity seems to be strictly related to aberrant expression of Dyrk1A [183]. Published studies showed that both brain tissue and immortalized lymphocytes of DS patients displayed a significant reduction in the yield of all the major cytoskeletal proteins co-immunoprecipitated with DYRK1A antibodies [184]. Similarly to DS cells, overexpression of DYRK1A in trisomic TgDYRK1A mice was shown to cause alterations in actin dynamic through increased stability of actin filaments [185]. Further, results from Ori-McKenney et al. demonstrated that the regulation of microtubule dynamics by DYRK1A-mediated phosphorylation is critical for dendritic patterning and

neuronal function, revealing a previously unidentified mode of post-translational microtubule regulation in neurons and uncovering a conserved pathway for a DS- associated kinase [183]. Conversely, Weitzdoerfer et al. reported the reduction of actin-related protein complex 2/3 in a fetal Down syndrome brain [186]. Our findings showing altered expression of cytoskeleton proteins in DS vs. healthy controls suggest that immune peripheral cell also retains the similar aberrant phenotype that is likely to play a central role in neurons. Dysfunction of cytoskeleton network may be considered a key pathological signature of DS.

Finally, we found the aberrant expression of several signaling proteins among which the reduced expression of protein kinase C (PKC) in DS group results in particular interest for the comprehension of the pathological processes. Reduced PKC activity was demonstrated in the brain of a DS mouse model [187] and in agreement with this, we support the decreased functionality of PKC signaling as pathological contributor of DS phenotype.

6. CONCLUSIONS

The characterization of several DS models, such as the primary cells from Ts2cje mice, the Ts2cje mice at 3 months and the human model of LCLs demonstrate the impairment of BACH-1/Nrf-2 pathway and its role in DS pathology. The reduced anti-oxidant response is confirmed by the evaluation of HO-1 and NQO1 gene and protein levels which result decreased. Tested the anti-oxidants compounds, CAPE and VP961 able to induce Nrf-2/HO-1 pathway, we demonstrate the possibility to modulate the alteration seen in human DS model.

Moreover, the comparative proteomic analysis on PBMCs from HD and DS young patients revealed a well-defined number of dysregulated pathways, including oxidative stress response in DS PBMCs compared to the control. This confirms the implication of OS in DS pathological features. In conclusion our study supports the role of OS in DS pathology as a chronic condition.

7. REFERENCES

1. Lejeune, J., M. Gautier, and R. Turpin, [*Study of somatic chromosomes from 9 mongoloid children*]. C R Hebd Seances Acad Sci, 1959. **248**(11): p. 1721-2.
2. Roizen, N.J. and D. Patterson, *Down's syndrome*. Lancet, 2003. **361**(9365): p. 1281-9.
3. Neale, N., et al., *Neuroimaging and other modalities to assess Alzheimer's disease in Down syndrome*. Neuroimage Clin, 2018. **17**: p. 263-271.
4. Wiseman, F.K., et al., *A genetic cause of Alzheimer disease: mechanistic insights from Down syndrome*. Nat Rev Neurosci, 2015. **16**(9): p. 564-74.
5. Antonarakis, S.E., et al., *Down syndrome*. Nat Rev Dis Primers, 2020. **6**(1): p. 9.
6. Bittles, A.H., et al., *The four ages of Down syndrome*. Eur J Public Health, 2007. **17**(2): p. 221-5.
7. de Graaf, G., F. Buckley, and B.G. Skotko, *Estimation of the number of people with Down syndrome in the United States*. Genet Med, 2017. **19**(4): p. 439-447.
8. Strauss, D. and R.K. Eyman, *Mortality of people with mental retardation in California with and without Down syndrome, 1986-1991*. Am J Ment Retard, 1996. **100**(6): p. 643-53.
9. Head, E., et al., *Aging and down syndrome*. Curr Gerontol Geriatr Res, 2012. **2012**: p. 412536.
10. Perluigi, M., F. Di Domenico, and D.A. Buttterfield, *Unraveling the complexity of neurodegeneration in brains of subjects with Down syndrome: insights from proteomics*. Proteomics Clin Appl, 2014. **8**(1-2): p. 73-85.
11. Head, E., et al., *Aging in Down Syndrome and the Development of Alzheimer's Disease Neuropathology*. Curr Alzheimer Res, 2016. **13**(1): p. 18-29.
12. Wang, C.C., et al., *Gene dosage imbalance of human chromosome 21 in mouse embryonic stem cells differentiating to neurons*. Gene, 2011. **481**(2): p. 93-101.
13. Glasson, E.J., et al., *The changing survival profile of people with Down's syndrome: implications for genetic counselling*. Clin Genet, 2002. **62**(5): p. 390-3.

14. Franceschi, M., et al., *Prevalence of dementia in adult patients with trisomy 21*. Am J Med Genet Suppl, 1990. **7**: p. 306-8.
15. Prasher, V.P. and A. Filer, *Behavioural disturbance in people with Down's syndrome and dementia*. J Intellect Disabil Res, 1995. **39 (Pt 5)**: p. 432-6.
16. Holland, A.J., et al., *Incidence and course of dementia in people with Down's syndrome: findings from a population-based study*. J Intellect Disabil Res, 2000. **44 (Pt 2)**: p. 138-46.
17. Oliver, C., et al., *A four year prospective study of age-related cognitive change in adults with Down's syndrome*. Psychol Med, 1998. **28(6)**: p. 1365-77.
18. Oliver, C., et al., *Effects of increasing task load on memory impairment in adults with Down syndrome*. Am J Ment Retard, 2005. **110(5)**: p. 339-45.
19. Lott, I.T. and E. Head, *Dementia in Down syndrome: unique insights for Alzheimer disease research*. Nat Rev Neurol, 2019. **15(3)**: p. 135-147.
20. Lao, P.J., et al., *Alzheimer-Like Pattern of Hypometabolism Emerges with Elevated Amyloid-beta Burden in Down Syndrome*. J Alzheimers Dis, 2018. **61(2)**: p. 631-644.
21. De-Paula, V.J., et al., *Alzheimer's disease*. Subcell Biochem, 2012. **65**: p. 329-52.
22. Di Domenico, F., et al., *Redox proteomics analysis of HNE-modified proteins in Down syndrome brain: clues for understanding the development of Alzheimer disease*. Free Radic Biol Med, 2014. **71**: p. 270-280.
23. Zana, M., Z. Janka, and J. Kalman, *Oxidative stress: a bridge between Down's syndrome and Alzheimer's disease*. Neurobiol Aging, 2007. **28(5)**: p. 648-76.
24. Doran, E., et al., *Down Syndrome, Partial Trisomy 21, and Absence of Alzheimer's Disease: The Role of APP*. J Alzheimers Dis, 2017. **56(2)**: p. 459-470.
25. Prasher, V.P., et al., *Molecular mapping of Alzheimer-type dementia in Down's syndrome*. Ann Neurol, 1998. **43(3)**: p. 380-3.
26. Cataldo, A.M., et al., *Down syndrome fibroblast model of Alzheimer-related endosome pathology: accelerated endocytosis promotes late endocytic defects*. Am J Pathol, 2008. **173(2)**: p. 370-84.
27. Shukkur, E.A., et al., *Mitochondrial dysfunction and tau hyperphosphorylation in Ts1Cje, a mouse model for Down syndrome*. Hum Mol Genet, 2006. **15(18)**: p. 2752-62.

28. Drewes, G., et al., *Dephosphorylation of tau protein and Alzheimer paired helical filaments by calcineurin and phosphatase-2A*. FEBS Lett, 1993. **336**(3): p. 425-32.
29. Dowjat, W.K., et al., *Trisomy-driven overexpression of DYRK1A kinase in the brain of subjects with Down syndrome*. Neurosci Lett, 2007. **413**(1): p. 77-81.
30. Liu, F., et al., *Overexpression of Dyrk1A contributes to neurofibrillary degeneration in Down syndrome*. FASEB J, 2008. **22**(9): p. 3224-33.
31. Busciglio, J. and B.A. Yankner, *Apoptosis and increased generation of reactive oxygen species in Down's syndrome neurons in vitro*. Nature, 1995. **378**(6559): p. 776-9.
32. Picard, M. and B.S. McEwen, *Mitochondria impact brain function and cognition*. Proc Natl Acad Sci U S A, 2014. **111**(1): p. 7-8.
33. Brooksbank, B.W., M. Martinez, and R. Balazs, *Altered composition of polyunsaturated fatty acyl groups in phosphoglycerides of Down's syndrome fetal brain*. J Neurochem, 1985. **44**(3): p. 869-74.
34. Odetti, P., et al., *Early glycoxidation damage in brains from Down's syndrome*. Biochem Biophys Res Commun, 1998. **243**(3): p. 849-51.
35. Cenini, G., et al., *Association between frontal cortex oxidative damage and beta-amyloid as a function of age in Down syndrome*. Biochim Biophys Acta, 2012. **1822**(2): p. 130-8.
36. de Haan, J.B., et al., *Elevation in the ratio of Cu/Zn-superoxide dismutase to glutathione peroxidase activity induces features of cellular senescence and this effect is mediated by hydrogen peroxide*. Hum Mol Genet, 1996. **5**(2): p. 283-92.
37. Shariati, S.A. and B. De Strooper, *Redundancy and divergence in the amyloid precursor protein family*. FEBS Lett, 2013. **587**(13): p. 2036-45.
38. Zhang, Y.W., et al., *APP processing in Alzheimer's disease*. Mol Brain, 2011. **4**: p. 3.
39. Choi, J.H., et al., *Age-dependent dysregulation of brain amyloid precursor protein in the Ts65Dn Down syndrome mouse model*. J Neurochem, 2009. **110**(6): p. 1818-27.
40. Cheon, M.S., et al., *Protein expression of BACE1, BACE2 and APP in Down syndrome brains*. Amino Acids, 2008. **35**(2): p. 339-43.
41. Seo, H. and O. Isacson, *Abnormal APP, cholinergic and cognitive function in Ts65Dn Down's model mice*. Exp Neurol, 2005. **193**(2): p. 469-80.

42. Teller, J.K., et al., *Presence of soluble amyloid beta-peptide precedes amyloid plaque formation in Down's syndrome*. Nat Med, 1996. **2**(1): p. 93-5.
43. Murray, A., et al., *Brief report: isogenic induced pluripotent stem cell lines from an adult with mosaic down syndrome model accelerated neuronal ageing and neurodegeneration*. Stem Cells, 2015. **33**(6): p. 2077-84.
44. Shi, Y., et al., *A human stem cell model of early Alzheimer's disease pathology in Down syndrome*. Sci Transl Med, 2012. **4**(124): p. 124ra29.
45. Di Domenico, F., et al., *Impairment of proteostasis network in Down syndrome prior to the development of Alzheimer's disease neuropathology: redox proteomics analysis of human brain*. Biochim Biophys Acta, 2013. **1832**(8): p. 1249-59.
46. Perluigi, M., F. Di Domenico, and D.A. Butterfield, *mTOR signaling in aging and neurodegeneration: At the crossroad between metabolism dysfunction and impairment of autophagy*. Neurobiol Dis, 2015. **84**: p. 39-49.
47. Witman, G.B., et al., *Tubulin requires tau for growth onto microtubule initiating sites*. Proc Natl Acad Sci U S A, 1976. **73**(11): p. 4070-4.
48. Rodriguez-Martin, T., et al., *Tau phosphorylation affects its axonal transport and degradation*. Neurobiol Aging, 2013. **34**(9): p. 2146-57.
49. Rahmani, Z., et al., *Expression of the mnb (dyrk) protein in adult and embryonic mouse tissues*. Biochem Biophys Res Commun, 1998. **253**(2): p. 514-8.
50. Marti, E., et al., *Dyrk1A expression pattern supports specific roles of this kinase in the adult central nervous system*. Brain Res, 2003. **964**(2): p. 250-63.
51. Lloret, A., et al., *Amyloid-beta toxicity and tau hyperphosphorylation are linked via RCAN1 in Alzheimer's disease*. J Alzheimers Dis, 2011. **27**(4): p. 701-9.
52. Conti, A., et al., *Altered expression of mitochondrial and extracellular matrix genes in the heart of human fetuses with - chromosome 21 trisomy*. BMC Genomics, 2007. **8**: p. 268.
53. Di Domenico, F., et al., *Bach1 overexpression in Down syndrome correlates with the alteration of the HO-1/BVR-a system: insights for transition to Alzheimer's disease*. J Alzheimers Dis, 2015. **44**(4): p. 1107-20.

54. Montine, T.J., et al., *Lipid peroxidation in aging brain and Alzheimer's disease*. *Free Radic Biol Med*, 2002. **33**(5): p. 620-6.
55. Butterfield, D.A. and B. Halliwell, *Oxidative stress, dysfunctional glucose metabolism and Alzheimer disease*. *Nat Rev Neurosci*, 2019. **20**(3): p. 148-160.
56. Halliwell, B., *Reactive oxygen species in living systems: source, biochemistry, and role in human disease*. *Am J Med*, 1991. **91**(3C): p. 14S-22S.
57. Cenini, G., A. Lloret, and R. Cascella, *Oxidative Stress in Neurodegenerative Diseases: From a Mitochondrial Point of View*. *Oxid Med Cell Longev*, 2019. **2019**: p. 2105607.
58. Capone, G.T., *Down syndrome: advances in molecular biology and the neurosciences*. *J Dev Behav Pediatr*, 2001. **22**(1): p. 40-59.
59. Pallardo, F.V., et al., *Multiple evidence for an early age pro-oxidant state in Down Syndrome patients*. *Biogerontology*, 2006. **7**(4): p. 211-20.
60. Nunomura, A., et al., *Oxidative damage is the earliest event in Alzheimer disease*. *J Neuropathol Exp Neurol*, 2001. **60**(8): p. 759-67.
61. Barone, E., et al., *HNE-modified proteins in Down syndrome: Involvement in development of Alzheimer disease neuropathology*. *Free Radic Biol Med*, 2017. **111**: p. 262-269.
62. Perluigi, M. and D.A. Butterfield, *Oxidative Stress and Down Syndrome: A Route toward Alzheimer-Like Dementia*. *Curr Gerontol Geriatr Res*, 2012. **2012**: p. 724904.
63. Butterfield, D.A., et al., *Redox proteomics in selected neurodegenerative disorders: from its infancy to future applications*. *Antioxid Redox Signal*, 2012. **17**(11): p. 1610-55.
64. Butterfield, D.A., A.M. Swomley, and R. Sultana, *Amyloid beta-peptide (1-42)-induced oxidative stress in Alzheimer disease: importance in disease pathogenesis and progression*. *Antioxid Redox Signal*, 2013. **19**(8): p. 823-35.
65. Mao, P. and P.H. Reddy, *Aging and amyloid beta-induced oxidative DNA damage and mitochondrial dysfunction in Alzheimer's disease: implications for early intervention and therapeutics*. *Biochim Biophys Acta*, 2011. **1812**(11): p. 1359-70.
66. Butterfield, D.A. and D. Boyd-Kimball, *Redox proteomics and amyloid beta-peptide: insights into Alzheimer disease*. *J Neurochem*, 2019. **151**(4): p. 459-487.
67. Head, E. and I.T. Lott, *Down syndrome and beta-amyloid deposition*. *Curr Opin Neurol*, 2004. **17**(2): p. 95-100.

68. Mehta, P.D., et al., *Increased amyloid beta protein levels in children and adolescents with Down syndrome*. J Neurol Sci, 2007. **254**(1-2): p. 22-7.
69. Anandatheerthavarada, H.K., et al., *Mitochondrial targeting and a novel transmembrane arrest of Alzheimer's amyloid precursor protein impairs mitochondrial function in neuronal cells*. J Cell Biol, 2003. **161**(1): p. 41-54.
70. Simon, A.M., et al., *Overexpression of wild-type human APP in mice causes cognitive deficits and pathological features unrelated to Abeta levels*. Neurobiol Dis, 2009. **33**(3): p. 369-78.
71. Zhang, X., et al., *Bach1: Function, Regulation, and Involvement in Disease*. Oxid Med Cell Longev, 2018. **2018**: p. 1347969.
72. Balcz, B., et al., *Increased brain protein levels of carbonyl reductase and alcohol dehydrogenase in Down syndrome and Alzheimer's disease*. J Neural Transm Suppl, 2001(61): p. 193-201.
73. Butterfield, D.A., et al., *Redox proteomics analysis to decipher the neurobiology of Alzheimer-like neurodegeneration: overlaps in Down's syndrome and Alzheimer's disease brain*. Biochem J, 2014. **463**(2): p. 177-89.
74. Butterfield, D.A. and D. Boyd-Kimball, *Oxidative Stress, Amyloid-beta Peptide, and Altered Key Molecular Pathways in the Pathogenesis and Progression of Alzheimer's Disease*. J Alzheimers Dis, 2018. **62**(3): p. 1345-1367.
75. Sultana, R., M. Perluigi, and D.A. Butterfield, *Oxidatively modified proteins in Alzheimer's disease (AD), mild cognitive impairment and animal models of AD: role of Abeta in pathogenesis*. Acta Neuropathol, 2009. **118**(1): p. 131-50.
76. Pratico, D., et al., *Down's syndrome is associated with increased 8,12-iso-iPF2alpha-VI levels: evidence for enhanced lipid peroxidation in vivo*. Ann Neurol, 2000. **48**(5): p. 795-8.
77. McMahon, M., et al., *Dimerization of substrate adaptors can facilitate cullin-mediated ubiquitylation of proteins by a "tethering" mechanism: a two-site interaction model for the Nrf2-Keap1 complex*. J Biol Chem, 2006. **281**(34): p. 24756-68.
78. Zhang, H., K.J.A. Davies, and H.J. Forman, *Oxidative stress response and Nrf2 signaling in aging*. Free Radic Biol Med, 2015. **88**(Pt B): p. 314-336.
79. Itoh, K., J. Mimura, and M. Yamamoto, *Discovery of the negative regulator of Nrf2, Keap1: a historical overview*. Antioxid Redox Signal, 2010. **13**(11): p. 1665-78.

80. Helguera, P., et al., *Adaptive downregulation of mitochondrial function in down syndrome*. Cell Metab, 2013. **17**(1): p. 132-40.
81. Swatton, J.E., et al., *Increased MAP kinase activity in Alzheimer's and Down syndrome but not in schizophrenia human brain*. Eur J Neurosci, 2004. **19**(10): p. 2711-9.
82. Oyake, T., et al., *Bach proteins belong to a novel family of BTB-basic leucine zipper transcription factors that interact with MafK and regulate transcription through the NF-E2 site*. Mol Cell Biol, 1996. **16**(11): p. 6083-95.
83. Ogawa, K., et al., *Heme mediates derepression of Maf recognition element through direct binding to transcription repressor Bach1*. EMBO J, 2001. **20**(11): p. 2835-43.
84. Sun, J., et al., *Heme regulates the dynamic exchange of Bach1 and NF-E2-related factors in the Maf transcription factor network*. Proc Natl Acad Sci U S A, 2004. **101**(6): p. 1461-6.
85. Kaspar, J.W. and A.K. Jaiswal, *Antioxidant-induced phosphorylation of tyrosine 486 leads to rapid nuclear export of Bach1 that allows Nrf2 to bind to the antioxidant response element and activate defensive gene expression*. J Biol Chem, 2010. **285**(1): p. 153-62.
86. Suzuki, H., et al., *Cadmium induces nuclear export of Bach1, a transcriptional repressor of heme oxygenase-1 gene*. J Biol Chem, 2003. **278**(49): p. 49246-53.
87. Suzuki, H., et al., *Heme regulates gene expression by triggering Crml-dependent nuclear export of Bach1*. EMBO J, 2004. **23**(13): p. 2544-53.
88. Sun, J., et al., *Hemoprotein Bach1 regulates enhancer availability of heme oxygenase-1 gene*. EMBO J, 2002. **21**(19): p. 5216-24.
89. Dhakshinamoorthy, S., et al., *Bach1 competes with Nrf2 leading to negative regulation of the antioxidant response element (ARE)-mediated NAD(P)H:quinone oxidoreductase 1 gene expression and induction in response to antioxidants*. J Biol Chem, 2005. **280**(17): p. 16891-900.
90. Ka, S.O., et al., *Hepatocyte-specific sirtuin 6 deletion predisposes to nonalcoholic steatohepatitis by up-regulation of Bach1, an Nrf2 repressor*. FASEB J, 2017. **31**(9): p. 3999-4010.
91. Sakoda, E., et al., *Regulation of heme oxygenase-1 by transcription factor Bach1 in the mouse brain*. Neurosci Lett, 2008. **440**(2): p. 160-5.

92. Kanno, H., et al., *Genetic ablation of transcription repressor Bach1 reduces neural tissue damage and improves locomotor function after spinal cord injury in mice*. J Neurotrauma, 2009. **26**(1): p. 31-9.
93. Shim, K.S., R. Ferrando-Miguel, and G. Lubec, *Aberrant protein expression of transcription factors BACH1 and ERG, both encoded on chromosome 21, in brains of patients with Down syndrome and Alzheimer's disease*. J Neural Transm Suppl, 2003(67): p. 39-49.
94. Ferrando-Miguel, R., et al., *Overexpression of transcription factor BACH1 in fetal Down syndrome brain*. J Neural Transm Suppl, 2003(67): p. 193-205.
95. Schipper, H.M., et al., *The sinister face of heme oxygenase-1 in brain aging and disease*. Prog Neurobiol, 2019. **172**: p. 40-70.
96. Barone, E., et al., *The Janus face of the heme oxygenase/biliverdin reductase system in Alzheimer disease: it's time for reconciliation*. Neurobiol Dis, 2014. **62**: p. 144-59.
97. Sferrazzo, G., et al., *Heme Oxygenase-1 in Central Nervous System Malignancies*. J Clin Med, 2020. **9**(5).
98. Baranano, D.E. and S.H. Snyder, *Neural roles for heme oxygenase: contrasts to nitric oxide synthase*. Proc Natl Acad Sci U S A, 2001. **98**(20): p. 10996-1002.
99. Bergeron, M., D.M. Ferriero, and F.R. Sharp, *Developmental expression of heme oxygenase-1 (HSP32) in rat brain: an immunocytochemical study*. Brain Res Dev Brain Res, 1998. **105**(2): p. 181-94.
100. Matz, P., et al., *Heme-oxygenase-1 induction in glia throughout rat brain following experimental subarachnoid hemorrhage*. Brain Res, 1996. **713**(1-2): p. 211-22.
101. Nakaso, K., et al., *Oxidative stress-related proteins A170 and heme oxygenase-1 are differently induced in the rat cerebellum under kainate-mediated excitotoxicity*. Neurosci Lett, 2000. **282**(1-2): p. 57-60.
102. Vincent, S.R., S. Das, and M.D. Maines, *Brain heme oxygenase isoenzymes and nitric oxide synthase are co-localized in select neurons*. Neuroscience, 1994. **63**(1): p. 223-31.
103. Maines, M.D., *The heme oxygenase system: a regulator of second messenger gases*. Annu Rev Pharmacol Toxicol, 1997. **37**: p. 517-54.
104. Maines, M.D., *The heme oxygenase system and its functions in the brain*. Cell Mol Biol (Noisy-le-grand), 2000. **46**(3): p. 573-85.
105. Mancuso, C., *Heme oxygenase and its products in the nervous system*. Antioxid Redox Signal, 2004. **6**(5): p. 878-87.

106. Tramutola, A., et al., *It Is All about (U)biqutin: Role of Altered Ubiquitin-Proteasome System and UCHL1 in Alzheimer Disease*. *Oxid Med Cell Longev*, 2016. **2016**: p. 2756068.
107. Tramutola, A., et al., *Polyubiquitylation Profile in Down Syndrome Brain Before and After the Development of Alzheimer Neuropathology*. *Antioxid Redox Signal*, 2017. **26**(7): p. 280-298.
108. Barone, E. and D.A. Butterfield, *Insulin resistance in Alzheimer disease: Is heme oxygenase-1 an Achille's heel?* *Neurobiol Dis*, 2015. **84**: p. 69-77.
109. Fao, L., S.I. Mota, and A.C. Rego, *Shaping the Nrf2-ARE-related pathways in Alzheimer's and Parkinson's diseases*. *Ageing Res Rev*, 2019. **54**: p. 100942.
110. Ramsey, C.P., et al., *Expression of Nrf2 in neurodegenerative diseases*. *J Neuropathol Exp Neurol*, 2007. **66**(1): p. 75-85.
111. Mota, S.I., et al., *Oxidative stress involving changes in Nrf2 and ER stress in early stages of Alzheimer's disease*. *Biochim Biophys Acta*, 2015. **1852**(7): p. 1428-41.
112. Torres-Lista, V., et al., *Neophobia, NQO1 and SIRT1 as premorbid and prodromal indicators of AD in 3xTg-AD mice*. *Behav Brain Res*, 2014. **271**: p. 140-6.
113. Resende, R., et al., *Brain oxidative stress in a triple-transgenic mouse model of Alzheimer disease*. *Free Radic Biol Med*, 2008. **44**(12): p. 2051-7.
114. Kanninen, K., et al., *Nuclear factor erythroid 2-related factor 2 protects against beta amyloid*. *Mol Cell Neurosci*, 2008. **39**(3): p. 302-13.
115. Buee, L., *Dementia Therapy Targeting Tau*. *Adv Exp Med Biol*, 2019. **1184**: p. 407-416.
116. Warnatz, H.J., et al., *The BTB and CNC homology 1 (BACH1) target genes are involved in the oxidative stress response and in control of the cell cycle*. *J Biol Chem*, 2011. **286**(26): p. 23521-32.
117. Koglsberger, S., et al., *Gender-Specific Expression of Ubiquitin-Specific Peptidase 9 Modulates Tau Expression and Phosphorylation: Possible Implications for Tauopathies*. *Mol Neurobiol*, 2017. **54**(10): p. 7979-7993.
118. Piras, S., et al., *Differentiation impairs Bach1 dependent HO-1 activation and increases sensitivity to oxidative stress in SH-SY5Y neuroblastoma cells*. *Sci Rep*, 2017. **7**(1): p. 7568.
119. Murtaza, G., et al., *Caffeic acid phenethyl ester and therapeutic potentials*. *Biomed Res Int*, 2014. **2014**: p. 145342.

120. Pittala, V., et al., *Novel Caffeic Acid Phenethyl Ester (Cape) Analogues as Inducers of Heme Oxygenase-1*. *Curr Pharm Des*, 2017. **23**(18): p. 2657-2664.
121. Magesh, S., Y. Chen, and L. Hu, *Small molecule modulators of Keap1-Nrf2-ARE pathway as potential preventive and therapeutic agents*. *Med Res Rev*, 2012. **32**(4): p. 687-726.
122. Park, J.H., et al., *Immunomodulatory effect of caffeic acid phenethyl ester in Balb/c mice*. *Int Immunopharmacol*, 2004. **4**(3): p. 429-36.
123. Liao, H.F., et al., *Inhibitory effect of caffeic acid phenethyl ester on angiogenesis, tumor invasion, and metastasis*. *J Agric Food Chem*, 2003. **51**(27): p. 7907-12.
124. Parlakpinar, H., et al., *Protective effect of caffeic acid phenethyl ester (CAPE) on myocardial ischemia-reperfusion-induced apoptotic cell death*. *Toxicology*, 2005. **209**(1): p. 1-14.
125. Wei, X., et al., *Caffeic acid phenethyl ester prevents neonatal hypoxic-ischaemic brain injury*. *Brain*, 2004. **127**(Pt 12): p. 2629-35.
126. Wei, X., et al., *Caffeic acid phenethyl ester prevents cerebellar granule neurons (CGNs) against glutamate-induced neurotoxicity*. *Neuroscience*, 2008. **155**(4): p. 1098-105.
127. Zhao, J., et al., *Caffeic Acid phenethyl ester protects blood-brain barrier integrity and reduces contusion volume in rodent models of traumatic brain injury*. *J Neurotrauma*, 2012. **29**(6): p. 1209-18.
128. Barros Silva, R., et al., *Caffeic acid phenethyl ester protects against the dopaminergic neuronal loss induced by 6-hydroxydopamine in rats*. *Neuroscience*, 2013. **233**: p. 86-94.
129. Scapagnini, G., et al., *Caffeic acid phenethyl ester and curcumin: a novel class of heme oxygenase-1 inducers*. *Mol Pharmacol*, 2002. **61**(3): p. 554-61.
130. Silva, T., et al., *Development of Blood-Brain Barrier Permeable Nitrocatechol-Based Catechol O-Methyltransferase Inhibitors with Reduced Potential for Hepatotoxicity*. *J Med Chem*, 2016. **59**(16): p. 7584-97.
131. Kumar, M., D. Kaur, and N. Bansal, *Caffeic Acid Phenethyl Ester (CAPE) Prevents Development of STZ-ICV Induced dementia in Rats*. *Pharmacogn Mag*, 2017. **13**(Suppl 1): p. S10-S15.
132. Morroni, F., et al., *Neuroprotective Effect of Caffeic Acid Phenethyl Ester in A Mouse Model of Alzheimer's Disease Involves Nrf2/HO-1 Pathway*. *Aging Dis*, 2018. **9**(4): p. 605-622.
133. Sorrenti, V., et al., *Protective Effects of Caffeic Acid Phenethyl Ester (CAPE) and Novel Cape Analogue as Inducers of Heme Oxygenase-1*

- in Streptozotocin-Induced Type 1 Diabetic Rats*. Int J Mol Sci, 2019. **20**(10).
134. Reinholdt, L.G., et al., *Molecular characterization of the translocation breakpoints in the Down syndrome mouse model Ts65Dn*. Mamm Genome, 2011. **22**(11-12): p. 685-91.
 135. Piano Mortari, E., et al., *The Vici syndrome protein EPG5 regulates intracellular nucleic acid trafficking linking autophagy to innate and adaptive immunity*. Autophagy, 2018. **14**(1): p. 22-37.
 136. Distler, U., et al., *Label-free quantification in ion mobility-enhanced data-independent acquisition proteomics*. Nat Protoc, 2016. **11**(4): p. 795-812.
 137. Greco, V., et al., *Proteomics and Toxicity Analysis of Spinal-Cord Primary Cultures upon Hydrogen Sulfide Treatment*. Antioxidants (Basel), 2018. **7**(7).
 138. Marini, F., et al., *Exploring the HeLa Dark Mitochondrial Proteome*. Front Cell Dev Biol, 2020. **8**: p. 137.
 139. Silva, J.C., et al., *Absolute quantification of proteins by LCMSE: a virtue of parallel MS acquisition*. Mol Cell Proteomics, 2006. **5**(1): p. 144-56.
 140. Vissers, J.P., J.I. Langridge, and J.M. Aerts, *Analysis and quantification of diagnostic serum markers and protein signatures for Gaucher disease*. Mol Cell Proteomics, 2007. **6**(5): p. 755-66.
 141. Butterfield, D.A., et al., *Mass spectrometry and redox proteomics: applications in disease*. Mass Spectrom Rev, 2014. **33**(4): p. 277-301.
 142. Lanzillotta, C., et al., *Early and Selective Activation and Subsequent Alterations to the Unfolded Protein Response in Down Syndrome Mouse Models*. J Alzheimers Dis, 2018. **62**(1): p. 347-359.
 143. Loboda, A., et al., *Role of Nrf2/HO-1 system in development, oxidative stress response and diseases: an evolutionarily conserved mechanism*. Cell Mol Life Sci, 2016. **73**(17): p. 3221-47.
 144. Lanzillotta, C., et al., *Proteomics Study of Peripheral Blood Mononuclear Cells in Down Syndrome Children*. Antioxidants (Basel), 2020. **9**(11).
 145. Aivazidis, S., et al., *The burden of trisomy 21 disrupts the proteostasis network in Down syndrome*. PLoS One, 2017. **12**(4): p. e0176307.
 146. Zamponi, E., et al., *Nrf2 stabilization prevents critical oxidative damage in Down syndrome cells*. Aging Cell, 2018. **17**(5): p. e12812.
 147. Antonarakis, S.E., *Down syndrome and the complexity of genome dosage imbalance*. Nat Rev Genet, 2017. **18**(3): p. 147-163.

148. Gardiner, K., *Gene-dosage effects in Down syndrome and trisomic mouse models*. *Genome Biol*, 2004. **5**(10): p. 244.
149. Parisotto, E.B., et al., *Antioxidant intervention attenuates oxidative stress in children and teenagers with Down syndrome*. *Res Dev Disabil*, 2014. **35**(6): p. 1228-36.
150. Valenti, D., et al., *The polyphenols resveratrol and epigallocatechin-3-gallate restore the severe impairment of mitochondria in hippocampal progenitor cells from a Down syndrome mouse model*. *Biochim Biophys Acta*, 2016. **1862**(6): p. 1093-104.
151. Korbil, J.O., et al., *The genetic architecture of Down syndrome phenotypes revealed by high-resolution analysis of human segmental trisomies*. *Proc Natl Acad Sci U S A*, 2009. **106**(29): p. 12031-6.
152. Epstein, C.J., et al., *Protocols to establish genotype-phenotype correlations in Down syndrome*. *Am J Hum Genet*, 1991. **49**(1): p. 207-35.
153. Gearhart, J.D., et al., *Developmental consequences of autosomal aneuploidy in mammals*. *Dev Genet*, 1987. **8**(4): p. 249-65.
154. Gardiner, K., et al., *Down syndrome: from understanding the neurobiology to therapy*. *J Neurosci*, 2010. **30**(45): p. 14943-5.
155. Reeves, R.H., L.L. Baxter, and J.T. Richtsmeier, *Too much of a good thing: mechanisms of gene action in Down syndrome*. *Trends Genet*, 2001. **17**(2): p. 83-8.
156. Lanzillotta, C., et al., *Chronic PERK induction promotes Alzheimer-like neuropathology in Down syndrome: Insights for therapeutic intervention*. *Prog Neurobiol*, 2021. **196**: p. 101892.
157. Lott, I.T. and E. Head, *Alzheimer disease and Down syndrome: factors in pathogenesis*. *Neurobiol Aging*, 2005. **26**(3): p. 383-9.
158. Perluigi, M. and D.A. Butterfield, *The identification of protein biomarkers for oxidative stress in Down syndrome*. *Expert Rev Proteomics*, 2011. **8**(4): p. 427-9.
159. Engidawork, E. and G. Lubec, *Molecular changes in fetal Down syndrome brain*. *J Neurochem*, 2003. **84**(5): p. 895-904.
160. Tramutola, A., et al., *Brain insulin resistance triggers early onset Alzheimer disease in Down syndrome*. *Neurobiol Dis*, 2020. **137**: p. 104772.
161. Perluigi, M., et al., *Aberrant protein phosphorylation in Alzheimer disease brain disturbs pro-survival and cell death pathways*. *Biochim Biophys Acta*, 2016. **1862**(10): p. 1871-82.

162. Mancuso, C., R. Siciliano, and E. Barone, *Curcumin and Alzheimer disease: this marriage is not to be performed*. J Biol Chem, 2011. **286**(3): p. 1e3; author reply 1e4.
163. Dierssen, M., et al., *Down Syndrome Is a Metabolic Disease: Altered Insulin Signaling Mediates Peripheral and Brain Dysfunctions*. Front Neurosci, 2020. **14**: p. 670.
164. Pfeffer, S.R., *Rab GTPases: master regulators that establish the secretory and endocytic pathways*. Mol Biol Cell, 2017. **28**(6): p. 712-715.
165. Zhen, Y. and H. Stenmark, *Cellular functions of Rab GTPases at a glance*. J Cell Sci, 2015. **128**(17): p. 3171-6.
166. Cenini, G., et al., *An investigation of the molecular mechanisms engaged before and after the development of Alzheimer disease neuropathology in Down syndrome: a proteomics approach*. Free Radic Biol Med, 2014. **76**: p. 89-95.
167. Kiral, F.R., et al., *Rab GTPases and Membrane Trafficking in Neurodegeneration*. Curr Biol, 2018. **28**(8): p. R471-R486.
168. English, A.R. and G.K. Voeltz, *Rab10 GTPase regulates ER dynamics and morphology*. Nat Cell Biol, 2013. **15**(2): p. 169-78.
169. Weitzdoerfer, R., et al., *Reduction of nucleoside diphosphate kinase B, Rab GDP-dissociation inhibitor beta and histidine triad nucleotide-binding protein in fetal Down syndrome brain*. J Neural Transm Suppl, 2001(61): p. 347-59.
170. Shisheva, A., S.R. Chinni, and C. DeMarco, *General role of GDP dissociation inhibitor 2 in membrane release of Rab proteins: modulations of its functional interactions by in vitro and in vivo structural modifications*. Biochemistry, 1999. **38**(36): p. 11711-21.
171. Schimmoller, F., I. Simon, and S.R. Pfeffer, *Rab GTPases, directors of vesicle docking*. J Biol Chem, 1998. **273**(35): p. 22161-4.
172. D'Adamo, P., et al., *Mutations in GDII are responsible for X-linked non-specific mental retardation*. Nat Genet, 1998. **19**(2): p. 134-9.
173. Botte, A. and M.C. Potier, *Focusing on cellular biomarkers: The endo-lysosomal pathway in Down syndrome*. Prog Brain Res, 2020. **251**: p. 209-243.
174. Chaudhari, N., et al., *A molecular web: endoplasmic reticulum stress, inflammation, and oxidative stress*. Front Cell Neurosci, 2014. **8**: p. 213.
175. Zhu, P.J., et al., *Activation of the ISR mediates the behavioral and neurophysiological abnormalities in Down syndrome*. Science, 2019. **366**(6467): p. 843-849.

176. Fullerton, H.J., et al., *Copper/zinc superoxide dismutase transgenic brain accumulates hydrogen peroxide after perinatal hypoxia ischemia*. *Ann Neurol*, 1998. **44**(3): p. 357-64.
177. Krapfenbauer, K., et al., *Aberrant expression of peroxiredoxin subtypes in neurodegenerative disorders*. *Brain Res*, 2003. **967**(1-2): p. 152-60.
178. Kreuz, S. and W. Fischle, *Oxidative stress signaling to chromatin in health and disease*. *Epigenomics*, 2016. **8**(6): p. 843-62.
179. Feser, J., et al., *Elevated histone expression promotes life span extension*. *Mol Cell*, 2010. **39**(5): p. 724-35.
180. Antonaros, F., et al., *Plasma metabolome and cognitive skills in Down syndrome*. *Sci Rep*, 2020. **10**(1): p. 10491.
181. Caracausi, M., et al., *Plasma and urinary metabolomic profiles of Down syndrome correlate with alteration of mitochondrial metabolism*. *Sci Rep*, 2018. **8**(1): p. 2977.
182. Barone, E., S. Mosser, and P.C. Fraering, *Inactivation of brain Cofilin-1 by age, Alzheimer's disease and gamma-secretase*. *Biochim Biophys Acta*, 2014. **1842**(12 Pt A): p. 2500-9.
183. Ori-McKenney, K.M., et al., *Phosphorylation of beta-Tubulin by the Down Syndrome Kinase, Minibrain/DYRK1a, Regulates Microtubule Dynamics and Dendrite Morphogenesis*. *Neuron*, 2016. **90**(3): p. 551-63.
184. Dowjat, K., et al., *Gene dosage-dependent association of DYRK1A with the cytoskeleton in the brain and lymphocytes of down syndrome patients*. *J Neuropathol Exp Neurol*, 2012. **71**(12): p. 1100-12.
185. Dowjat, K., et al., *Abnormalities of DYRK1A-Cytoskeleton Complexes in the Blood Cells as Potential Biomarkers of Alzheimer's Disease*. *J Alzheimers Dis*, 2019. **72**(4): p. 1059-1075.
186. Weitzdoerfer, R., M. Fountoulakis, and G. Lubec, *Reduction of actin-related protein complex 2/3 in fetal Down syndrome brain*. *Biochem Biophys Res Commun*, 2002. **293**(2): p. 836-41.
187. Siarey, R.J., et al., *Altered signaling pathways underlying abnormal hippocampal synaptic plasticity in the Ts65Dn mouse model of Down syndrome*. *J Neurochem*, 2006. **98**(4): p. 1266-77.

8. APPENDIX

Appendix A

Life Sciences 284 (2021) 119913

Contents lists available at ScienceDirect

Life Sciences

journal homepage: www.elsevier.com/locate/lifebsci

ELSEVIER

Open Access

Life Sciences

Biliverdin reductase-A protein levels are reduced in type 2 diabetes and are associated with poor glycometabolic control

Flavia Agata Cimini^{a,1}, Ilaria Barchetta^{a,1}, Ilaria Zuliani^b, Sara Pagnotta^b, Laura Bertocchini^a, Sara Dule^a, Michele Zampieri^a, Anna Reale^a, Marco Giorgio Baroni^{a,c,d}, Maria Gisella Cavallo^a, Eugenio Barone^{b,c}

^a Department of Experimental Medicine, Sapienza University of Rome, Italy
^b Department of Biochemical Sciences "A. Rossi-Fanelli", Sapienza University of Rome, Piazzale A. Moro 5, 00185 Rome, Italy
^c Department of Clinical Medicine, Public Health, Life and Environmental Sciences (MIGS), University of Laquila, Italy
^d Neuroendocrinology and Metabolic Diseases, IRCCS Neuroend, Pavia, Italy

ARTICLE INFO

Keywords:
Biliverdin reductase-A
Type 2 diabetes
Glucose homeostasis
Heme oxygenase
Inflammation
Metabolic disorders

ABSTRACT

Aim: Biliverdin reductase-A (BVR-A) other than its canonical role in the degradation pathway of heme as partner of heme oxygenase-1 (HO1), has recently drawn attention as a protein with pleiotropic functions involved in lipid-glucose homeostasis. However, whether BVR-A expression is altered in type 2 diabetes (T2D) has never been evaluated.

Main methods: BVR-A protein levels were evaluated in T2D (n = 44) and non-T2D (n = 29) subjects, who underwent complete clinical workup and routine biochemistry. In parallel, levels HO1, whose expression is regulated by BVR-A as well as levels of tumor necrosis factor α (TNF α), which is a known repressor for BVR-A with pro-inflammatory properties, were also assessed.

Key findings: BVR-A levels were significantly lower in T2D subjects than in non-T2D subjects. Reduced BVR-A levels were associated with greater body mass, systolic blood pressure, fasting blood glucose (FBG), glycated hemoglobin (HbA1c), triglycerides, transaminases and TNF α , and with lower high-density lipoproteins (HDL) levels. Lower BVR-A levels are associated with reduced HO1 protein levels and the multivariate analysis showed that BVR-A represented the main determinant of HO1 levels in T2D after adjustment. In addition, reduced BVR-A levels were able to predict the presence of T2D with AUROC = 0.69, for potential confounders.

Significance: Our results demonstrate for the first time that BVR-A protein levels are reduced in T2D individuals, and that this alteration strictly correlates with poor glycometabolic control and a pro-inflammatory state. Hence, these observations reinforce the hypothesis that reduced BVR-A protein levels may represent a key event in the dysregulation of intracellular pathways finally leading to metabolic disorders.

1. Introduction

Type 2 diabetes (T2D) is a metabolic disorder characterized by alterations in glucose homeostasis, as insulin resistance and progressive defects in insulin secretion [1]. In the last decades, considering the well-known link among T2D, inflammation, oxidative stress and insulin resistance, several studies have explored the role of the heme oxygenase 1 (HO1)/biliverdin reductase-A (BVR-A) system in the context of metabolic diseases, although predominantly focusing on the role for HO1 (reviewed in [2,3]).

The HO1/BVR-A system is traditionally known for its activity in the degradation pathway of heme and the production of bilirubin and represents one of the strongest endogenous antioxidant systems [4,5]. However, over the canonical role, several studies highlighted new functions for both HO1 and BVR-A, that can even work independently from each other [2,6,7]. These new functions mostly rely on the regulation of cellular metabolism whereby alterations at the expenses of HO1 and BVR-A were associated with metabolic disorders [2,6,7].

While HO1 role in metabolic disorders has been largely investigated *in vitro*, in animal models and in humans [2,3], the role for BVR-A

^{*} Corresponding author at: Department of Biochemical Sciences "A. Rossi-Fanelli", Sapienza University of Rome, Piazzale Aldo Moro 5, 00185 Rome, Italy.
E-mail address: eugenio.barone@uniroma1.it (E. Barone).

[†] These authors equally contributed.

<https://doi.org/10.1016/j.lfs.2021.119913>

Received 14 July 2021; Received in revised form 9 August 2021; Accepted 9 August 2021

Available online 26 August 2021

0024-3205/© 2021 Elsevier Inc. All rights reserved.

Appendix B

Neurotherapeutics
https://doi.org/10.1007/s13311-020-00978-4

ORIGINAL ARTICLE



The Dysregulation of OGT/OGA Cycle Mediates Tau and APP Neuropathology in Down Syndrome

Ilaria Zuliani¹ · Chiara Lanzillotta¹ · Antonella Tramutola¹ · Antonio Francioso¹ · Sara Pagnotta¹ · Eugenio Barone¹ · Marzia Perluigi¹ · Fabio Di Domenico¹

Accepted: 18 November 2020
© The Author(s) 2020

Abstract

Protein O-GlcNAcylation is a nutrient-related post-translational modification that, since its discovery some 30 years ago, has been associated with the development of neurodegenerative diseases. As reported in Alzheimer's disease (AD), flaws in the cerebral glucose uptake translate into reduced hexosamine biosynthetic pathway flux and subsequently lead to aberrant protein O-GlcNAcylation. Notably, the reduction of O-GlcNAcylation involves also tau and APP, thus promoting their aberrant phosphorylation in AD brain and the onset of AD pathological markers. Down syndrome (DS) individuals are characterized by the early development of AD by the age of 60 and, although the two conditions present the same pathological hallmarks and share the alteration of many molecular mechanisms driving brain degeneration, no evidence has been sought on the implication of O-GlcNAcylation in DS pathology. Our study aimed to unravel for the first time the role of protein O-GlcNAcylation in DS brain alterations positing the attention of potential trisomy-related mechanisms triggering the aberrant regulation of OGT/OGA cycle. We demonstrate the disruption of O-GlcNAcylation homeostasis, as an effect of altered OGT and OGA regulatory mechanism, and confirm the relevance of O-GlcNAcylation in the appearance of AD hallmarks in the brain of a murine model of DS. Furthermore, we provide evidence for the neuroprotective effects of brain-targeted OGA inhibition. Indeed, the rescue of OGA activity was able to restore protein O-GlcNAcylation, and reduce AD-related hallmarks and decreased protein nitration, possibly as effect of induced autophagy.

Key Words O-GlcNAcylation · Down syndrome · OGT/OGA · APP · tau · autophagy

Introduction

Down syndrome (DS; Trisomy 21) is the most common chromosomal disorder and the most frequent genetic cause of intellectual disability affecting about 6 million people worldwide [1, 2]. Because of the advances in health care and management of co-occurring illnesses, the life expectancy of people with DS has largely improved [3, 4]. The triplication of genes on chromosome 21 and of their products can alter diverse pathways, including those involved with brain development, metabolism, and neuronal networks [5, 6]. Individuals with DS are also more likely to develop certain pathological

conditions, including hypothyroidism, autoimmune diseases, epilepsy, hematological disorders, and Alzheimer-like dementia [7]. The clinical manifestation of Alzheimer-like dementia in DS resembles that occurring in the general population [8, 9], with slight differences in early presentation [10]. Nearly all individuals with full trisomy 21 aged 40 and older are found to have typical signs of Alzheimer's disease (AD) neuropathology, including extracellular amyloid plaques and intracellular neurofibrillary tangles [11]. The extra copy of amyloid precursor protein (APP) gene on chromosome 21 is associated with a 4- to 5-fold overexpression of APP that leads to an early onset and rapid accumulation of β -amyloid protein ($A\beta$) with age [9, 12]. Cortical deposits of $A\beta$ 1-42 have even been discovered as early as at 12 years of age [13]. Triplication of specific kinases (e.g., DYRK-1) interacting with APP and tau represents a further link between gene imbalance and neuropathological features DS [14]. Furthermore, brain hypoglycemia and insulin resistance are emerging as common mechanisms of neurodegeneration in DS and AD [15-17]. Several

✉ Fabio Di Domenico
fabio.didomenico@uniroma1.it

¹ Department of Biochemical Sciences "A. Rossi Fanelli", Laboratory affiliated to Istituto Pasteur Italia-Fondazione Cenci Bolognietti, Sapienza University of Rome, P.le Aldo Moro 5, 00185 Rome, Italy

Published online: 30 November 2020

Springer

Appendix C



Article

Proteomics Study of Peripheral Blood Mononuclear Cells in Down Syndrome Children

Chiara Lanzillotta ^{1†}, Viviana Greco ^{2,3†}, Diletta Valentini ⁴, Alberto Villani ⁵,
Valentina Folgiero ⁶, Matteo Caforio ^{1,3}, Franco Locatelli ^{3,4}, Sara Pagnotta ¹, Eugenio Barone ⁷,
Andrea Urbani ^{2,3}, Fabio Di Domenico ¹ and Marzia Perluigi ^{1,*}

¹ Department of Biochemical Sciences "A. Rossi Fanelli", Laboratory Affiliated to Istituto Pasteur Italia-Fondazione Cenci Bolognietti, Sapienza University of Rome, 00185 Rome, Italy; chiara.lanzillotta@uniroma1.it (C.L.); matteo.caforio@opbg.net (M.C.); sara.pagnotta@uniroma1.it (S.P.); eugenio.barone@uniroma1.it (E.B.); fabio.didomenico@uniroma1.it (F.D.D.)

² Department of Basic Biotechnological Sciences, Intensive Care and Perioperative Clinics, Università Cattolica del Sacro Cuore, 00168 Rome, Italy; viviana.greco@unicatt.it (V.G.); andrea.urban@policlinico.gemelli.it (A.U.)

³ Department of Laboratory Diagnostic and Infectious Diseases, Fondazione Policlinico Universitario Agostino Gemelli-IRCCS, 00168 Rome, Italy

⁴ Pediatric and Infectious Disease Unit, Bambino Gesù Children's Hospital, 00165 Rome, Italy; diletta.valentini@opbg.net (D.V.); alberto.villani@opbg.net (A.V.)

⁵ Department of Pediatric Hematology/Oncology and of Cell and Gene Therapy, Bambino Gesù Children's Hospital, 00165 Rome, Italy; franco.locatelli@opbg.net

⁶ Department of Gynecology/Obstetrics and Pediatrics, Sapienza University of Rome, 00185 Rome, Italy

* Correspondence: marzia.perluigi@uniroma1.it

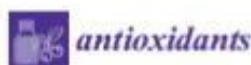
† The authors contributed equally to the work.

Received: 29 September 2020; Accepted: 09 November 2020; Published: 11 November 2020

Abstract: Down syndrome (DS) is the most common chromosomal disorder and the leading genetic cause of intellectual disability in humans, which results from the triplication of chromosome 21. To search for biomarkers for the early detection and exploration of the disease mechanisms, here, we investigated the protein expression signature of peripheral blood mononuclear cells (PBMCs) in DS children compared with healthy donors (HD) by using an in-depth label-free shotgun proteomics approach. Identified proteins are found associated with metabolic pathways, cellular trafficking, DNA structure, stress response, cytoskeleton network, and signaling pathways. The results showed that a well-defined number of dysregulated pathways retain a prominent role in mediating DS pathological features. Further, proteomics results are consistent with published study in DS and provide evidences that increased oxidative stress and the increased induction of stress related response, is a participant in DS pathology. In addition, the expression levels of some key proteins have been validated by Western blot analysis while protein carbonylation, as marker of protein oxidation, was investigated. The results of this study propose that PBMCs from DS children might be in an activated state where endoplasmic reticulum stress and increased production of radical species are one of the primary events contributing to multiple DS pathological features.

Keywords: proteomics; Down syndrome; peripheral blood mononuclear cells (PBMCs); unfolded protein response; oxidative stress

Appendix D



Review

The BACH1/Nrf2 Axis in Brain in Down Syndrome and Transition to Alzheimer Disease-Like Neuropathology and Dementia

Mazia Perluigi ^{1,*}, Antonella Tramutola ^{1,2}, Sara Pagnotta ¹, Eugenio Barone ^{1,2} and D. Allan Butterfield ^{2,3,*}

- ¹ Department of Biochemical Sciences, Sapienza University of Rome, 00185 Rome, Italy; antonella.tramutola@uniroma1.it (A.T.); sara.pagnotta@uniroma1.it (S.P.); eugenio.barone@uniroma1.it (E.B.)
² Department of Chemistry, University of Kentucky, Lexington, KY 40506, USA
³ Sanders-Brown Center on Aging, University of Kentucky, Lexington, KY 40536, USA
* Correspondence: mazia.perluigi@uniroma1.it (M.P.); dabcs@uky.edu (D.A.B.)

Received: 29 July 2020; Accepted: 17 August 2020; Published: 21 August 2020



Abstract Down syndrome (DS) is the most common genetic cause of intellectual disability that is associated with an increased risk to develop early-onset Alzheimer-like dementia (AD). The brain neuropathological features include alteration of redox homeostasis, mitochondrial deficits, inflammation, accumulation of both amyloid beta-peptide oligomers and senile plaques, as well as aggregated hyperphosphorylated tau protein-containing neurofibrillary tangles, among others. It is worth mentioning that some of the triplicated genes encoded are likely to cause increased oxidative stress (OS) conditions that are also associated with reduced cellular responses. Published studies from our laboratories propose that increased oxidative damage occurs early in life in DS population and contributes to age-dependent neurodegeneration. This is the result of damaged, oxidized proteins that belong to degradative systems, antioxidant defense system, neuronal trafficking, and energy metabolism. This review focuses on a key element that regulates redox homeostasis, the transcription factor Nrf2, which is negatively regulated by BACH1, encoded on chromosome 21. The role of the Nrf2/BACH1 axis in DS is under investigation, and the effects of triplicated BACH1 on the transcriptional regulation of Nrf2 are still unknown. In this review, we discuss the physiological relevance of BACH1/Nrf2 signaling in the brain and how the dysfunction of this system affects the redox homeostasis in DS neurons and how this axis may contribute to the transition of DS into DS with AD neuropathology and dementia. Further, some of the evidence collected in AD regarding the potential contribution of BACH1 to neurodegeneration in DS are also discussed.

Keywords: oxidative stress; BACH1; Nrf2; Down syndrome; Alzheimer disease

1. Genetics of Oxidative Stress in Down Syndrome

Down syndrome (DS) or trisomy 21 is one of the most common genetic disorder displaying phenotypic features that include neurodevelopmental defects, neuronal dysfunction, and accelerated aging, among others Cerini, Dowling [1–3]. Further, DS individuals are at increased risk to develop a type of dementia that mimics the clinical and pathological features course of Alzheimer disease (AD), with the deposition of amyloid plaques and neurofibrillary tangles. Interestingly, DS is emerging as a disorder etiologically related to oxidative stress (OS) mainly due to triplication of Cu, Zn-superoxide dismutase (SOD-1), encoded on chromosome 21 (Hsa21). However, recent reports showed that OS is driven not only from overexpression of some *Hsa21* genes, but also from a dysregulation of gene/protein expression associated with the trisomy [4].

Ringraziamenti

Ringrazio Marzia, per avermi dato la possibilità, tre anni di fa, di entrare a far parte di questo gruppo; grazie per essere stata una guida, un riferimento ma soprattutto un esempio per la passione e la determinazione che dimostri ogni giorno nel tuo lavoro.

Eugenio, per ogni consiglio e suggerimento.

Fabio, per la costante disponibilità

Il ringraziamento più grande è per Antonella, tutto quello che ho imparato in questi anni è grazie a te, sei stata il mio punto fermo, il mio faro. Grazie per esserci stata in ogni momento di questo percorso, per tutti gli insegnamenti e per la passione che mi hai trasmesso per questo lavoro.

Chiara, grazie per la tua presenza, il tuo aiuto e per ogni momento condiviso.

Simona, grazie perchè hai reso questo mio ultimo anno migliore, sei stato il pezzo mancante del puzzle.

Ringrazio i miei genitori, per avermi sempre sostenuto, per il vostro esempio ed i preziosi insegnamenti. Grazie perchè questo traguardo è anche merito vostro.

Ringrazio Giovanni ed Eleonora, per il vostro supporto e per essere sempre al mio fianco.

Ringrazio mia nonna, lo so che hai sempre fatto il tifo per me.

Ringrazio Alessandro, per essere sempre stato al mio fianco, sostenuto in questo cammino ed aver creduto in me. Niente sarebbe stato possibile senza te accanto.